UNCERTAINTY-BASED ROBUST OPTIMAL DESIGN AND CONTROL OF CLEANROOM AIR-CONDITIONING SYSTEMS

ZHUANG CHAOQUN

PhD

The Hong Kong Polytechnic University

2020

Temporary Binding for Examination Purposes

The Hong Kong Polytechnic University

Department of Building Services Engineering

UNCERTAINTY-BASED ROBUST OPTIMAL DESIGN AND CONTROL OF CLEANROOM AIR-CONDITIONING SYSTEMS

ZHUANG CHAOQUN

A thesis submitted in partial fulfillment of the requirements for the degree of Doctor of Philosophy

Sept 2019

CERTIFICATE OF ORIGINALITY

I hereby declare that this thesis is my own work and that, to the best of my knowledge and belief, it reproduces no materials previously published or written, nor material that has been accepted for the award of any other degree or diploma, except where due acknowledgement has been made in the text.

_____(Signed)

ZHUANG Chaoqun (Name of student)

ABSTRACT

Abstract of thesis entitled: Uncertainty-based robust optimal design and control of cleanroom air-conditioning systems

Submitted by : ZHUANG Chaoqun

For the degree of : Doctor of Philosophy

at The Hong Kong Polytechnic University in September, 2019

The total floor area and energy consumption of buildings with spaces requiring strict temperature and humidity control, such as pharmaceutical cleanrooms, hospitals, semiconductor/microchip factories (denoted as “cleanrooms” for brevity), have been growing rapidly worldwide. The energy intensity of cleanroom air-conditioning systems is usually 10-100 times greater than the average energy intensity of office buildings, due to the complexity of the systems and their operational needs for strict temperature and humidity control. However, the energy conservation issue in cleanrooms has not attracted sufficient attention. This PhD study attempts to comprehensively explore the ventilation strategy including the energy-efficient design and control of cleanroom air-conditioning systems by addressing the following questions which are not well answered in existing studies:

- What is the most suitable ventilation strategy for cleanroom air-conditioning systems that can be adaptive to changes in different working conditions?
- How to design cleanroom air-conditioning systems that can maximize their potentials in energy saving and cost reduction under uncertainties?

- How to control cleanroom air-conditioning systems in operation that can enable systems to operate at high energy efficiency and reliability under measurement uncertainties?

To ensure the high performance of air-conditioning systems as its design expectation, the ventilation strategy adopted should be adaptive to changes in internal sensible/latent load and ambient conditions. An “adaptive full-range decoupled ventilation (ADV) strategy” is proposed to minimize the system energy consumption by incorporating the advantages of existing ventilation strategies and adopting a novel “adaptive economizer”. The main advantage of the ADV strategy is that it can select the optimal operation mode (i.e. with the minimum estimated energy use) from available/multiple operation modes. It avoids sub-cooling and reheating as far as beneficial via the best use of MAU and economizer for cooling and dehumidification. The energy and economic performance of the proposed ADV strategy are further evaluated under different climatic conditions. The results show that adopting the ADV strategy can offer significant and promising energy savings. The payback periods are attractive for both existing system retrofit and new system design in most climates.

The design for cleanroom air-conditioning systems is a complicated task due to the coupling operation and counteraction/interaction among their components. An uncertainty-based robust optimal design method for cleanroom air-conditioning systems is developed for implementing the ADV strategy considering uncertainties. To address the issue of asynchronous loads in different zones/spaces with reduced computation demand, a probabilistic diversity factor method is developed to quantify the effects of uncertainties of space load diversities in multiple zones/spaces. The robust optimal design method is validated based on the actual air-conditioning systems in an existing pharmaceutical building. The test results show that the air-conditioning

system, which is designed for the ADV strategy using the proposed design method, offers superior economic performance and satisfaction of service.

Besides the robust optimal design, an online supervisory control strategy is also essentially needed for practical implementations of the ADV strategy. A risk-based online robust optimal control strategy is developed for multi-zone air-conditioning systems considering component performance degradation and measurement uncertainties. The core element of this strategy is the robust decision-making scheme, which is developed for selecting the optimal control mode of the air-conditioning systems online by compromising between the potential risks and benefits. This online control strategy is validated on a dynamic system simulation platform constructed on the basis of existing air-conditioning systems at full scale. The test results show the proposed control strategy can successfully determine the best operation mode allowing for component performance degradation and measurement uncertainties, and ensure air-conditioning systems to operate at high reliability and energy efficiency.

To conclude, the developed adaptive ventilation strategy, the system robust optimal design and robust online optimal control methods can provide significant improvements to current design and control practice of cleanroom air-conditioning systems.

PUBLICATIONS ARISING FROM THIS THESIS

Journal Papers

2018 Howard Cheung, Shengwei Wang, **Chaoqun Zhuang**, Jiefan Gu. (2018). A simplified power consumption model of information technology (IT) equipment in data centers for energy system real-time dynamic simulation. *Applied energy*, 222, 329-342.

2019 **Chaoqun Zhuang**, Shengwei Wang, Kui Shan. (2019). Adaptive full-range decoupled ventilation strategy and air-conditioning systems for cleanrooms and buildings requiring strict humidity control and their performance evaluation. *Energy*, 168, 883-896.

2019 **Chaoqun Zhuang**, Shengwei Wang, Kui Shan. (2019). Probabilistic optimal design of cleanroom air-conditioning systems facilitating optimal ventilation control under uncertainties. *Applied Energy*, 253, 113576.

2020 **Chaoqun Zhuang** and Shengwei Wang. (2020). An adaptive full-range decoupled ventilation strategy for buildings with spaces requiring strict humidity control and its applications in different climatic conditions. *Sustainable Cities and Society*, 52, 101838.

2020 **Chaoqun Zhuang** and Shengwei Wang. (2020). Risk-based online robust optimal control of air-conditioning systems for buildings requiring strict humidity control considering measurement uncertainties. *Applied Energy*, 261, 114451.

2020 **Chaoqun Zhuang** and Shengwei Wang. (2020). Uncertainty-based robust optimal design of cleanroom air-conditioning systems considering life-cycle performance. *Indoor and Built Environment*, 1420326X19899442.

Conference Papers

2017 Howard Cheung, Shengwei Wang, **Chaoqun Zhuang**. (2017). Development of a simple power consumption model of information technology (IT) equipment for building simulation. *9th International Conference on Applied Energy.* August 21 to 24, 2017, Cardiff, UK.

2018 **Chaoqun Zhuang**, Shengwei Wang, Rui Tang. (2018). Optimal design of multi-zone air-conditioning systems for buildings requiring strict humidity control. *10th International Conference on Applied Energy*. August 22 to 25, 2018, Hong Kong, China.

2018 **Chaoqun Zhuang**, Shengwei Wang, Kui Shan. (2018). Optimal control strategy of air-conditioning systems for buildings requiring strict humidity control. *39th AIVC - 7th TightVent & 5th Venticool Conference: Smart ventilation for buildings*. September 18 to 19 2018, Antibes, France.

2019 **Chaoqun Zhuang** and Shengwei Wang. (2019). Coordinated probabilistic optimal design of cleanroom air-conditioning systems facilitating optimal ventilation control strategies under uncertainties. *The 11th International Symposium on Heating, Ventilation and Air Conditioning*. July 12 to 15, 2019, Harbin, China. **(Best Paper Award)**

2019 **Chaoqun Zhuang** and Shengwei Wang. (2019). Adaptive full-range decoupled ventilation strategy and air-conditioning systems for cleanrooms:

concepts and coordinated optimal design. *The 1st international Chinese Conference on Energy and Built Environment*. July 19 to 22, 2019, Chengdu, China.

ACKNOWLEDGEMENTS

This thesis would have been not completed timely without help and support from many people.

First and foremost, I would like to express my sincerest appreciation to Professor Shengwei Wang, my supervisor, for his readily available supervision, valuable suggestions, patient encouragement and continuous support during my PhD study. Also, I would like to thank Professor Fu Xiao, for her suggestions and support to me over the entire period of my PhD study.

I would also like to thank all colleagues in IB&BA research group, especially Dr. Kui Shan, Dr. Diance Gao, Dr. Rui Tang, Dr. Jing Kang, Dr. Lei Xu and Dr. Maomao Hu. Their talents and diligence always inspire and encourage me to be better.

Finally, I am truly grateful for the love, support and patience from my parents and my wife (Yunran). Without them, I would not have been able to thrive in my doctoral program. I am incredibly grateful for those friends who provide tacit and powerful support over the past three years. This thesis is dedicated to them.

TABLE OF CONTENTS

LIST OF FIGURES

LIST OF TABLES

NOMENCLATURE

a_1-a_2, b_1-b_2, c_1-c_4	coefficients
ACH	air change rates per hour
ADV	adaptive full-range decoupled ventilation
AHU	air-handling unit
CAP	capacity (kW)
c_p	air specific heat ratio (kJ/(m^3·K)
C_{OT}	overall annualized total cost (USD)
C_C	capital cost (USD)
C_M	maintenance cost (USD)
C_O	operation cost (USD)
C_P	penalty cost (USD)
COP_c	overall coefficient of performance of cooling system
COP_{he}	overall coefficient of performance of heating system
COP_{hu}	overall coefficient of performance of humidification system
CRF	capital recovery factor
D_{sen}	sensible cooling demand of zones (W/m^2)
D_{lat}	latent cooling demand of zones (W/m^2)
DV	dedicated outdoor air ventilation
E	electrical load (kW)
e	white noise
ΔE	dead band
FL	following latent load
FS	following sensible load
h	enthalpy of air (kJ/kg)
h_{fg}	latent heat of vaporization (kJ/kg)
IC	interactive control
Inc	investment cost (USD)
LL	lower-limit humidity control
m	air mass flowrate (kg/s)
MAU	make-up air-handling unit
N	lifetime (year)

PAU	primary air-handling unit
PD	partially decoupled control
Δp	total pressure rise (kPa)
SHR	sensible heat ratio
Q_{sen}	space sensible cooling load (W/m^2)
Q_{lat}	space latent cooling load (W/m^2)
Q_{tot}	space total cooling load (W/m^2)
$Q_{cc,MAU}$	cooling coil cooling load of make-up air-handling unit (kW)
$Q_{cc,AHU}$	cooling coil cooling load of supply air-handling unit (kW)
$Q_{he,AHU}$	heater heating load of supply air-handling unit (kW)
$Q_{hu,AHU}$	humidification load of supply air-handling unit (kW)
t,T	temperature (°C)
w	humidity ratio (kg/kg)
$w_{MAU,min}$	MAU minimum outlet humidity ratio (kg/kg)
W_f	fan power (kW)
i'	real discount rate
i_d	discount rate
i_e	energy inflation rate
i_g	general inflation rate
i''	effective discount rate
V	air volumetric flow rate (m^3/s)
Z_{sen}	zone sensible cooling load (W/m^2)
Z_{lat}	zone latent cooling load (W/m^2)

Subscripts

ave	average
c	cooling system
cc	cooling coil
e	electricity
f	fan
fh	outdoor air
fic	fictitious
he	heating system
hu	humidification system

in	initial
inp	input
k,j	time instant
lat	latent
ma	maintenance
min	minimum
mf	make-up fan
nb	net benefit
pen	penalty
r	room
s	supply air
sen	sensible
sf	supply fan
thr	threshold
tot	total
out	outlet
otp	output

Greek symbols

α	outdoor air ratio
α_t, γ_t	threshold value
ε	motor installation factor
η_f	fan efficiency
γ_{pen}	penalty price ratio
β	diversity factor
£	price
Δ	standard deviation
λ	filtering weight factor
ρ	air density (kg/m^3)

CHAPTER 1 INTRODUCTION

This chapter presents an outline of this thesis in the following three sections. The background and motivation of this study are described in Section 1.1. The aim and objectives are presented in Section 1.2. Section 1.3 shows the organization of this thesis and gives a brief description of each chapter.

1.1 Background and motivation

The depletion of fossil fuels, global climate change and dramatic growth of energy consumption are the main challenges to the governments and society today. Buildings consume 30-40% of primary energy globally (Duić et al., 2013), and this percentage is even higher (60% of primary energy and over 90% of electricity) in Hong Kong (EMSD, 2018). In response to these challenges, the Hong Kong government has set a target to achieve an energy intensity reduction target as a whole of 40% by 2025 using 2005 as the base (ENVB, 2015).

Buildings with spaces requiring strict temperature and humidity controls, such as pharmaceutical cleanrooms, hospitals, semiconductor/microchip factories, laboratories and museums (hereafter denoted as “cleanrooms” for brevity), have been growing rapidly in terms of total floor area and energy consumption. For instance, in the USA, the total area of cleanrooms increased from 4.2 million m^2 in 1993 to about 15.5 million m^2 in 2015 (Mills, 1996). It increases even faster in South China (Pearl Delta Region) due to the rapid increase of semiconductor fabrication (Li, He, Shan, & Cai, 2018). Meanwhile, the energy intensity of air-conditioning systems in such

buildings/applications can be 30 to 50 times more energy-intensive than typical commercial buildings (Mathew, 2008), or 10 to 100 times more energy-intensive than typical office buildings (Mills et al., 2008; Tschudi & Xu, 2001). However, the annual energy intensity in cleanrooms has not seen a significant reduction over the last two decades (Kircher, Shi, Patil, & Zhang, 2010; Mills, 1996). The industries, which may need cleanroom production environments, usually involve highly skilled and knowledge-intensive manufacturing processes. The efforts on cleanroom air-conditioning systems in the past are mainly on the means to provide a satisfactory indoor environment in order to maintain the reliable operation of the machines/equipment. Therefore, the energy conservation issue in cleanrooms has not gained sufficient attention. The increased total floor area, high energy intensity and the complex system design and control of cleanrooms have raised widespread concerns over their rapidly growing energy consumption, leading to considerable interest in the potential for energy savings.

According to the investigation and system retrofitting work by Shan and Wang (2017) in pharmaceutical factory buildings in Hong Kong, up to 42% of annual energy cost saving could be achieved by optimizing the system control without any hardware modification. This indicates that the energy-saving potential of air-conditioning systems is very high in spaces where strict and simultaneous temperature and humidity control is required. However, many problems need to be solved in order to realize this energy-saving potential, due to the complexity of air-conditioning systems and their operation for achieving strict humidity and temperature control. The challenges in solving these problems are particularly associated with ever-changing working conditions, the uncertainties in the information used for the air-conditioning system design as well as the uncertainties of measurements used for system online control

decisions. These challenges are summarized as follows, which are the main issues to be addressed in this PhD study.

i. The energy performance of existing ventilation strategies is unsatisfactory under off-design conditions. Although most existing popular ventilation strategies today are energy-efficient under specific ranges of working conditions, their actual performance in operation often deviates significantly from their design expectations due to the fact that they cannot adjust to "off-design" changing ambient and load conditions. Furthermore, the counteractions and interactions among different air-conditioning processes often result in great energy waste.

ii. Mismatches widely exist between air-conditioning system design and operation/control in current engineering practice. Although individual components are well designed and systems may work at high energy efficiency at design working conditions, mismatches are commonplace in practice. This is because the coordination and interaction between different components under off-design conditions are usually not comprehensively considered.

iii. The practical operation of ventilation strategies often deviates significantly from expectations due to measurement uncertainties/errors and model errors. Although models can be well trained at the initial stage, most models for online use today cannot adapt themselves to component performance degradation. The model prediction errors of component capacities and the errors in measuring cooling loads and working conditions result in the improper selection of control modes and consequently great energy waste.

1.2 Aim and objectives

This study, therefore, aims to develop a new energy-efficient ventilation strategy, robust optimal design and online optimal control methods for cleanrooms air-conditioning systems, which enable the systems to operate at high energy efficiency over a wide range of ever-changing load and ambient conditions. It is accomplished by addressing the following objectives and research tasks:

i. Develop an "adaptive full-range decoupled ventilation (ADV) strategy", which can provide superior energy performance over the full range of internal loads and ambient conditions;
ii. Assess the energy and economic performance when implementing the proposed ADV strategy, as well as identify the applicable regions for different operation modes in different climate zones;
iii. Develop and validate an uncertainty-based robust optimal design method for cleanroom air-conditioning systems facilitating the proposed ADV strategy. The robust optimal design method should be able to offer the systems with high energy efficiency at a wide range of internal loads and ambient conditions, taking into account design input uncertainties and load diversities of multiple spaces;
iv. Develop and validate a risk-based online robust optimal control strategy for implementing the proposed ADV strategy. The control strategy should be able to determine/select the optimal control mode with high energy efficiency and reliability considering component performance degradation and measurement uncertainties.

1.3 Organization of this thesis

Chapter 1 introduces the background and the motivation of the research by presenting the need of a comprehensive energy-conservative approach for cleanrooms air-conditioning systems, including the ventilation strategy, system robust optimal design and control methods. The aim and main objectives are also presented in this chapter.

Chapter 2 presents a comprehensive literature review of related existing studies, including the existing ventilation strategies and their limitations, as well as design and control optimization methods for air-conditioning systems. This chapter also elaborates on the research gaps which are addressed in this PhD study.

Chapter 3 describes the mechanism and advantages of the proposed ADV strategy. It minimizes system energy consumption by avoiding sub-cooling and reheating as far as beneficial via the best use of make-up air handling units for dehumidification. In addition, a new "adaptive economizer", with three modes of operation, is incorporated in the proposed strategy to optimize the outdoor air intake. Component and system modelling of cleanroom air-conditioning systems is also presented in this chapter.

Chapter 4 illustrates the performance evaluation and applications of the proposed ADV strategy in different climate zones. Nine cities in five main climate zones are selected to test the application potentials of the proposed ventilation strategy. Energy and economic performance, the needs for existing system retrofits and new system designs, as well as the preferable operation modes are presented.

Chapter 5 presents the design optimization of cleanroom air-conditioning systems considering uncertainties for implementing the ADV strategy. To consider the effects of asynchronous loads in different zones/spaces with reduced computation demand, a probabilistic diversity factor method is proposed to quantify the effects of

uncertainties of space load diversities in multiple zones/spaces. The proposed design method is implemented and validated in the design optimization of air-conditioning systems for implementing four different ventilation control strategies considering possible and uncertain off-design conditions.

Chapter 6 presents a risk-based online robust optimal control strategy for cleanroom air-conditioning systems considering component performance degradation and measurement uncertainties. An online control decision is made by compromising between the failure risks and energy benefits of different operation modes considering measurement uncertainties. The proposed control strategy is tested and validated on a dynamic simulation test platform constructed based on an existing pharmaceutical manufacturing building.

Chapter 7 summarizes the main contributions of this PhD study and gives recommendations for future research on the subject concerned.

The interconnection between the main chapters of the thesis is illustrated as shown in Figure 1.1. The development of a novel ADV strategy, as well as component and system energy models, which are the basic tasks of the whole study, are presented in Chapter 3. The performance evaluation and optimal design are addressed in Chapters 4 & 5, based on the component and system energy models presented in Chapter 3. In Chapter 4, the energy and economic performance adopting the ADV strategy in different climate zones are presented. In Chapter 5, the optimal design of cleanroom air-conditioning systems for implementing the ADV strategy is presented. In Chapter 6, a risk-based online robust optimal control strategy is presented. A robust online decision-making scheme is developed for selecting the best operation mode of air-conditioning systems. A realistic dynamic simulation platform involving the

cleanroom air-conditioning component and system models is built for evaluating the actual performance of the proposed real-time control strategy.

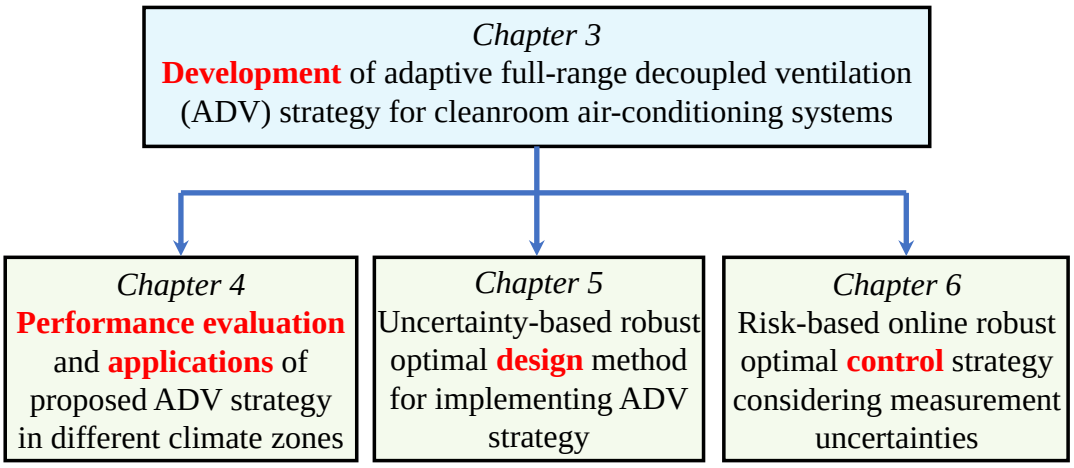

Figure 1.1 Organization of main chapters

CHAPTER 2 LITERATURE REVIEW

Cleanrooms today are technology-intensive solutions with high demands on the indoor air cleanliness, pressurization, temperature and humidity controls. The energy conservation opportunities are prevalent for cleanroom air-conditioning systems due to high energy intensity and strict control requirements. Comprehensive approaches, including a proper ventilation strategy, optimal design and control methods, are essentially needed for achieving energy-efficient operation of cleanrooms. This chapter presents a comprehensive literature review on the existing ventilation strategies, design and control methods for air-conditioning systems for different applications. Section 2.1 briefly introduces the basic information about the cleanroom air-conditioning systems, including indoor environment control requirements and typical system configurations. Section 2.2 presents the existing ventilation strategies for cleanrooms or spaces requiring strict humidity control. The review of the studies on design and control optimization methods for general air-conditioning systems are presented in Section 2.3 and Section 2.4, respectively. Conclusive remarks of the reviews are given in Section 2.5.

2.1 Overview of cleanroom air-conditioning systems and configurations

2.1.1 Why are cleanrooms energy-intensive?

Cleanrooms are special spaces that maintain the controlled environments (e.g. cleanliness, temperature, humidity, and pressure) required for the specific

manufacturing processes. The causes of high energy consumption in most cleanroom air-conditioning systems are mainly due to *i.*) high air recirculation rates and high airflow resistance (due to the use of filters) to ensure the indoor cleanliness; and *ii.*) some counteraction processes (i.e. overcooling and reheating) to ensure simultaneous indoor temperature and humidity control.

Cleanrooms are usually designed with air changes per hour (ACH) between 20 to 160 depending on theirs cleanliness level, which is much higher than the value (e.g. 5 ACH) in spaces of normal use (Schneider, 2001). Higher ACHs equate to higher airflows and more energy use. For instance, it is reported that the air recirculation system in the cleanroom accounts for about 10% of the total power consumption in semiconductor fabrication plants (Hu & Chuah, 2003; Lin, Hu, & Xu, 2015). In addition, compared with conventional air-conditioning systems with the general purpose of thermal comfort, adding humidity as a critical control objective in cleanrooms would raise the challenge of energy-efficient operation/control since cooling and dehumidification processes are highly coupled, leading to some unavoidable counteraction and interaction processes.

Specifically, the energy consumed by air conditioning systems (e.g. chiller water, hot water, steam and fans) is approximately 58% of the total energy consumption in cleanrooms (Tschudi, Sartor, Mills, & Xu, 2002) as shown in Figure 2.1. Energy conservation opportunities of Heating, Ventilation and Air Conditioning (HVAC) systems are prevalent in cleanroom applications (Tschudi & Xu, 2001).

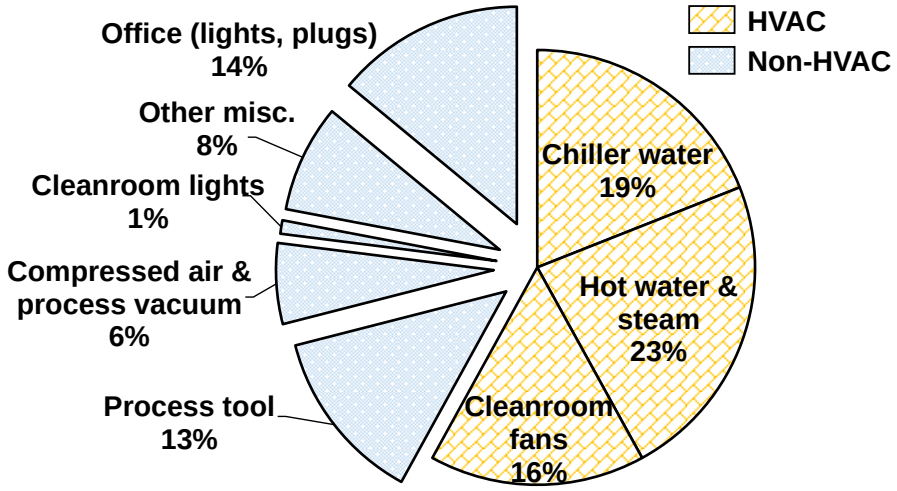

Figure 2.1 Energy end-use in production cleanrooms. (Tschudi et al., 2002)

2.1.2 Typical system configurations

Cleanroom air-conditioning systems suitable for the low-cleanliness requirement cleanrooms, i.e., IOS-8 (ISO, 2015), can be categorized into three typical types referring to existing design practice (Hu & Tsao, 2007; PG&E, 2011), as described below. They are concerned in this study. For the high cleanliness cleanrooms with strict contamination control, some specific configurations may be required (e.g. mini environments) due to their high ACH requirements, which is not included in the scope of this study.

I - Single supply air-handling unit system: The configuration of the single supply air-handling unit (AHU) system is shown in Figure 2.2. The AHU contains a cooling coil, a heater, a fan, a humidifier and filters for conditioning the supply air. The chilled water to AHU cooling coils is supplied by a chiller plant. This system only resorts an AHU to control the indoor temperature and relative humidity. All makeup air and recirculation air are mixed, conditioned and supplied from this unit in one airflow loop. Return and supply air are both via large plenum chambers under the floor and above the ceiling. Generally, cleanrooms require positive static pressure to avoid the

infiltration of pollutants from the outdoor air or adjacent area. The pressure stabilizer (i.e. adjustable automatic relief damper) controls the difference between the total supply and return air flowrates in order to maintain a positive pressure in cleanrooms. The amount of the exhaust air, which needs to be discharged, highly depends on the amount of induced outdoor air (i.e. make-up air) and leakage air.

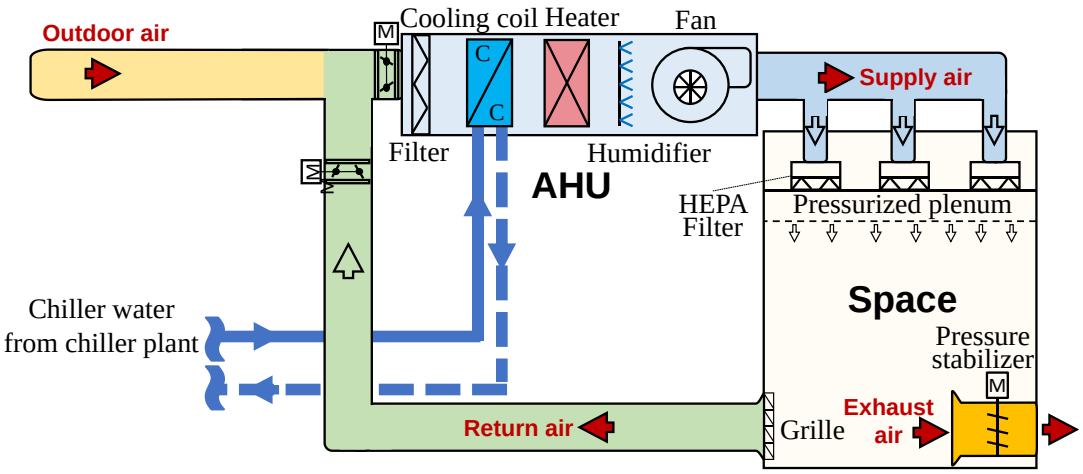

Figure 2.2 Configuration of single AHU system

II - Make-up air-handling unit integrated with local axial fan and dry cooling coil:

The configuration of a make-up air-handling unit (MAU) integrated with a local axial fan and a dry cooling coil (DCC) is shown in Figure 2.3. The MAU consists of a cooling coil, a fan and filters for conditioning the outdoor air. The MAU is used for handling all the indoor latent heat and part of indoor sensible heat while the DCC is used for handling residual indoor sensible heat only. Dual-temperature chilled water is required for such configuration. Low-temperature chiller water is supplied to the MAU. The medium-temperature chiller water is supplied to the DCC to avoid terminal condensation. Total supply air is transported in air aisle by the local axial fan.

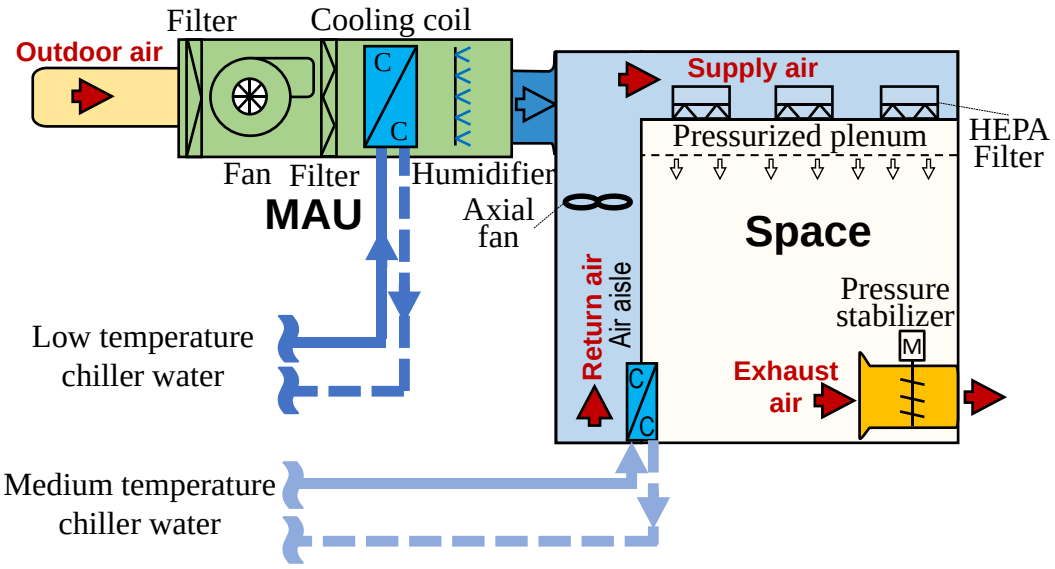

Figure 2.3 Configuration of MAU integrated with local axial fan and DCC

III - MAU integrated with AHU: The configuration of an MAU integrated with an AHU is shown in Figure 2.4. The MAU is used for conditioning the outdoor air and the AHU is used for conditioning the total supply air. The chilled water to both MAU and AHU cooling coils is supplied by a chiller plant. Both the MAU and AHU can handle the indoor sensible and latent heat depending on the ventilation strategy adopted.

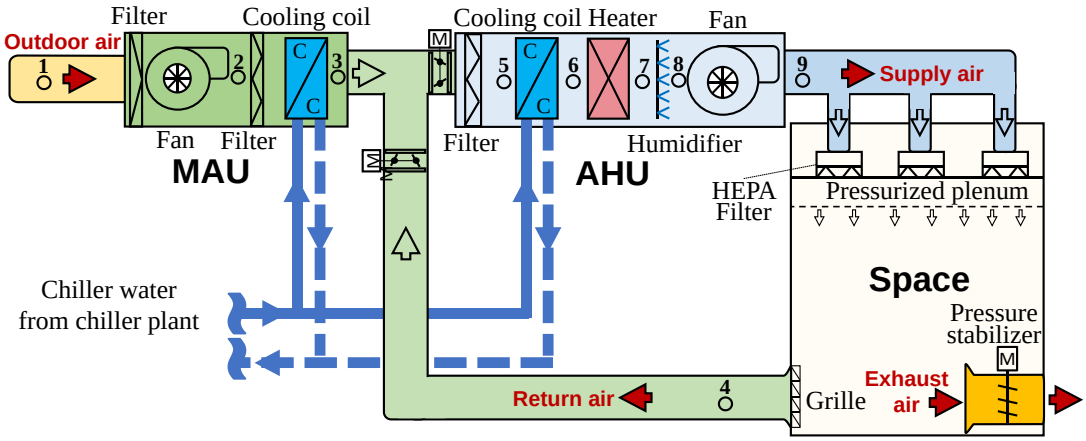

Figure 2.4 Configuration of MAU integrated with AHU

For cleanroom air-conditioning systems, selection of the system configuration is a key issue for achieving high energy efficiency due to the required high recirculation

airflow rate and high-pressure losses at filters (Xu, 2003). The first configuration requires the least initial cost while the energy consumption in such configuration is high due to the need of overcooling and reheating processes to control the indoor temperature and relative humidity. The second configuration is recommended by some design guides because of its low-pressure drop characteristics and high energy efficiency (Hu & Tsao, 2007; PG&E, 2011). But such a configuration is not widely used due to the high initial cost and system complexity (e.g. the need for dual-temperature chillers and additional air aisle construction) and the inconvenience of maintenance. The combined use of an MAU together with AHUs (i.e. third configuration) is still the mainstream configuration in real applications (Li, Lee, & Jia, 2016; Shiue et al., 2011).

2.2 Existing ventilation strategies for cleanrooms and their limitations

2.2.1 Ventilation strategies under hot and humid outdoor conditions

In a particular working condition, the matching between sensible heat ratio (SHR) of the space and the SHR of the system (i.e. system capacity) depends on the ventilation strategy used. The existing typical ventilation strategies for space temperature and humidity controls, as well as their limitations are summarized in Table 2.1.

Table 2.1 Typical ventilation strategies under hot and humid outdoor conditions

Operational strategy	Mechanism	Description	Limitations
Interactive control (IC)	Cooling (or sub-cooling) and reheating processes are adopted to eliminate the coupling between temperature and humidity control loops.	Outdoor air is treated to be close to the indoor air enthalpy. Outdoor airflow is always set at the minimum.	Simultaneous cooling and reheating
Dedicated outdoor air ventilation (DV)	MAU handles all the latent heat and part of space sensible heat while the AHUs remove the rest of space sensible heat.	Outdoor air is treated below the indoor air dewpoint. Outdoor airflow can be set higher than the minimum.	High ventilation energy demand
Partially decoupled control (PD)	MAU handles all the latent heat and part of space sensible heat while the AHUs remove the rest of space sensible heat under low internal loads.	Outdoor air is treated below the indoor air dewpoint. Outdoor airflow is always set at the minimum.	Simultaneous cooling and reheating under high internal latent loads

Interactive control (IC) strategy: IC strategy (Cui, Watanabe, Ryu, Akashi, & Nishiyama, 1999; Jouhara, 2009; Yau, 2007), which is the most commonly used ventilation strategy in cleanrooms, employs cooling (or sub-cooling) and reheating processes to eliminate the coupling between temperature and humidity control loops. Figure 2.5(A) shows the air-handling process (state points shown in Figure 2.4) on the psychrometric chart adopting the IC strategy. The minimum required outdoor airflow is first introduced by the MAU with some temperature rise due to heat generation from the MAU fan motor (1→2). The MAU cools the outdoor air down to its apparatus dew point (2→3), which is near the indoor air enthalpy. The cooled outdoor air is then mixed with the recirculation air in the AHU (3→5, 4→5) before being handled by the AHU cooling coil (5→6) for space dehumidification and then reheated by the heater (6→7) if necessary. The supply air further gains heat from the AHU fan motor (7→9) and eventually reaches the supply air temperature set-point.

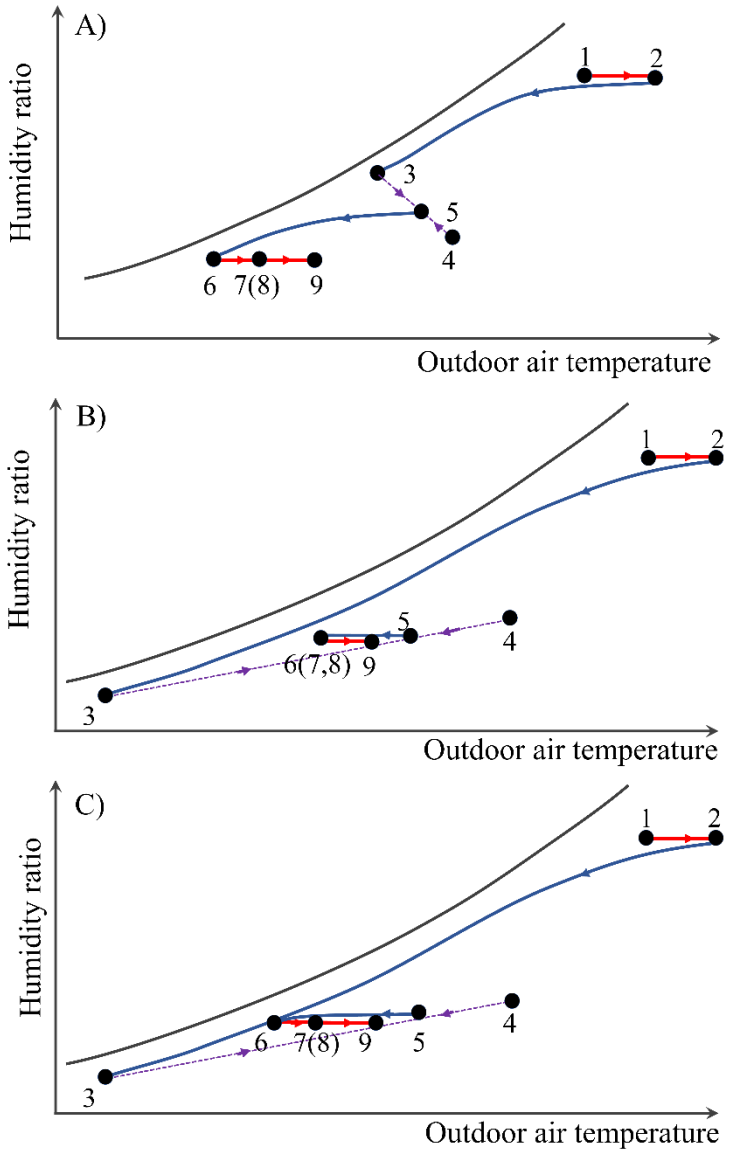

Figure 2.5 Psychrometric process of different ventilation strategies for hot and humid outdoor conditions *(A: IC strategy B: DV strategy or PD strategy under low internal latent loads C: PD strategy under high internal latent loads)*

Dedicated outdoor air ventilation (DV) strategy: DV strategy (Li et al., 2016; Tsao, Hu, Chan, Hsu, & Lee, 2008), also named "fully decoupled control strategy", fully decouples cooling and dehumidification by coordinated use of make-up air-handling units (MAUs) (or primary air-handling units, PAUs) and air-handling units (AHUs). For a system adopting this ventilation strategy, the MAU deals with all the latent load

and part of the space sensible load while the AHUs deal with the rest of space sensible load. As such, no sub-cooling and reheating is necessary to achieve the desired humidity control. However, to remove moisture produced by machines/processes/occupants, the necessary outdoor airflow rate may exceed, from time to time, the outdoor airflow rate required to maintain acceptable indoor air quality and/or positive pressure. Thus, a large MAU cooling capacity is usually required to meet the high cooling demand to handle outdoor air. The outdoor air treatment accounts for 30% to 65% of total air-conditioning energy consumption in the subtropics (Brown, 1990).

The air-handling process of the DV strategy is shown in Figure 2.5(B). The indoor relative humidity and dry-bulb temperature are controlled by the MAU and AHU respectively. Different from the IC strategy, the outdoor air is cooled below the dewpoint of the indoor air (2→3) and the MAU outlet air temperature set-point can be adjusted/reset according to the internal latent load. The MAU can induce higher outdoor airflow than its minimum requirement for the purpose of space dehumidification if the internal latent load is high. By adopting this strategy, no reheating is needed.

Partially-decoupled control (PD) strategy: PD strategy was proposed by Shan and Wang (2017) to overcome the drawbacks of the fully decoupled ventilation strategy (DV strategy). It decouples the dehumidification/cooling processes while working at the required minimum outdoor airflow. This strategy has been implemented in retrofitting a few existing conventional air-conditioning systems with significant energy savings. However, this strategy is only applicable to systems serving spaces with relatively low internal latent loads due to the fact that simultaneous cooling and reheating would occur when the internal latent load is high.

The mechanisms and air-handling processes of the PD strategy are elaborated in Figure 2.5 (B-C). Figure 2.5 (B) illustrates the air-handling process of the PD strategy when the internal latent load is relatively low. In this circumstance, since the outdoor air is dried effectively by the MAU which can handle all outdoor and indoor latent loads, there is no need to subcool and reheat the supply air in the AHU (State 6 and State 7 overlapping). When the internal latent load increases, the air-handling process is shown in Figure 2.5 (C), where the AHU only undertakes part of the latent load restricted by the use of fixed outdoor airflow set-point. To handle the rest of the latent load, the supply air needs to be cooled by the AHU cooling coil (5→6). The air is then reheated by the heater (6→7) (unless the indoor sensible load is high enough), which is similar to the air-handling process of the IC strategy.

The above review shows that each of the above existing strategies achieves good energy performance only in ambient and load conditions specifically favourable to that strategy. However, actual working conditions often deviate from design/ favourable conditions when adopting the existing ventilation strategies, resulting in significant energy waste. A ventilation strategy with high energy efficiency at different ambient and load conditions is essentially needed.

2.2.2 Ventilation strategies with economizer under cold or cool outdoor conditions

In cool or cold outdoor conditions, adopting an economizer system can be a superior option to reduce cooling energy use. An economizer system can save energy by strategically introducing outdoor air into occupied spaces based on the comparison of the outdoor and return air states (i.e. temperature, enthalpy, or humidity differences). Many studies have investigated the energy-saving potentials of the economizer in commercial and office buildings. Fasiuddin and Budaiwi (2011) found adopting

an enthalpy economizer in a shopping mall can achieve energy saving by 3% in Saudi Arabia. Yao and Wang (2010) evaluated potential energy conservation brought by different air-side economizers in office buildings, and the results indicate that energy savings by adopting the economizer are about 10-20% under hot climate zones and 5-10% under cold climate zones. Budaiwi (2001) obtained up to 13% energy savings by utilizing an economizer based on a dry-bulb temperature differential control in a nine-story office building under the hot-dry summer and cold winter climatic conditions. Son and Lee (2016) obtained around 10% energy savings by using a differential enthalpy control method in a three-story office building in Korea.

The above review shows that current economizer operation strategies are generally developed for buildings requiring thermal comfort control only, where the main purpose of utilizing the economizer is for energy conservation. For the buildings with spaces requiring strict temperature and humidity controls, the existing economizer operations are required to be improved, to meet the strict control requirements. For instance, during very dry outdoor conditions, the amount of outdoor air should be properly induced to ensure the indoor air humidity is not lower than its lower limit. Although several studies were carried out to demonstrate the potential energy benefits of utilizing the economizer in data centers (Cho, Lim, & Kim, 2012; Cho, Chang, Jung, & Yoon, 2017; Ham, Park, & Jeong, 2015; Lee & Chen, 2013; Shehabi, 2008), the economizer operation for other types of buildings, especially for the buildings/spaces with the high internal latent load, are still not fully investigated.

2.3 Optimal design of air-conditioning systems

2.3.1 Component design

ASHRAE handbooks (2016) summarized the design approaches for generic air-conditioning system equipment and components, such as fans, humidifiers, heaters, cooling/heating coils and heat recovery equipment. Some optimal design methods were also developed in an attempt to enhance the performance of temperature and humidity controls. Sekhar & Tan (2009) improved the dehumidifying performance of the oversized cooling coil by changing the effective surface area through simple manipulation of the effective number of rows of coil operation. Tsao et al. (2008) investigated the influence of fan location on the energy performance of a semiconductor cleanroom. The results show that a draw-through type MAU required less electrical power than a blow-off type MAU. Suzuki et al. (2000) found that 3% of electricity savings can be achieved by improving the heat transfer of cooling coils to remove fin condensation. Jo et al. (2017) employed a pressurized water atomizer in the humification system achieving more than 8% energy savings.

However, although the air-conditioning components may be well designed, a mismatch between system design and operation still widely exists because the coordination and interaction among these components/processes are not considered sufficiently. For example, a cleanroom facility site study (PG&E, 2011) has shown that the actual cooling load of the MAU in operation was only about one-fourth of its design value. Improper system design leading to control disorders and lower energy efficiency during operation is often observed and well-understood by engineers today.

2.3.2 Design optimization methods

Many design optimization methods/algorithms have been proposed to establish systematic design approaches for air-conditioning systems of general use. Wright (1996) employed a genetic algorithm to optimize the design parameters of components, including cooling coils, heating coils, fans and ducts. Hanby and Angelov (2000) adopted a gradient-based technique for plant design optimization. Bichiou and Krarti (2011) adopted three optimization algorithms, including a genetic algorithm, a particle swarm algorithm and a sequential search algorithm, to minimize life-cycle costs of air-conditioning systems. Lee et al. (2009) applied a particle swarm algorithm to minimize the life cycle cost of ice-storage air-conditioning systems and obtained the optimal capacity of the ice storage tank. Doodman et al. (2009) combined global sensitivity analysis and a harmony search algorithm for the design optimization of air-cooled heat exchangers. The results show that, compared with the genetic algorithm, the harmony search algorithm converged to optimum solutions with higher accuracy. Such approaches are effective and commonly adopted but not certainly produce an optimal system design due to the settings of deterministic design inputs/parameters. The actual energy performance of air-conditioning systems may often deviate significantly from their design expectations due to the fact that even well-selected data/information used as design inputs can be rather different from that in real operation. Such inherent deviations are regarded as “uncertainties”.

In conventional design practice, the capacities of the air-conditioning components for a building are determined under the design condition which is certain and presumed in a climate region (Lu, 2008). For the design of building air-conditioning systems, cooling load calculation considering uncertainties have been considered when conducting performance estimates or optimizing the design of building energy systems

(De Wit & Augenbroe, 2002). Accurate and reliable prediction of cooling/heating loads is very important for building energy system design (Huang, Huang, & Sun, 2018), and uncertainties in predicting cooling/heating loads have been studied widely to solve the under-sizing and over-sizing problems that widely exist in practical applications (Brohus, Frier, Heiselberg, & Haghighat, 2012; Hopfe, Augenbroe, & Hensen, 2013). Domínguez et al. (2010) quantified the uncertainties of building models and divided the input factors into three groups: certain factors, scenario elements, and uncertain factors. Sun et al. (2014) proposed a design method to size building energy systems considering uncertainties in weather conditions, building envelope and internal loads. There have also been a few studies on the design of central cooling plant design which considered the impacts of the cooling load uncertainties (Cheng, Wang, & Yan, 2016; Huang, Huang, Augenbroe, & Li, 2018) .

The above review shows that although design optimization approaches are available for air-conditioning systems of general use, comprehensive design methodology suitable for cleanroom systems is not yet available, especially for cleanroom air-conditioning system design considering inherent uncertainties in the design inputs and load diversities.

2.4 Optimal control of air-conditioning systems

Online supervisory control is important for achieving energy-efficient operation of air-conditioning systems in practical applications (Dounis & Caraiscos, 2009). Supervisory control, often named optimal control, seeks to minimize or maximize a real function by systematically choosing the values of variables within allowed ranges (Wang & Ma, 2008). The building automation system (BAS) allows HVAC systems

to operate effectively and efficiently through supervisory control, improving the building energy or cost-efficiency with superior performance.

Many studies have shown that supervisory control strategies greatly improve the indoor comfort and thermal environment while minimizing the energy input under dynamic working conditions (Wang & Ma, 2008). Nassif et al. (2005) used a two-objective genetic algorithm to formulate a model-based supervisory control strategy for heating, ventilating, and air-conditioning (HVAC) systems, achieving an energy saving of 16% over an existing conventional air-conditioning system. West et al. (2014) adopted an optimized supervisory model predictive control (MPC) for HVAC systems in commercial buildings. Average energy reductions of 19% and 32% were achieved in the two buildings, respectively. Ferreira et al. (2012) applied a neural-network-based predictive control strategy for HVAC real-time control in an educational building, achieving a satisfactory thermal comfort level and 50% energy savings. However, the existing supervisory control strategies are generally developed for buildings requiring thermal comfort control, implying that the system relies on temperature-based control to remove indoor moisture. Adding humidity as an objective complicates the task of control, necessitating a supervisory control strategy for optimizing the simultaneous control of space temperature and humidity.

Due to the complexity of air-conditioning systems with counteractant processes and dynamic working conditions, errors and uncertainties in the measurements can lead to improper choices of system control modes, resulting in huge energy waste. For example, it has been reported that the measurement uncertainties of outdoor airflow can lead to 17% waste in cooling energy use and 43% waste in heating energy use (Yan, Li, Malkawi, & Augenbroe, 2017). The uncertainty in the occupancy measurements, meanwhile, can cause an increase of 18% in the total energy

consumption (Goyal, Ingley, & Barooah, 2012). Several online fault-tolerant control strategies have been developed and applied in air conditioning systems (Yu, Woradechjumroen, & Yu, 2014) to enable the systems to operate at high efficiency and reliability in the presence of sensor faults/errors. Yang et al. (2014) developed a fault-tolerant supervisory control scheme by correcting the faulty measurements and reconstructing the controller inputs. Wang and Chen (2002) used neural network models to diagnose the measurement faults of airflow sensors, and realized the fault-tolerant control of outdoor airflow in the presence of sensor faults. Jin and Du (2006) proposed a fault-tolerant control method to regulate the outdoor airflow and adjust the air-handling unit (AHU) supply air temperature, based on principal component analysis, the joint angle method and compensatory reconstruction. The basic idea of these online fault-tolerant control strategies is to detect and identify the faults of the control systems, and then recover or correct the sensor measurements. However, due to the propagation and interaction of different measurement uncertainties in the control process, it is difficult to fix or remove the bias faults in cases with simultaneous multiple sensor biases. Simultaneous multiple sensor biases are a common issue in practical operation as the physical properties of sensors change over time. As a result, the measurement uncertainties significantly influence the proper selection of control modes.

The above review shows that no effective optimal control method can be found for the energy-efficient control of cleanroom air-conditioning systems subject to various ambient and internal load conditions, particularly to avoid unhealthy counteraction and interaction among components. The quantification methods of measurement uncertainties to support robust online optimization decisions (or online control) cannot be found in the HVAC field.

2.5 Summary

This chapter presented a comprehensive review on the existing studies on air-conditioning systems. The typical configurations and components of cleanroom air-conditioning systems were introduced briefly. The optimal design and control methods for air-conditioning systems of general use were presented. From the above review, the existing gaps can be summarized as follows:

i. Existing ventilation strategies can achieve good energy performance only in ambient and load conditions specifically favourable to that strategy. However, actual conditions are often unfavourable, resulting in significant energy waste. A ventilation strategy with high energy efficiency at different ambient and load conditions is essentially needed.

ii. Comprehensive optimal design methodology suitable for cleanrooms or spaces requiring strict humidity control is not yet available, especially when different sources of uncertainties are concerned. Effective design methods for multi-zone cleanroom air-conditioning systems cannot be found.

iii. The existing online control strategies are not suitable for the energy-efficient control of cleanroom air-conditioning systems subject to various ambient and internal load conditions. They particularly lack the ability to avoid unhealthy counteraction and interaction among components. The online control strategies considering component performance degradation and measurement uncertainties towards robust supervisory control for air-conditioning systems (including that for cleanrooms) needs to be developed.

CHAPTER 3 DEVELOPMENT OF AN ADAPTIVE FULL-RANGE DECOUPLED VENTILATION STRATEGY

This chapter presents the mechanism and main advantages of the proposed "adaptive full-range decoupled ventilation (ADV) strategy". The energy performance of the proposed ventilation strategy is evaluated under different ambient and internal load conditions and compared with the most updated strategies available. Section 3.1 presents and elaborates the typical configuration of cleanroom air-conditioning systems concerned. Section 3.2 presents and elaborates the mechanism and advantages of the proposed ADV strategy. Section 3.3 presents the energy models for the cleanroom air-conditioning systems. Energy performance maps of the ADV strategy under different ambient and internal load conditions are presented in Section 3.4. Conclusive remarks of this chapter are presented in Section 3.5.

3.1 Description of the systems concerned

The system configuration and air-conditioning components concerned, i.e. a blow-through type MAU and a draw-through AHU, serve for cleanrooms or spaces with strict temperature and humidity controls, as presented in Figure 2.4. This configuration is common in real applications, especially for hot and humid regions. Due to the high supply air flowrate requirements of cleanrooms to meet the air cleanliness, the peak cooling/heating demands can be met even under the lower limit of supply air flowrate (i.e. 20 ACH for the Class ISO 8 cleanrooms (ISO, 2015)). The cleanroom air-

conditioning systems of such configuration are usually designed as constant air volume (CAV) systems.

3.2 Mechanism and advantages of adaptive full-range decoupled ventilation strategy

To full use of the cooling/dehumidification capacity of outdoor air and avoid unnecessary reheating processes, a novel ADV strategy is developed. This strategy contains non-economizer operation modes (i.e. PD and DV modes) and economizer operation modes (i.e. FL, FS and FL modes) for different application situations. The mechanisms and descriptions of non-economizer and economizer operation modes of the ADV strategy are highlighted in Table 3.1. Due to the combination of the advantages of different operation modes, the ADV strategy can offer superior energy performance over the full range of internal load and ambient conditions. It avoids sub-cooling and reheating as far as beneficial via the best use of MAU and economizer for cooling and dehumidification.

Table 3.1 Mechanisms and descriptions of operation modes of ADV strategy

Operation mode		Mechanism	Description
Non-economizer operation mode	Dedicated outdoor air ventilation (DV)	MAU handles all latent heat and part of space sensible heat while the AHUs remove the rest of space sensible heat	Outdoor air is treated below the indoor air dewpoint. Outdoor airflow is adjusted according to the internal latent load
	Partially decoupled control (PD)	MAU handles all latent heat and part of space sensible heat while the AHUs remove the rest of space sensible heat under low internal load conditions	Outdoor air is treated below the indoor air dewpoint. Outdoor airflow is always set at the minimum
Economizer operation mode	Following sensible load (FS)	The indoor temperature is controlled by properly setting the outdoor airflow	Outdoor airflow is adjusted according to the internal sensible load
	Following latent load (FL)	The indoor relative humidity is controlled at the upper limit by properly setting the outdoor airflow	Outdoor airflow is adjusted to control the indoor relative humidity at the upper limit
	Lower-limit humidity control (LL)	The indoor relative humidity is controlled at the lower limit by properly setting the outdoor airflow	Outdoor airflow is adjusted to control the indoor relative humidity at the lower limit

3.2.1 Non-economizer operation mode

The air-handling processes of the DV and PD modes are identical to the DV and PD ventilation strategies as illustrated in Section 2.2.1. The required outdoor air intake for each mode is elaborated as follows.

Dedicated outdoor air ventilation (DV)

For the DV mode, the MAU cools and dehumidifies the outdoor airflow to handle all internal latent load and part of the internal sensible load, and the AHU removes the residual internal sensible heat. The outdoor air ratio of the DV mode is determined according to the internal latent load, which is allowed to be higher than the minimum requirements under high internal latent load conditions, as shown in Eq. 3.1, where α_{DV} is the outdoor air ratio when adopting the DV mode. Q_{lat} is the internal latent load

(W/m^2). $w_{MAU,min}$ is the minimum outlet humidity ratio determined by MAU lower-limit outlet temperature (kg/kg). h_{fg} (2501 kJ/kg) is the latent heat of vaporization.

$$\alpha_{DV} = min(max\left(\frac{Q_{lat}}{h_{fg}(w_4 - \min(w_2, w_{MAU,min})}, \alpha_{min}\right), 1) \quad (3.1)$$

Partially decoupled control (PD)

The system adopting the PD mode keeps the outdoor airflow rate at its lower limit, which is expressed as Eq. 3.2, where α_{PD} is the outdoor air ratio when adopting the PD mode.

$$\alpha_{PD} = \alpha_{min} \quad (3.2)$$

3.2.2 Economizer operation mode

A new "adaptive economizer" is incorporated into the proposed strategy, which considers the need for both temperature and humidity controls comprehensively during the cool and cold seasons. The adaptive economizer adopts three economizer control modes, named "following sensible load" (FS), "following latent load" (FL) and "lower-limit humidity control" (LL) as shown in Figure 3.1.

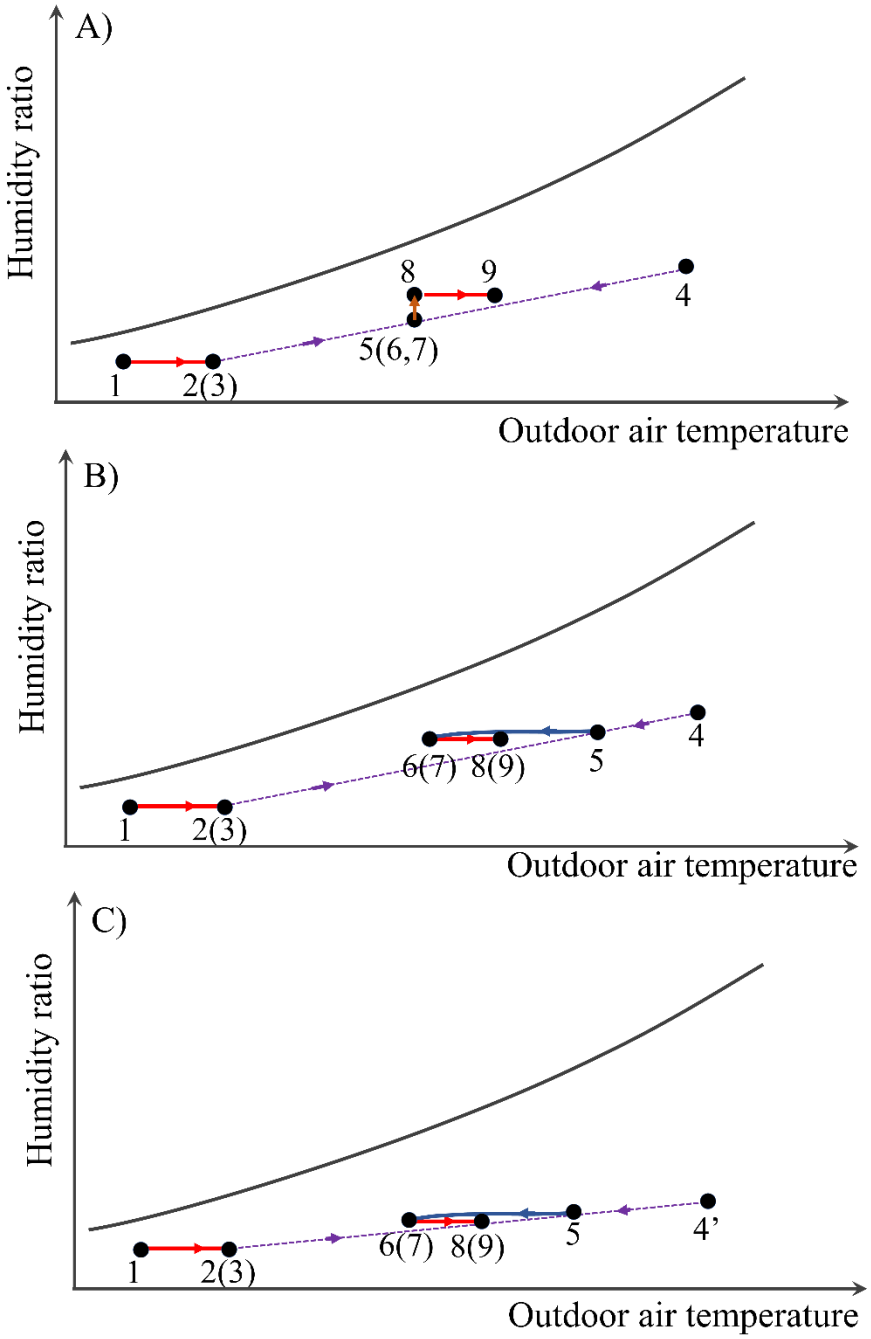

Figure 3.1 Psychrometric processes of economizer for cool/cold and dry outdoor conditions *(A. Free cooling; B. Free dehumidification; C. Lower-limit humidity control)*

Figure 3.1 (A) shows the air-handling process on the psychrometric chart adopting the FS mode. In this mode, the outdoor airflow is adjusted according to the internal sensible load and the humidification might be needed if the internal sensible load is

high (5→8). Figure 3.1 (B) shows the air-handling process on the psychrometric chart adopting the FL mode. In this mode, the latent heat is removed by adjusting the outdoor airflow rate, keeping indoor relative humidity at the upper limit, while the remaining sensible cooling load is handled by the AHU cooling coil (5→6). Figure 3.1 (C) shows the air-handling process on the psychrometric chart adopting the LL mode. Compared with the FL mode, the indoor relative humidity is always controlled at the lower limit (State 4'), so more outdoor air can be induced to remove the internal sensible heat.

The outdoor air ratios of different economizer modes are listed in Table 3.2. Here, α_{FS} is the outdoor air ratio of adopting the FS mode. α_{FL} is the outdoor air ratio of adopting the FL mode. α_{FL} is the outdoor air ratio of adopting the LL mode. w_4 *and* $w_{4'}$ are upper and lower limit settings of indoor humidity respectively (kg/kg). Q_{sen} is the internal sensible load (W/m^2). W_{sf} is the supply fan power (W). ε is the motor installation factor, which is used to indicate the motor location.

Table 3.2 Outdoor air ratios of different control modes of adaptive economizer

Control mode	Outdoor air ratio
Following sensible load	$\alpha_{FS} = min\left(max\left(\frac{Q_{sen}+\varepsilon W_{sf}}{c_p(t_4-t_2)}, \alpha_{min}\right), 1\right)$ (3.3)
Following latent load	$\alpha_{FL} = min\left(max\left(\frac{Q_{lat}}{(w_4-w_1)}, \alpha_{min}\right), 1\right)$ (3.4)
Lower-limit humidity control	$\alpha_{LL} = min\left(max\left(\frac{Q_{lat}}{(w_{4'}-w_1)}, \alpha_{min}\right), 1\right)$ (3.5)

In operation, the proposed ventilation strategy identifies the economic operation mode under the dynamic ambient and internal load conditions. Under hot and humid outdoor conditions, if "inducing more outdoor air" is identified to be the most economical way, the air-conditioning system will operate as the displayed way in Figure 2.5(B). This operation mode allows the outdoor airflow to exceed the minimum outdoor airflow

rate required for maintaining an acceptable indoor air quality or space positive pressure in a space. Otherwise, the air-handling will follow the process shown in Figure 2.5 (C) using the minimum outdoor airflow rate. In the cool/cold and dry outdoor conditions, the proposed ventilation strategy will choose the economizer operation modes which have the best energy performance.

The procedure and steps of selecting the optimal mode using the ADV strategy are illustrated in Figure 3.2. At each time step, the design indoor condition, outdoor condition, internal sensible and latent load, etc., are measured directly or computed based on measurements. The required supply air state including the temperature and humidity can then be determined. By considering the outdoor condition (air temperature and humidity) and required supply air state, the required outdoor air ratios of different operation modes (i.e. PD, DV and economizer modes) can be obtained using Eqs. 3.1-3.5. The feasibilities of utilizing particular operation modes are therefore assessed by verifying whether the required outdoor air ratio is within the required range (i.e. lower than 1). The electrical loads of the feasible operation modes can thus be calculated according to their corresponding working principles using Eqs. (3.6-3.7, 3.11-3.16). The ADV strategy will eventually select the operation mode with the minimum electrical load.

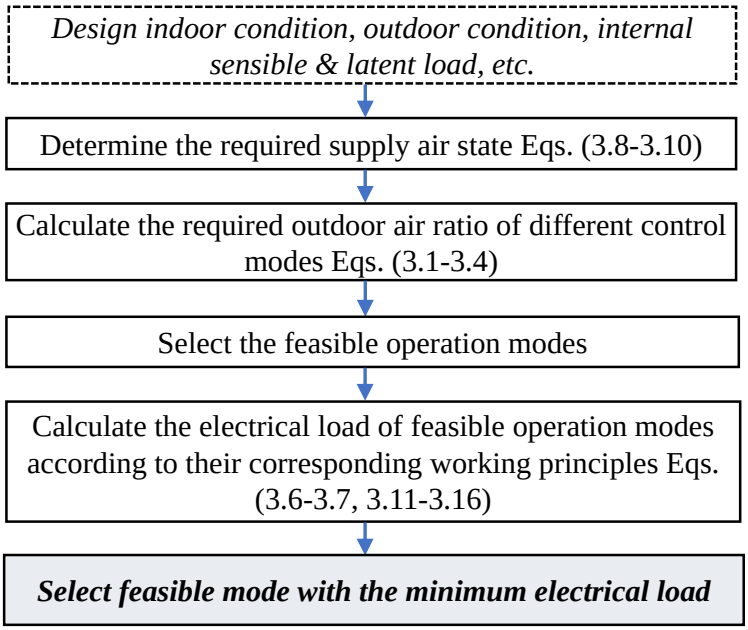

Figure 3.2 Proceduce and steps of selecting optimal operation mode by ADV strategy

3.3 Component and system models

The total electrical load of the air-side components is calculated using Eq. 3.6, which includes the electrical load of the MAU/AHU cooling coils, the AHU heater and humidifier, the make-up air fan and the supply air fan.

$$E_{tot} = \frac{Q_{cc,MAU}+Q_{cc,AHU}}{COP_c} + \frac{Q_{he,AHU}}{COP_{he}} + \frac{Q_{hu,AHU}}{COP_{hu}} + W_{mf} + W_{sf} \quad (3.6)$$

where, COP_c is the overall coefficient of performance of the cooling system. COP_{he} is the overall coefficient of performance of the heating system. COP_{hu} is the overall coefficient of performance of the humidification system. $Q_{cc,MAU}$ is the cooling coil cooling load of the make-up air-handling unit (kW). $Q_{cc,AHU}$ is the cooling coil cooling load of the supply air-handling unit (kW). $Q_{he,AHU}$ is the heater heating load of the supply air-handling unit (kW). $Q_{hu,AHU}$ is the humidification load of the supply air-handling unit (kW). W_{mf} is the fan power of the make-up air-handling unit (kW). W_{sf} is the fan power of the supply air-handling unit (kW).

The energy models of the subsystems are described as follows.

3.3.1 Fan model

The fan powers of MAU/AHU fans are characterized by their volumetric flow rate, pressure rise and efficiency, as shown in Eq. 3.7, where W_f is total fan power (kW). V is air volumetric flow rate (m^3/s). Δp is total pressure rise (kPa). η_f is fan efficiency.

$$W_f = \frac{V\Delta p}{\eta_f} \tag{3.7}$$

3.3.2 System energy balance model

The thermodynamic states of the system are determined by heat balance Eqs. 3.8-3.15 with the following main assumptions: *i*) The pressure drops through the ducts are constant and the air heat loss through the duct is neglected. *ii*) The minimum outlet temperatures of both MAU and AHU are set at 13 °C, a setting typically used in practice (Wang & Song, 2012), which are the lower limit of AHU and MAU outlet temperatures in design calculation when dehumidification requirements are concerned. *iii*) The saturated relative humidity is set at 95% when the processed air reaches the apparatus dew point. *iv*) The air is perfectly mixed inside all ducts and the thermal space. *v*) The ducts are well-sealed without air leakage. *vi*) The air states at the outlets of MAU and AHU vary simultaneously with the instantaneous sensible and latent cooling demands. *vii*) The overall coefficient of performance of the cooling system (COP_c), heating system (electric heater) (COP_h) and humidification system (electric humidifier) (COP_{hu}) are assumed to be 2.5, 1.0 and 1.0 respectively as constants.

After determining the air states for each ventilation strategy (Figure 2.5), the cooling/heating loads for the cooling coils/heater can be estimated using Eqs. 3.13-3.15, where m_s is the supply air mass flow rate (kg/s). h is the enthalpy of air (kJ/kg). The fan motor installation factor ε is used to indicate the motor location. It equals 1.0

if the fan motors are installed inside the MAU/AHU, and it equals the motor efficiency if motors are installed outside the MAU/AHU. The fan motor installation factor η equals 1 in the case study.

$$Q_{sen} = m_s c_p (t_4 - t_9) \tag{3.8}$$

$$Q_{lat} = Q_{sen}(\frac{1\text{-}SHR}{SHR}) \tag{3.9}$$

$$Q_{lat} = m_s h_{fg} (w_4 - w_9) \tag{3.10}$$

$$w_5 = \alpha w_3 + (1 - \alpha) w_4 \tag{3.11}$$

$$t_8 = t_4 - \frac{1}{m_s c_p}(Q_{sen} + \varepsilon W_{sf}) \tag{3.12}$$

$$Q_{cc,AHU} = (m_s - \alpha m_s) h_4 + \alpha m_s h_3 - m_s h_6 \tag{3.13}$$

$$Q_{he,AHU} = m_s (h_7 - h_6) - \varepsilon W_{sf} \tag{3.14}$$

$$Q_{cc,MAU} = \alpha m_s (h_1 - h_3) + \varepsilon W_{mf} \tag{3.15}$$

During the transient seasons and winter, when the outside air is dry, the humidifier may be activated to avoid too low space humidity (i.e. lower than its lower limits). The humidification load of the humidifier is shown in Eq. 3.16.

$$Q_{hu,AHU=} m_s h_{fg} (w_8 - w_7) \tag{3.16}$$

3.4 Energy performance of adaptive full-range decoupled ventilation strategy and comparison with existing strategies

3.4.1 Test building and design conditions

A pharmaceutical factory building located in Tai Po district of Hong Kong was selected for the comparison study. It has five floors and the total cleanroom area is about 3,620 m^2. All the production areas were designed as Class ISO 8 cleanrooms (ISO, 2015). The configuration of a typical cleanroom air-conditioning system, i.e. the system serving part of the cleanrooms at the 2nd floor, is shown in Figure 2.4. A typical

air-conditioning system of the cleanrooms consists of the axial fans, chilled water-cooling coils, an electric heater, an electric steam humidifier and other accessories.

For the cleanrooms concerned, the minimum total supply and outdoor airflow rates were designed as 20 ACH and 2 ACH respectively to meet the requirements of indoor cleanliness and pressurization (ASHRAE, 2007; ASHRAE 62.1, 2016; ISO, 2015). The cleanroom air-conditioning systems usually adopt constant air volume (CAV) systems in practice. The height of the cleanrooms concerned is 2.8 m. The design room conditions, fan specification and control requirements are summarized in Table 3.3.

Table 3.3 Design room conditions, fan specification, and control requirements

Description	Parameter	Value
Indoor design conditions	Temperature (°C)	20±3
	RH (%)	55±10
Outdoor and supply airflow rate	Outdoor air changes per hour	≥2
	Supply air changes per hour	≥20
Installed fan specification	MAU fan pressure (Pa)	1,600
	AHU fan pressure (Pa)	1,350
	Fan efficiency (%)	60

In order to compare the energy performance of the cleanroom air-conditioning system of utilizing the proposed ADV strategy, three existing ventilation strategies (i.e. IC, DV and PD) were selected for comparison purposes. The working principles of three existing ventilation strategies are presented in Section 2.2.1. It is worth noticing that an enthalpy-based economizer was incorporated into the IC strategy. The economizer is activated according to the enthalpy differential between outdoor air and indoor air. If the outdoor air enthalpy is higher than indoor air enthalpy, the minimum outdoor airflow would be set. Otherwise, the outdoor airflow would be adjusted according to

the AHU cooling coil outlet temperature, and the MAU cooling coil value would be closed.

3.4.2 Energy performance under different internal load conditions

The system performance maps for the IC, DV, PD and ADV strategies are presented in Figure 3.3(A)-(D), which represents the situation at Hong Kong outdoor design condition where no economizer control is adopted. As recommended by ASHRAE fundamentals 14.6 (ASHRAE, 2013), the dew-point temperature corresponding to 1% annual cumulative frequency of occurrence (ASHRAE 1% DP-MCDB) was used as the outdoor design condition (i.e. 29.1 °C, 84.4%) when space dehumidification was the duty of the outdoor air ventilation system (i.e. make-up air-handling units). The total electrical load (Eq. 3.7) of each strategy was calculated under 6,147,072 working points/conditions (3,072×2,001), with an interval of 0.05 W/m^2 and 5×10^{-4} in terms of space sensible cooling load (Q_{sen}) and sensible heat ratio (SHR), respectively. Here, the total electrical load is the sum of the electrical loads of the cooling coils, the heater, the humidifier (if needed) and fans as calculated by Eqs. 3.8-3.16. It is worth noticing that although the selected outdoor condition is hot and humid without involving the economizer, the induced outdoor air flowrates of different ventilation strategies were still different and the outdoor air flowrates of some ventilation strategies may exceed the lower limits of their set-points. This is due to different MAU dehumidification requirements of different strategies. For the IC and PD strategies, the outdoor air flowrate was set at the lower limit as a constant value (i.e. 2 ACH or outdoor air ratio 0.1 in the case study). For the DV and ADV strategies, the outdoor air flowrate was adjusted according to the internal latent load, allowing the amount of outdoor air higher than the lower limit to remove moisture under relatively high internal latent load conditions, as shown in Figure 3.4(A) and (B), respectively.

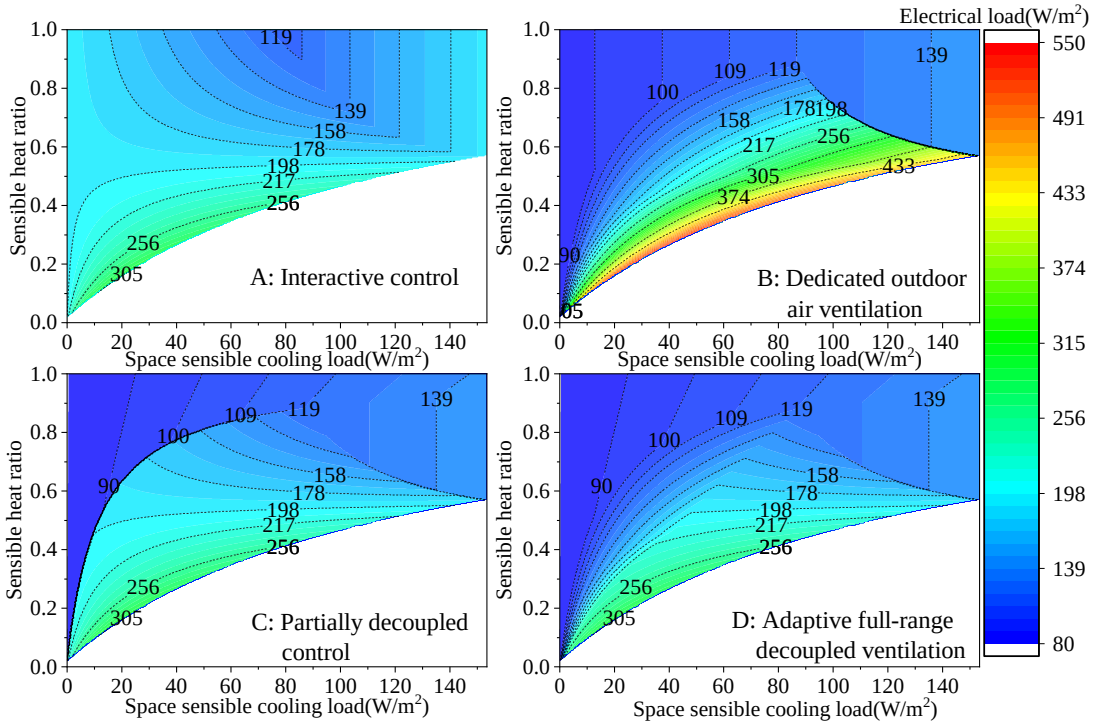

Figure 3.3 Space air-conditioning energy maps of four ventilation strategies under Hong Kong design outdoor condition *(A: Interactive control; B: Dedicated outdoor air ventilation; C: Partially decoupled control; D: Adaptive full-range decoupled ventilation)*

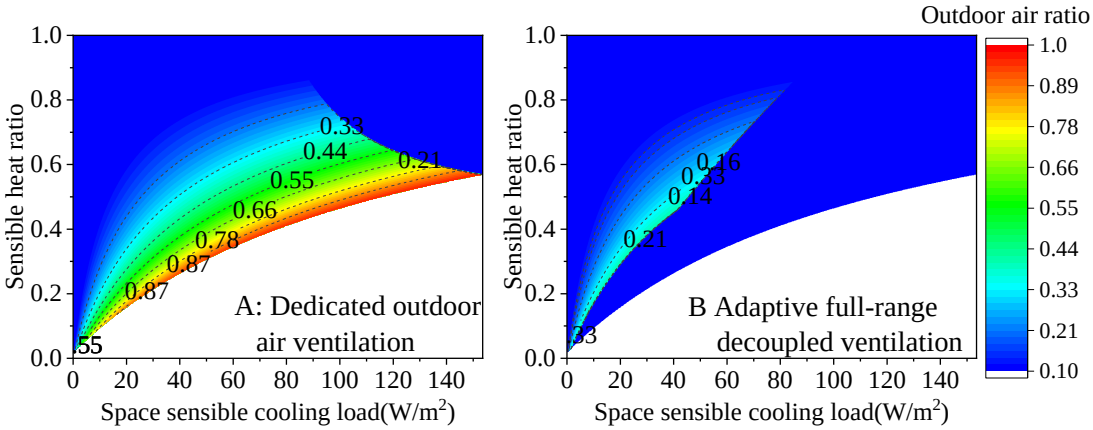

Figure 3.4 Outdoor air ratio of two ventilation strategies under Hong Kong design outdoor condition *(A: Dedicated outdoor air ventilation; B: Adaptive full-range decoupled ventilation)*

By comparing the energy performance of the existing and proposed strategies under different internal load regions, the preferred ventilation strategies (i.e. most energy-efficient strategy) in different regions are shown in Figure 3.5. Here, blue dot lines are

the contour lines of energy-saving ratio. The energy-saving ratio of the proposed ADV strategy ranged up to 59.2% compared with that of the least energy-efficient strategy. In Region 1, the proposed ADV strategy, as well as the PD and DV strategies, had superior energy performance compared with the IC strategy, where the space had a comparatively high sensible heat ratio. In Region 2, the proposed ADV strategy and the DV strategy had superior energy performance compared with the other two strategies, where the space had a medium sensible heat ratio. In Region 3, the proposed ADV strategy, as well as the IC and PD strategies, were the superior options, where the space had a low sensible heat ratio.

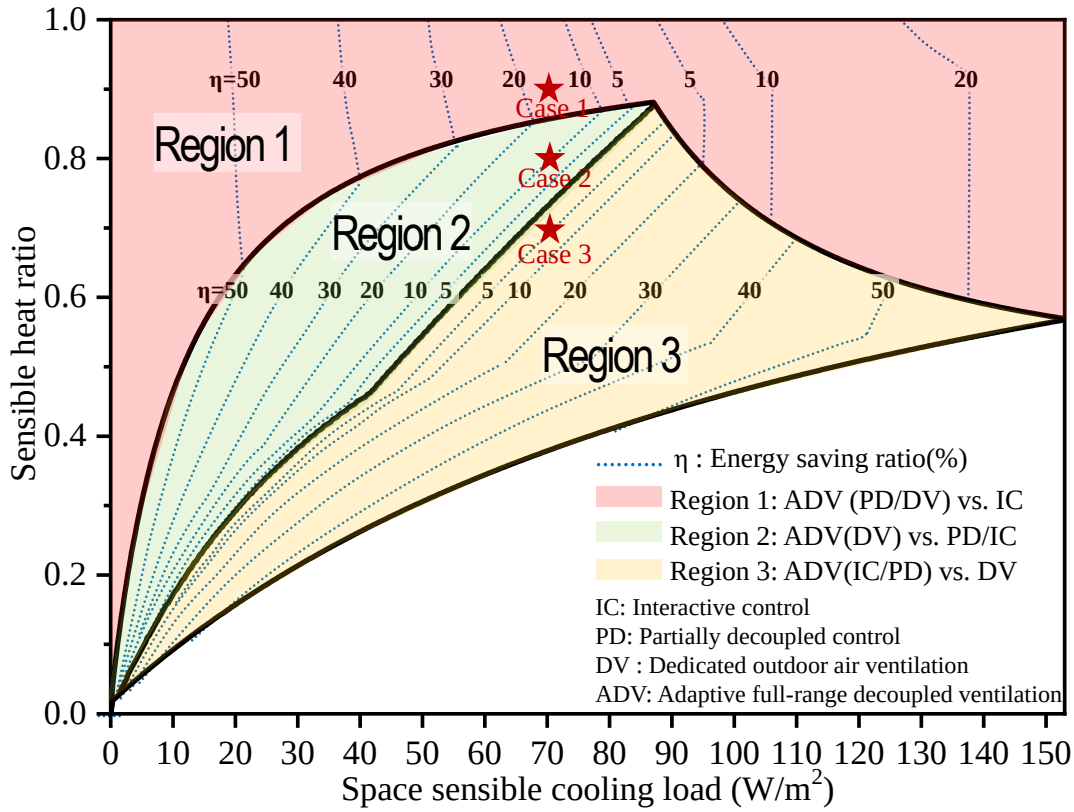

Figure 3.5 Preferred ventilation modes/strategies and their energy-saving ratio in different internal load regions under the Hong Kong design outdoor condition

It can be summarized that although the energy performance of some existing ventilation strategies was as good as that of the proposed strategy in some of the three

regions, the proposed strategy was always the superior strategy in all regions or working conditions concerned. Table 3.4 shows the preferred ventilation strategies in different regions of working conditions according to the energy performance comparison results. It can be seen that the proposed ventilation strategy offered superior energy-efficiency over the full range of internal loads under the Hong Kong outdoor design condition.

Table 3.4 Superior ventilation strategies in different internal load regions under the Hong Kong outdoor design condition

Strategy	Region 1	Region 2	Region 3
ADV	√	√	√
IC			√
PD	√		√
DV		√	

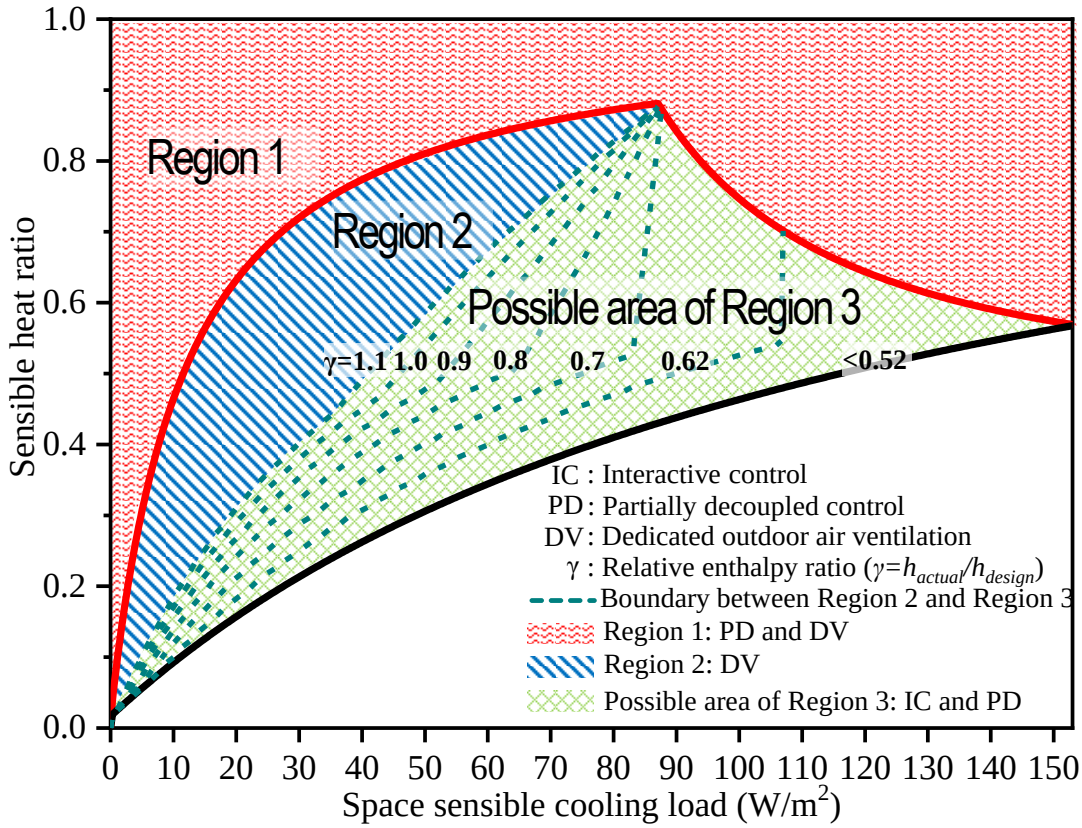

Figure 3.6 Boundary changes of preferred ventilation modes/strategies of ADV strategy in different internal load regions under different outdoor conditions

The preferred ventilation modes of the ADV strategy in different internal load regions under the Hong Kong outdoor design condition are presented in Figure 3.5. However, it is also worth noticing that the boundary for selecting superior ventilation mode is affected significantly by the ambient conditions. As mentioned in Section 3.2, the proposed ADV strategy consists of three operation modes in hot and humid outdoor conditions and it operates at its most economical mode at a particular state. To illustrate how the most economical mode is affected by different indoor and outdoor conditions, further analysis was therefore conducted. Figure 3.6 presents the boundary of preferred ventilation strategies in different internal load regions, which moves when the outdoor condition varies. This map was made under the condition when the absolute humidity of the outdoor air was no less than that of the indoor air or the economizer is not applicable. Similar to Figure 3.5, in Region 1, the PD and DV

modes/strategies were the preferred modes, i.e., better than the IC mode/strategy. In Region 2, the DV mode/strategy was the preferred mode, i.e., better than the IC and PD modes/strategies. In Region 3, the IC and PD modes/strategies were the preferred options. The key difference between Figure 3.6 and Figure 3.5 was that, in Figure 3.6, the boundary between Region 2 and Region 3 moved when outdoor enthalpy changed. When the enthalpy of outdoor air reduced, this boundary line moved down and the area of Region 2 increased. Here, relative enthalpy ratio (γ) of the outdoor air is defined as the ratio of its actual enthalpy (h_{actual}) to that of the air at the outdoor design condition (h_{design}) (29.1 °C, 84.4%), as shown in Eq. 3.17. When the relative enthalpy ratio of the outdoor air was 0.62, which was equal to the enthalpy of the indoor design condition (23 °C, 65%), the area where the DV mode/strategy was the preferred mode covered most of the possible working conditions as indicated by 88.4% of the total operation area in the figure. It is worth noticing that, when the relative enthalpy ratio of the outdoor air decreased to 0.52 or below (equivalent to that at (19.2 °C, 70%) or (17.3 °C, 85%)), the DV mode/strategy was the preferred mode for all possible working conditions if no economizer was adopted and the Region 3 disappeared practically.

$$\gamma = \frac{h_{actual}}{h_{design}} \tag{3.17}$$

3.4.3 Energy performance under different outdoor conditions

Figure 3.7 (A)-(D) present the system performance maps for the IC, DV, PD strategies and the proposed ADV strategy at a given typical internal load condition (Qs=90 W/m^2, SHR=0.8). The total electrical load (Eq. 3.6) of each strategy was calculated under 1,806,301 working points/conditions (6,001×301), with an interval of 0.01 °C and 1×10^{-4} in terms of outdoor air temperature and humidity ratio, respectively.

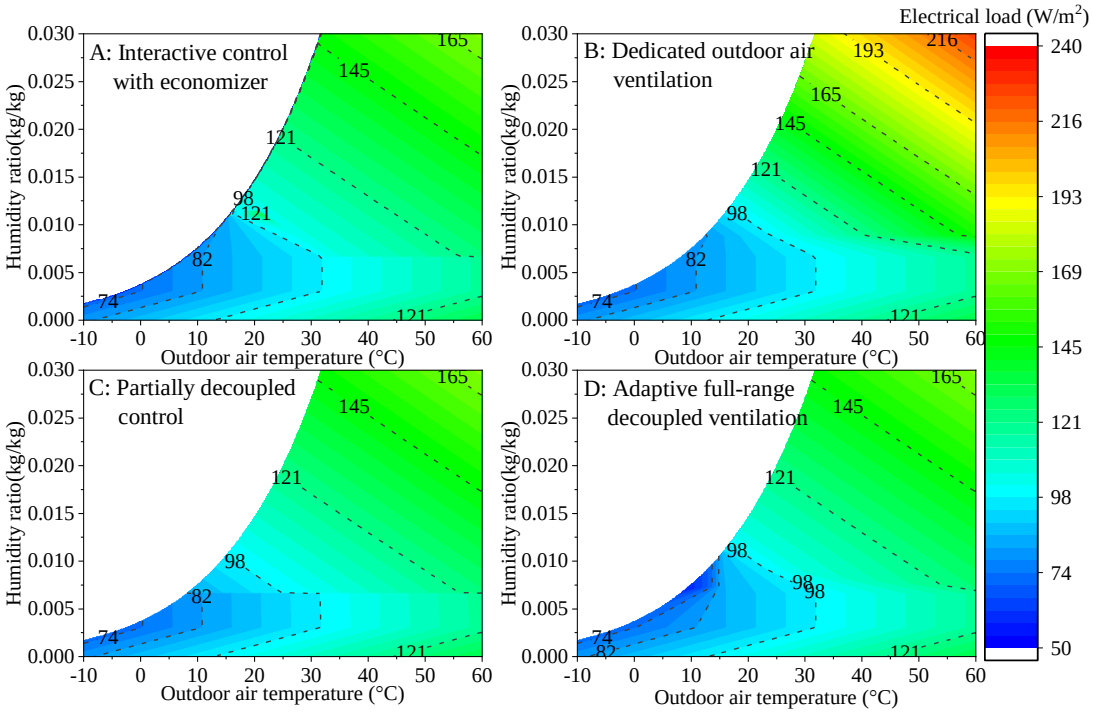

Figure 3.7 Space air-conditioning energy maps of four ventilation strategies under a typical internal load condition (Qs=90 W/m^2, SHR=0.8) *(A: Interactive control with economizer; B: Dedicated outdoor air ventilation; C: Partially decoupled control; D: Adaptive full-range decoupled ventilation)*

An adaptive economizer, which involves three economizer operation modes, marked as “following sensible load” (FS), “following latent load” (FL) and “lower-limit humidity control” (LL), was investigated and adopted by the proposed ADV strategy. Figure 3.8(A) shows the applicable outdoor condition regions for activating the adaptive economizer. The adaptive economizer was not applicable in Regions 1-3 since the enthalpy of outdoor air was comparatively high (i.e. Region 1 and 2) or the minimum outdoor airflow was enough for “free dehumidification” (i.e. Region 3). By contrast, the adaptive economizer was beneficial and more energy-efficient in Regions 4-6 compared with that of the ventilation strategy without the economizer. The preferred economizer modes in different outdoor condition regions are shown in Figure 3.8(B), which is actually the enlarged figure of Regions 4-6 in Figure 3.8(A). The energy-saving ratio of the proposed ADV strategy adopting the adaptive

economizer ranged up to 27.4% compared with that of the ADV strategy without adopting an economizer. In Region 4, the proposed ADV strategy adopting the FL mode had the superior energy performance, where the outdoor airflow rate was adjusted to control the indoor humidity at its upper limit. In Region 5, the proposed ADV strategy adopting the FS mode had the superior energy performance, where the outdoor airflow rate was adjusted to control the indoor temperature while the indoor humidity varied in an allowable range. In Region 6, the proposed ADV strategy adopting the LL mode was the superior option, where the outdoor airflow rate was adjusted to control the indoor humidity to its lower limit.

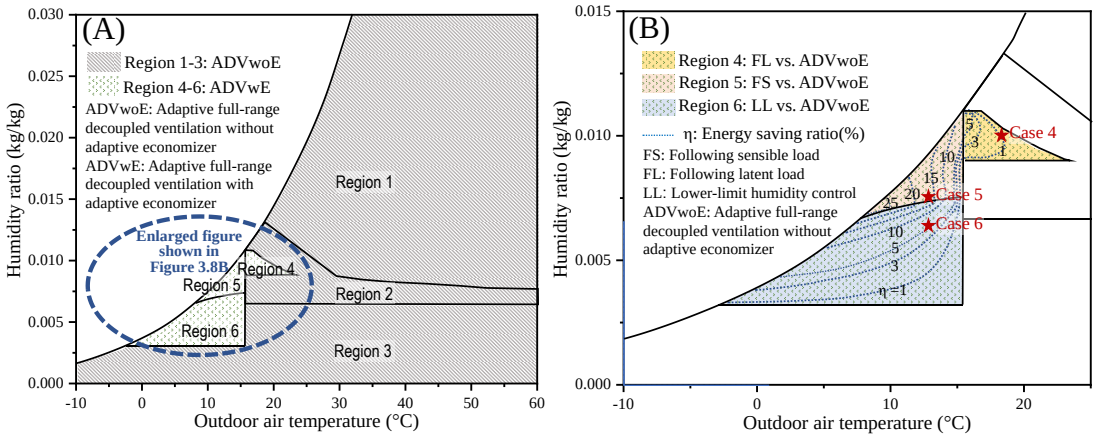

Figure 3.8 Applicable outdoor condition regions for adaptive economizer and preferred economizer modes at a typical internal load condition (Qs=90 W/m^2, SHR=0.8)

Table 3.5 shows the preferred ventilation strategies in different regions of ambient conditions according to the energy performance comparison results. It can be seen that the proposed ventilation strategy offered superior energy-efficiency over the full range of ambient conditions under a typical internal load condition (Qs=90 W/m^2, SHR=0.8). In Region 1, the proposed ADV strategy, as well as the IC and PD strategies, were the most energy-efficient compared with the DV strategy, where the outdoor air had high enthalpy. In Region 2, the proposed ADV strategy and the DV strategy had superior

energy performance compared with the other two strategies, where the outdoor air enthalpy was not high. In Region 3, all the ventilation strategies had the same energy performance, where the minimum outdoor airflow was enough for "free dehumidification" since the outdoor air was extremely dry. In Region 4, the proposed ADV strategy and the IC strategy offered superior energy performance compared with the other two strategies due to the adoption of the economizer. In Regions 5-6, the proposed ADV strategy was the superior option since it adopted the adaptive economizer and made full use of the "free cooling and dehumidification" capacity of the outdoor air.

Table 3.5 Superior ventilation strategies under different ambient conditions and the typical internal load condition

Strategy	Region 1	Region 2	Region 3	Region 4	Region 5	Region 6
ADV	**√**	**√**	**√**	**√**	**√**	**√**
IC	√		√	√		
PD	√		√			
DV		√	√			

3.4.4 Limitations of existing strategies and benefits of proposed strategy

To justify the limitations of the existing ventilation strategies and the benefits of the proposed strategy, six typical and representative cases were selected to assess and compare the energy performance of the proposed and the existing most-updated ventilation strategies, as shown in Table 3.6. It is worth noticing that, in this table, the electrical loads of the MAU/AHU cooling coils, AHU heater and AHU humidifier were their cooling/heating loads (Eqs. 3.13-3.16) divided by the cooling/heating COPs respectively (i.e. 2.5/1.0 in this case study). The powers of MAU/AHU fans were calculated using Eq. 3.7.

The energy performance of different ventilation strategies under different internal load conditions was assessed in Case 1-3 (marked in Figure 3.5), where their performance under low/medium/high internal latent load conditions was compared. Similarly, the energy performance of different ventilation strategies under different outdoor conditions was assessed in Case 4-6 (marked in Figure 3.8B), where the space sensible cooling load (Q_{sen}) and sensible heat ratio (SHR) in three cases were set the same.

Case 1 represents the condition when indoor had a relatively low latent load, where all the latent gains can be removed by the MAU with the minimum outdoor airflow. The electrical load of the IC strategy was the largest, which was 16.3% more than that of the proposed ADV strategy as well as the PD and DV strategies, due to the sub-cooling and reheating process for removing the latent gains. Case 2 represents the condition when indoor had a medium latent load, where only part of the latent gains can be removed by the MAU with the minimum outdoor airflow using the PD strategy and therefore the reheating occurred. The electrical loads of the IC strategy and the PD strategy were the same, which were 10.6% more than that of the proposed ADV strategy and the DV strategy. Case 3 represents the condition when indoor had a high latent load. The DV strategy had a higher electrical load compared with the proposed ADV strategy as well as the IC and PD strategies since the amount of the AHU electrical load decrease overtook that of increased the MAU electrical load due to excessive high-enthalpy outdoor airflow. Case 4 represents the condition when the outdoor air was cool and dry. The FS strategy had the highest electrical load, which was 12.6% more than that of the most energy-efficient strategy (the proposed ADV strategy adopting the FL mode or the IC strategy), due to the excessive outdoor air intake. In this case, the electrical loads of the PD and DV strategies were also 6.1% and 1.1% more than that of the proposed ADV strategy respectively, since these two

strategies cannot make full use of the “free dehumidification” capacity of the outdoor air. Case 5 represents the condition when the outdoor air was cold and dry. The energy electrical loads of the PD and LL strategies were 21.7% and 20.0% more than that of the proposed ADV strategy (adopting the FS mode) respectively, due to the activation of heating processes. In addition, the electrical loads of the DV, IC and FL strategies were 15.3% more than that of the proposed ADV strategy (adopting the FS mode), since these three strategies cannot make full use of the “free cooling” capacity of the outdoor air. Case 6 represents the condition when the outdoor air was cold and extremely dry. The FS strategy had the highest electrical load, which was 22.5% more than that of the proposed ADV strategy (adopting the LL mode) since the humidification needed to be activated due to the excessive dry outdoor air intake. In this case, the electrical loads of the PD and DV strategies were also 5.3% more than that of the proposed ADV strategy (adopting the LL mode), since these two strategies cannot make full use of the “free cooling and dehumidification” capacity of the outdoor air.

Table 3.6 Electrical loads of studied cases under different internal load and ambient conditions

Case	Internal load		Outdoor condition		Ventilation strategy	Outdoor air ratio	Electrical load/ power (W/m^2)						
	Q_{sen} (W/m^2)	SHR	Temperature (°C)	RH (%)			MAU cooling	MAU fan	AHU cooling	AHU heating	AHU humidifier	AHU fan	Total
1	70	0.9	29.1	84.4	IC	0.1	25.90	4.16	52.04	14.70	0.00	35.03	131.84
					ADV/PD/DV	0.1	35.61	4.16	35.57	0.00	0.00	35.03	**110.37**
2	70	0.8			IC	0.1	25.90	4.16	58.18	20.11	0.00	35.03	143.38
					PD	0.1	38.44	4.16	45.64	20.11	0.00	35.03	143.38
					ADV/DV	0.146	56.04	6.05	31.01	0.00	0.00	35.03	**128.13**
3	70	0.7			DV	0.25	96.11	10.38	23.16	0.00	0.00	35.03	164.67
					PD	0.1	38.44	4.16	53.60	27.24	0.00	35.03	158.48
					ADV(FL)/IC	0.1	25.90	4.16	66.14	27.24	0.00	35.03	**158.48**
4	90	0.8	18	78	FS	1	0.00	41.46	28.89	0.00	0.00	35.03	105.37
					PD	0.1	7.74	4.16	48.82	2.97	0.00	35.03	98.72
					DV	0.187	14.51	7.78	35.87	0.00	0.00	35.03	93.19
					ADV(FL)/IC	0.272	0.00	14.49	42.64	0.00	0.00	35.03	**92.15**
5			13	80	PD	0.1	1.66	4.16	45.95	2.97	0.00	35.03	89.77
					LL	0.937	0.00	38.86	0.00	12.81	0.00	35.03	86.70

Case	Internal load		Outdoor condition		Ventilation strategy	Outdoor air ratio	Electrical load/ power (W/m^2)						
	Q_{sen} (W/m^2)	SHR	Temperature (°C)	RH (%)			MAU cooling	MAU fan	AHU cooling	AHU heating	AHU humidifier	AHU fan	Total
6			13	70	IC/FL	0.118	0.00	4.86	43.05	0.00	0.00	35.03	82.94
					DV	0.118	1.95	4.86	41.10	0.00	0.00	35.03	82.94
					ADV(FS)	0.85	0.00	35.24	0.00	0.00	0.00	35.03	**70.27**
					FS	0.85	0.00	35.24	0.00	0.00	31.57	35.03	101.84
					IC/FL	0.1	0.00	4.16	44.11	0.00	0.00	35.03	83.30
					PD/DV	0.1	1.66	4.16	42.44	0.00	0.00	35.03	83.30
					ADV(LL)	0.353	0.00	14.65	29.21	0.00	0.00	35.03	**78.89**

By comparing the energy performance of six typical working conditions (Cases 1-6), it can be concluded that each of the existing ventilation strategies has its limitations under certain internal load or ambient conditions. The proposed ADV strategy, having incorporated the advantages of different ventilation strategies and an adaptive economizer, could offer the superior energy performance in all cases by setting optimal outdoor airflow and activating the most energy-efficient operation mode of the adaptive economizer.

3.5 Summary

An “adaptive full-range decoupled ventilation strategy” (ADV) was developed to enhance the energy performance of cleanroom air-conditioning systems over the full range of internal load and ambient conditions. The mechanism, main advantages and energy performance of the proposed ADV strategy were studied and compared with the other three existing strategies based on the cleanroom air-conditioning systems of a pharmaceutical manufacturing building located in Hong Kong. The following conclusions can be made:

i. Compared with the existing ventilation strategies, the proposed strategy has superior energy performance over the full range of internal load and ambient conditions.
ii. Under hot and humid outdoor conditions, while the economizer is not activated, the proposed strategy can minimize system energy consumption by avoiding sub-cooling and reheating as far as beneficial via the best use of MAU for dehumidification.

iii. Under dry and cool outdoor conditions, while the economizer is activated, the proposed strategy can optimize the outdoor air intake by the full use of the outdoor air “free cooling” and “free dehumidification” capacities.

CHAPTER 4 PERFORMANCE EVALUATION AND APPLICATIONS OF PROPOSED STRATEGY IN DIFFERENT CLIMATE ZONES

Although the proposed "adaptive full-range decoupled ventilation (ADV) strategy" shows superior energy performance, the successful and full applications of the ADV strategy in practical applications are still facing the following questions: *i)* actual energy performance in different climates; *ii)* the new design and the needs of modifications in retrofitting existing systems and their cost-benefits; and *iii)* proper selection of the optimal alternatives from various operation modes in different climatic conditions.

These questions are addressed by annual energy simulation tests with following tasks: *i)* evaluation of the energy and economic performance when implementing the ADV strategy in different climate zones, *ii)* investigation of the air-conditioning system design and the needs for existing system retrofitting, and *iii)* identification of the most suitable operation modes of the proposed ADV strategy when implemented in different climatic conditions. This chapter is organized as follows. Section 4.1 introduces the test locations in typical climate zones and design conditions. Section 4.2 presents the annual energy saving potential and the preferable operation modes of the ADV strategy in different climatic conditions. Required air-conditioning system design and cost-benefit are evaluated and analysed in Section 4.3. The results of the tests and investigation are presented in Section 4.4.

4.1 Selection of test locations in typical climate zones and design conditions

4.1.1 Selection of test locations

Due to the large land area across a wide range of latitudes and complexities of topography, the climates are of large diversities in China (He, Yang, & Ye, 2014). In terms of the thermal design of buildings, a major climate classification is developed to distinct climatic features (MOHURD, 1993). The five major climate zones of this classification are as follows: severe cold, cold, hot summer and cold winter, temperate as well as hot summer and warm winter. Figure 4.1 shows the overall layout of the five major climate zones. Due to varying topology and elevation, the five climate zones are further divided into two or three subregions although they are not shown in the figure (MOHURD, 2015). Nine test locations, including Harbin (severe cold, 45.8°N and 126.8°E), Urumqi (severe cold, 43.8°N and 87.6°E), Beijing (cold, 39.9°N and 116.3°E), Lhasa (cold, 29.7°N and 91.0°E), Shanghai (hot summer and cold winter, 31.2°N and 121.4°E), Chongqing (hot summer and cold winter, 29.9°N and 108.6°E), Kunming (temperate, 25.0°N and 102.7°E), Nanning (Hot summer and warm winter, 22.8°N and 108.4°E) and Hong Kong (Hot summer and warm winter, 22.3°N and 114.2°E), within each of the five climate zones were selected for the analysis.

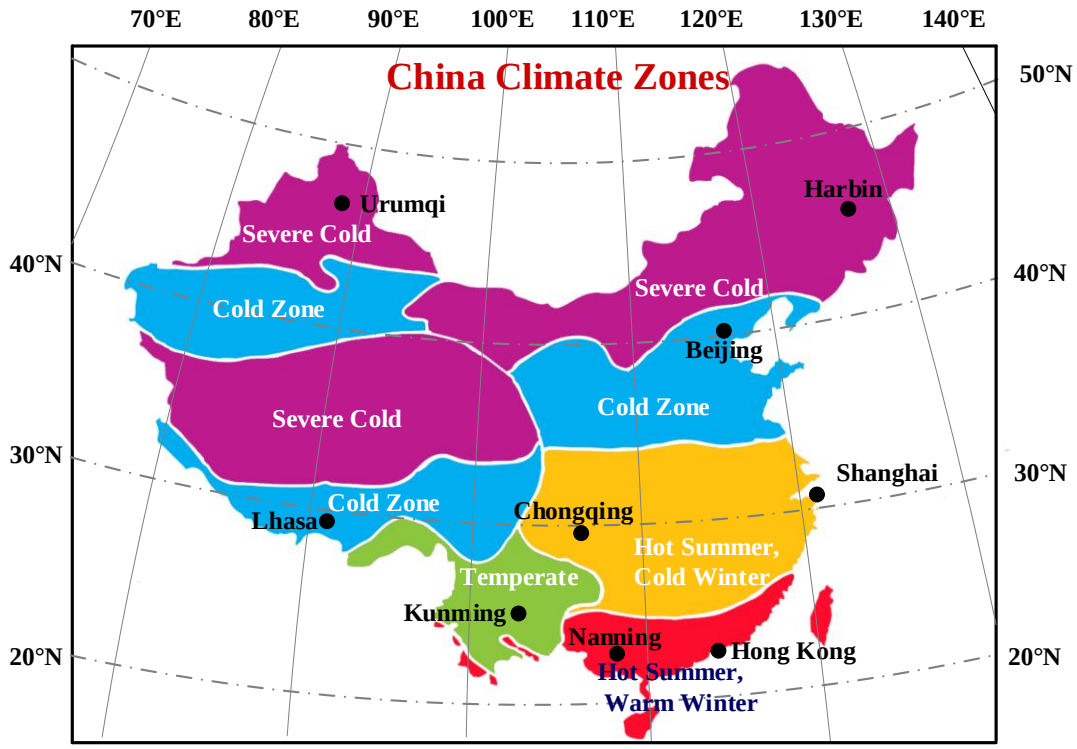

Figure 4.1 Geographical distribution of five major climates and nine cities (MOHURD, 1993)

4.1.2 Building parameters

The air-conditioning subsystem concerned (i.e. serving the space with a total floor area of 369.7 m^2) has the system configuration as shown in Figure 2.4, containing the axial fans, chilled water-cooling coils, an electric heater, an electric steam humidifier and other accessories. It is worth noticing that no infiltration was considered in the load calculation due to the positive pressure control requirement on cleanrooms. The pharmaceutical building model was assigned envelope parameters, ventilation rates, internal loads, operating schedules, as well as indoor temperature and relative humidity setpoints compliant with prescriptive requirements or recommended design values in Chinese building energy efficiency standards (Wang & Zhang, 2015). The detailed characteristics of the simulated building are shown in Table 4.1. The load patterns of lighting, occupancy and equipment are shown in Figure 4.2.

Table 4.1 Characteristics of the simulated building

Description	Parameter	Value
Envelope details (MOHURD, 2015)	Roof thermal transmittance ($W/m^2 \cdot K$)	0.28 (Harbin), 0.35 (Urumqi), 0.45 (Beijing & Lhasa), 0.5 (Shanghai & Chongqing), 0.8 (Kunming, Nanning & Hong Kong)
	Wall thermal transmittance ($W/m^2 \cdot K$)	0.38 (Harbin), 0.43 (Urumqi), 0.5 (Beijing & Lhasa), 0.8 (Shanghai & Chongqing), 1.5 (Kunming, Nanning & Hong Kong)
	Window thermal transmittance ($W/m^2 \cdot K$)	2.7 (Harbin), 2.9 (Urumqi), 3.0 (Beijing & Lhasa), 3.5 (Shanghai & Chongqing), 5.2 (Kunming, Nanning & Hong Kong)
	Window to wall ratio (WWR)	0.2
Indoor design conditions	Temperature (°C)	20 ± 3
	Relative humidity (RH) (%)	55 ± 10
	Concerned space volume (m^3) (length × width × height)	1,035 (23.7×15.6×2.8)
Outdoor and supply airflow	Outdoor air changes per hour (ACH)	2
	Supply air changes per hour (ACH)	20
Installed fans specification	MAU fan pressure (Pa)	1,100
	AHU fan pressure (Pa)	850
	Fan efficiency (%)	60
Internal loads (Sensible & latent heat)	Lighting (W/m^2)	13.9 + 0
	Occupants (W/m^2)	22 + 37
	Equipment (W/m^2)	57 + 19
Internal load pattern	Lighting Occupancy Equipment	See Figure 4.2, referring to the defaults given in BEAM Plus (Burnett, Yik, Lee, Powell, & Tang, 2001)

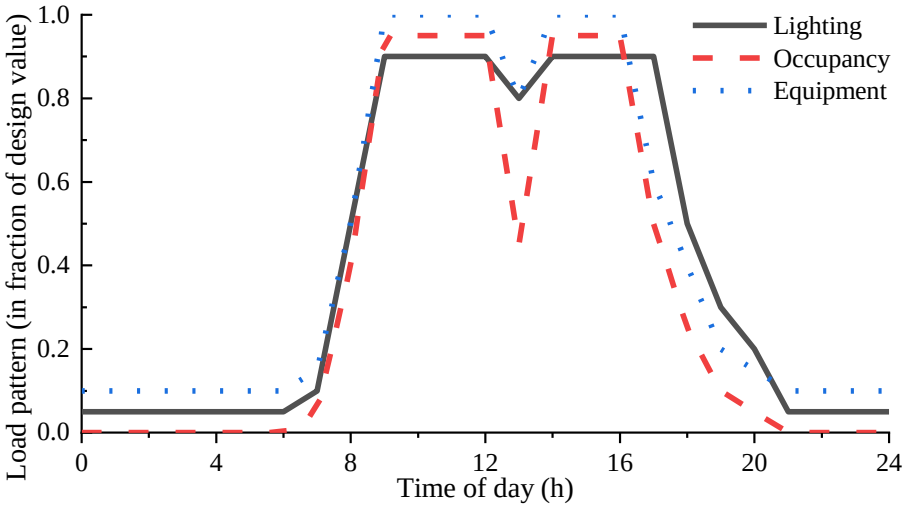

Figure 4.2 Load patterns of lighting, occupancy and equipment in the simulated building

4.1.3 Weather conditions

Typical Meteorological Year of different locations (Marion & Urban, 1995), which contains typical hourly weather data obtained from the Meteonorm database (Remund, Kunz, & Lang, 1999), were used for the whole-year building energy analysis. Figure 4.3 presents the hourly TMY2 weather data on the psychrometric chart and the distribution of outdoor conditions in different regions for one year in Hong Kong. By selecting the indoor humidity at the lower-limit (23 °C, 45%) and upper-limit (23 °C, 65%) as reference indoor conditions (point O_1 and O_2), the psychrometric chart can be divided into four regions based on differences between the outdoor and indoor air states. The air-conditioning systems should operate using non-economizer modes (i.e. the economizer is not activated) in regions I and II, while the systems were of high probability to operate using economizer modes in regions III and IV. Region I represents the humid outdoor conditions. The outdoor air humidity was higher than the upper-limit humidity of indoor air, so the MAU needed to dehumidify the outdoor air for removing the moisture. Region II represents the hot-dry outdoor air conditions. It was possible to remove all the indoor moisture by the introduction of the proper

outdoor airflow under low internal latent load conditions, while the cooling was still required to remove the sensible heat. Region III represents the cool-dry outdoor conditions. Through the introduction of cool outdoor air by the economizer cycle, the indoor environment was likely to be controlled at the allowable range even without additional cooling/dehumidification. Region IV represents the cold-dry outdoor conditions. Due to low temperature and humidity of outdoor air, heating and humidification were possibly needed to maintain the required indoor temperature and relative humidity.

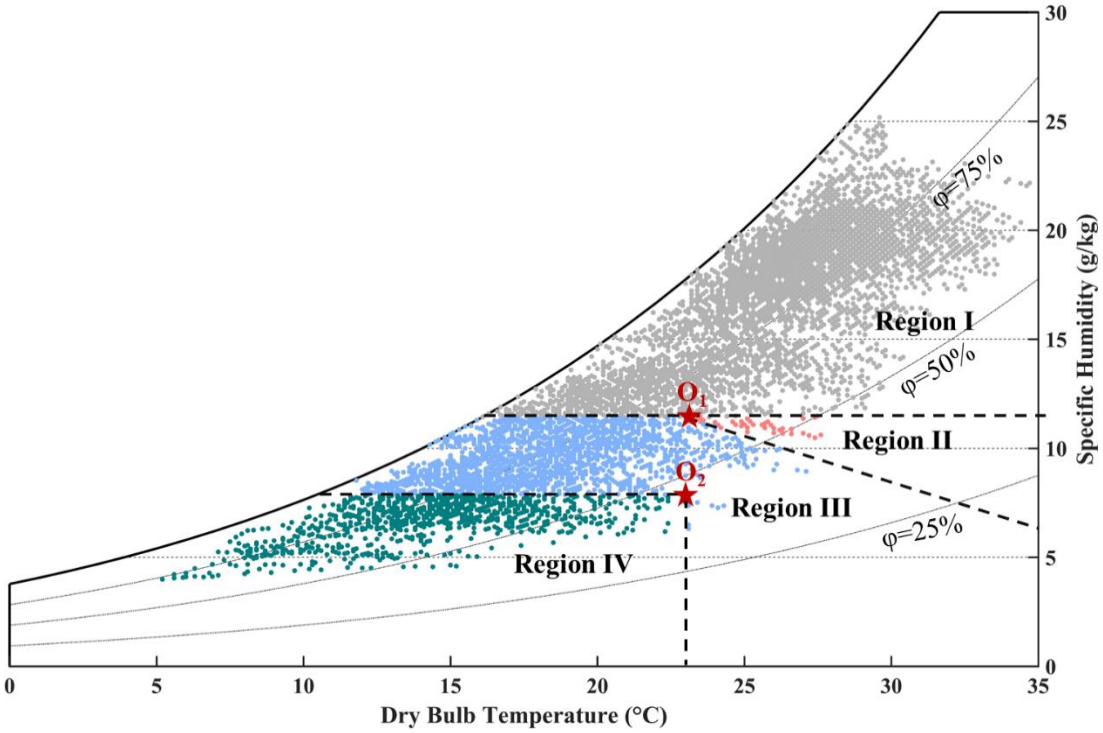

Figure 4.3 Hourly outdoor conditions for one year in Hong Kong

Figure 4.4 presents the fraction of outdoor conditions that fell into each psychrometric region for nine selected cities. Nanning and Hong Kong, located in hot summer and warm winter climate zone, were hot and humid with over 60% of outdoor conditions fell into region I. Harbin, Urumqi, Beijing and Lhasa, located in the cold/severe cold zones, had more than 60% of time in the cold-dry region (i.e. region IV). Shanghai

and Chongqing, located in hot summer and cold winter climate zone, had more than 30% of the time in both region I and region IV, with distinct dry and wet climates. Kunming, located in temperate climate zone, had more than 30% of the time in cool-dry outdoor conditions (region III), significantly higher than that of the other cities. It can also be seen that, in moderate, cold and severe cold climate zones, the ambient conditions had a significant fraction falling into regions III and IV. These were the regions in which the economizer modes should be well-selected and applied. For the cities in hot climatic conditions, the non-economizer modes operated for the most time through a year.

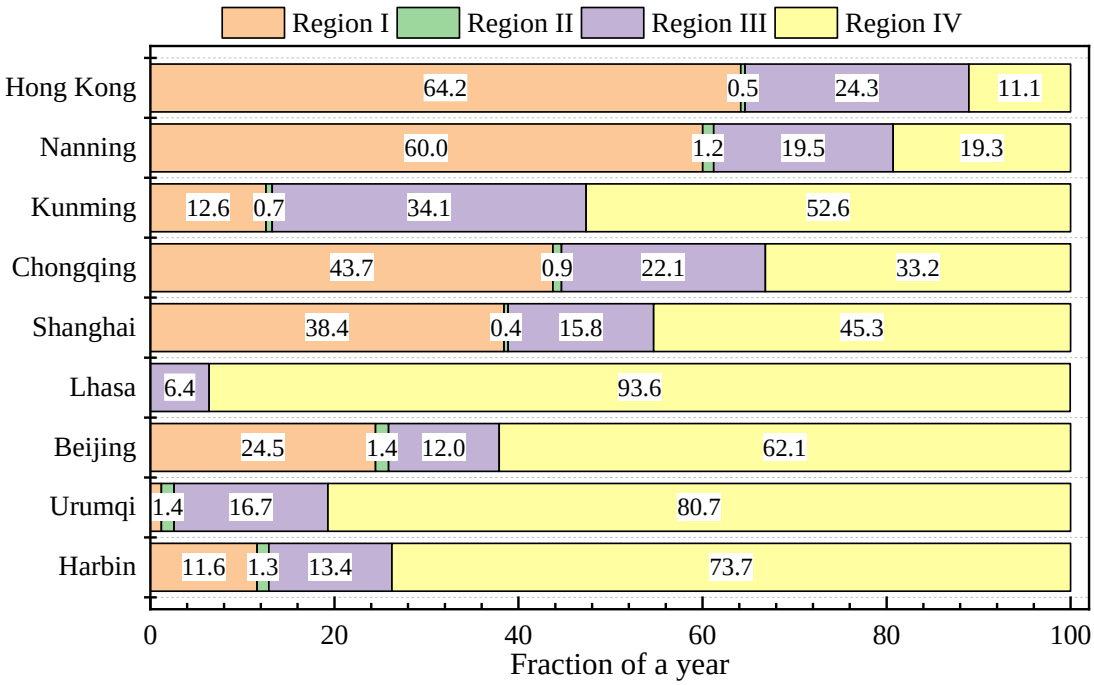

Figure 4.4 Fraction of a year for different psychrometric chart regions in different cities

4.1.4 Load conditions

Assuming that the indoor temperature and relative humidity of the cleanrooms were controlled at its upper limit (23 °C, 65%), the hourly space cooling loads of cleanrooms in nine cities were calculated in TRNSYS 18 (2017) as shown in Figure 4.5. Here the

cooling loads resulted from heat transfer processes through the building envelope (external elements) and internal sources while the outdoor air load (or ventilation load) was not taken into account. This is due to the outdoor air load was determined by the ventilation strategy adopted and handled by the MAU before entering the spaces. The mean sensible cooling loads varied between 23.6 W/m^2 (Kunming) and 36.4 W/m^2 (Hong Kong), and the mean total cooling loads varied between 44.3 W/m^2 (Kunming) and 57.4 W/m^2 (Hong Kong). Although the selected cities are located in different climate zones, the space cooling load distributions had no significant difference when the outdoor air load was not taken into account.

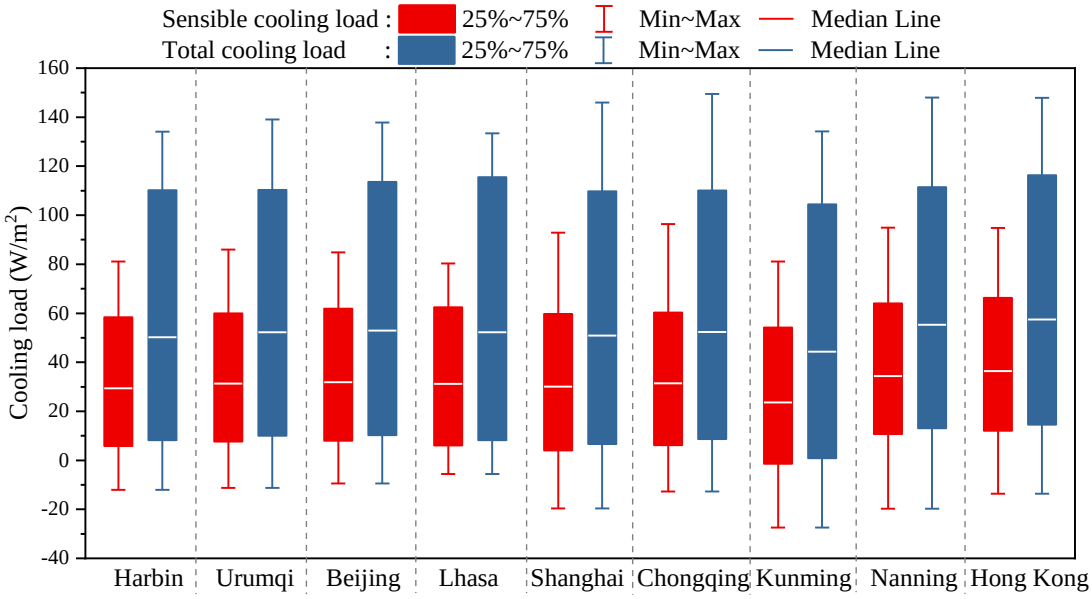

Figure 4.5 Space cooling load distributions of cleanrooms in nine cities

4.2 Energy-saving potentials and preferable operation modes in different conditions

The total electrical load of the cleanroom air-conditioning system was evaluated using the component and system energy models as introduced in Section 3.3. This total load

is composed of electrical loads from the MAU/AHU cooling coil, AHU heater, AHU humidifier, make-up air fan and supply air fan.

In order to demonstrate the energy and economic performance of the proposed ADV strategy, the interactive control (IC) strategy was selected as a reference ventilation strategy for comparison purposes. The IC strategy is the most commonly used in cleanroom air-conditioning systems as presented in Section 2.2.1. In addition, an enthalpy-based economizer was incorporated into the IC strategy to improve the energy performance under cool/cold outdoor conditions.

The energy performance of the ADV strategy was assessed and compared with the existing IC strategy in the selected nine cities. Figure 4.6 shows the annual energy consumption of different components adopting the IC strategy and ADV strategy. It can be seen that the annual energy consumption of the air-conditioning systems adopting the ADV strategy can be 6.8-40.8% less than that of the IC strategy. Compared with adopting the IC strategy, although more MAU cooling was required, a large amount of AHU cooling and heating energy consumption was reduced. This indicates that the overcooling and reheating processes were significantly reduced when adopting the proposed ADV strategy. In addition, for the cities in hot/temperate regions (i.e. Shanghai, Chongqing, Nanning, Hong Kong and Kunming), the energy savings (over 34%) were more significant than that in cold regions (i.e. Harbin, Urumqi, Beijing and Lhasa). It is worth noticing that applying the ADV strategy in Urumqi can only achieve 6.8% energy saving, which was the least among all the cities. The reason is that Urumqi is cool/cold and dry throughout a year, and the dry outdoor air can be directly induced for removing the indoor latent heat to avoid overcooling and reheating processes, resulting in little difference between using the ADV strategy and IC strategy in most operation time.

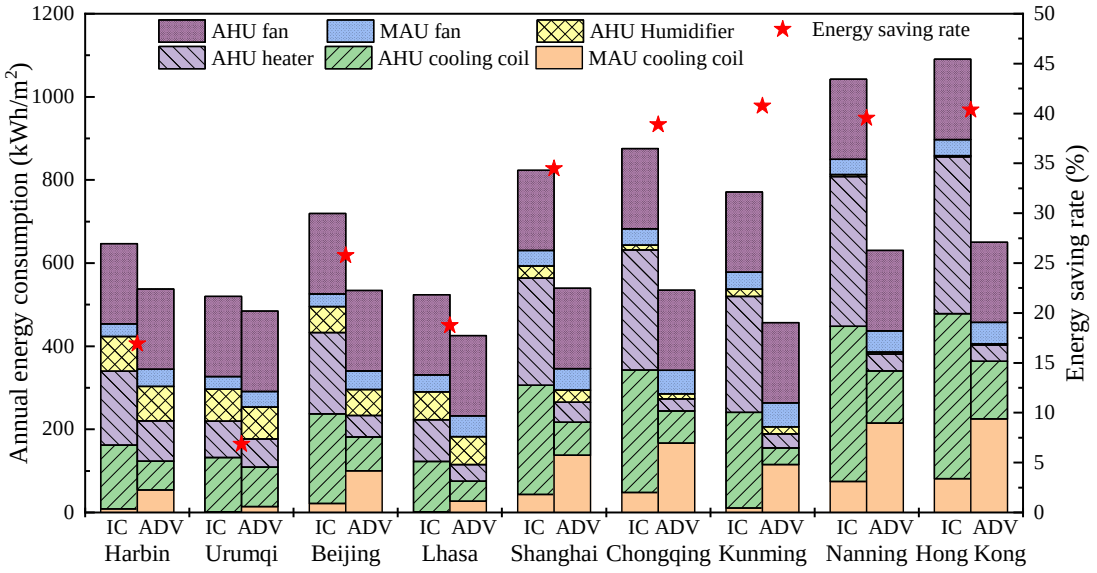

Figure 4.6 Annual energy consumption of adopting existing IC strategy and proposed ADV strategy in nine cities

The running frequencies (%) of different control modes of the ADV strategy are presented as in Figure 4.7, to illustrate how the significant energy savings were achieved. The non-economizer modes accounted for more than 50% running time through a year in all selected cities. In this figure, the PD/DV mode represents that there is no difference between the PD mode and DV mode, which indicates all moisture heat can be removed at the minimum required outdoor airflow (i.e. 2 ACH in this case). The PD/DV mode accounted for the largest proportion among all operation modes (more than 42%). It is worth noticing that overcooling and reheating processes (i.e. represented by PD mode in this figure) to remove the internal latent load were seldom used in cold and temperate regions. However, for the cities in hot climate regions, such as Hong Kong, the overcooling and reheating processes were still adopted due to the high internal latent load and outdoor air enthalpy. The FL mode had the lowest running frequency in all cities. The running frequency of economizer mode was highest in Lhasa (45.6%), due to the high cooling/dehumidification potentials under plateau climatic conditions.

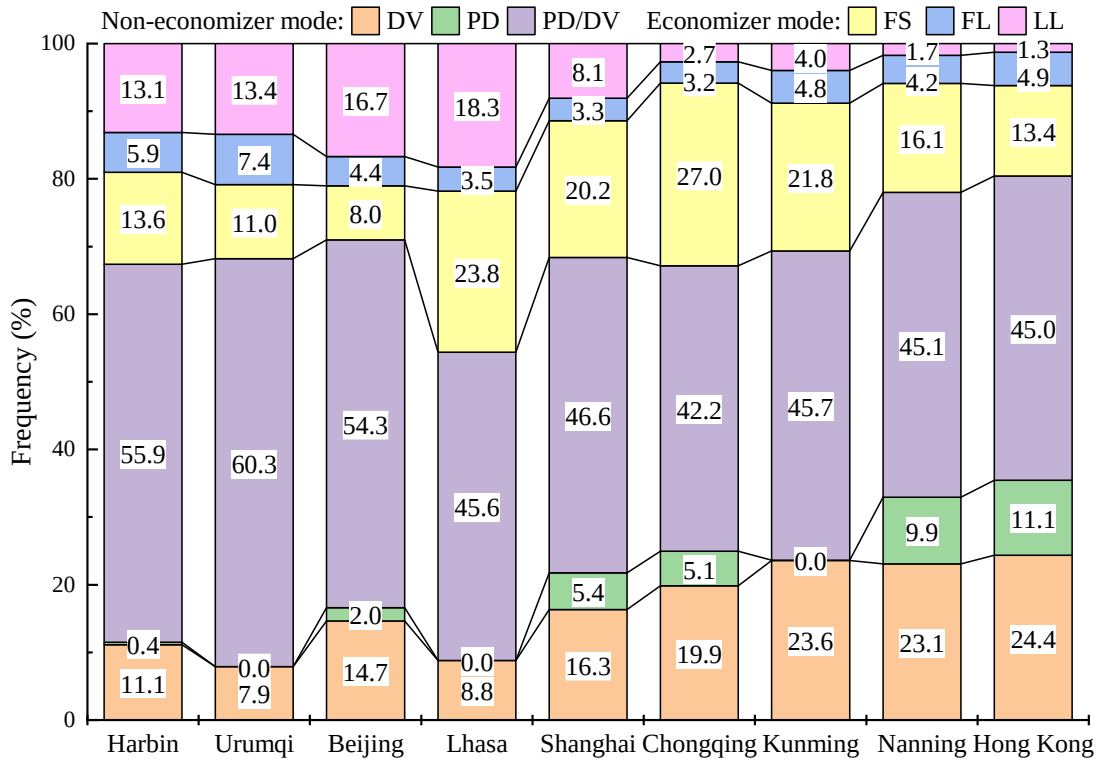

Figure 4.7 Running frequencies (%) of different control modes of ADV strategy

To simplify the operations adopting the ADV strategy in real applications, it is recommended to only use DV mode in severe cold/cold and moderate regions due to the low running frequency of using PD mode (less than 2%). In addition, when the economizer was activated, the FL and FS modes were the main economizer modes in severe cold and cold regions (Harbin, Urumqi, Beijing and Lhasa), while the FS mode was the main economizer mode in hot or temperate regions (Shanghai, Chongqing, Nanning, Hong Kong and Kunming).

Both the operation frequencies of economizer mode and energy-saving ratios when adopting the ADV strategy had a high correlation with the outdoor air humidity of locations as shown in Figure 4.8. Figure 4.8A presents the relations between the annual mean absolute humidity of outdoor air and frequencies of economizer mode in different locations. It can be seen that economizer modes were more frequently used for the cities in dry climatic conditions. Figure 4.8B presents that the overall energy

saving ratios were higher in humid climates than that in dry climates when adopting the ADV strategy. This indicates climate conditions, especially the outdoor air humidity, significantly influence the selection of best operation modes, and thus the energy performance of the systems.

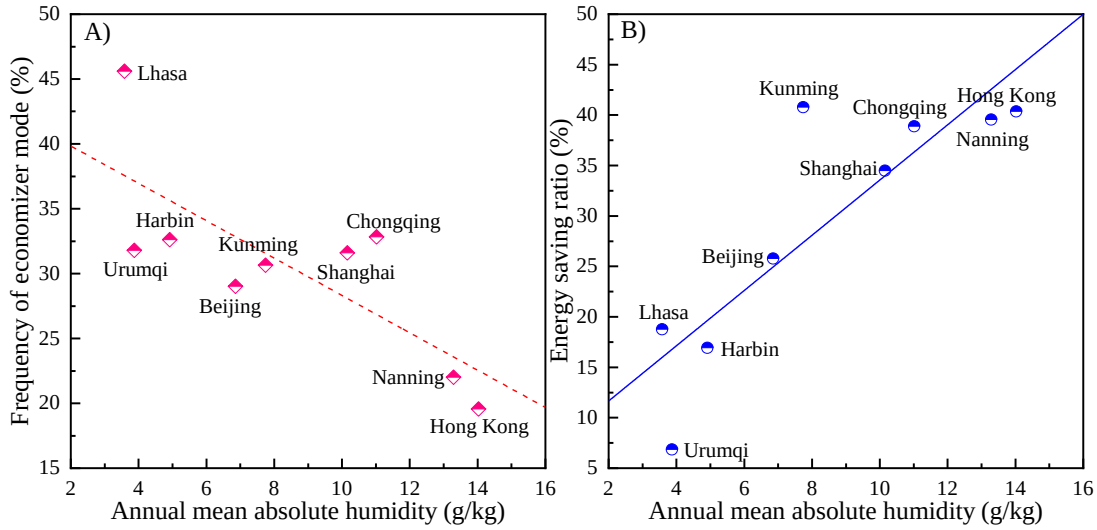

Figure 4.8 Annual mean absolute humidity of outdoor air vs. A) frequencies of economizer mode B) energy-saving ratios in different locations

4.3 Requirements on air-conditioning system design and cost-benefit analysis

Due to the strict requirements on temperature and humidity controls in cleanrooms, it is assumed that the component capacities should meet the maximum cooling/heating demands of a year. Therefore, the required capacities of the cooling coils, heater and humidifier were determined by the hourly maximum cooling, heating and humidification demands, respectively. The required powers of the MAU and AHU fans were determined by the maximum outdoor and supply airflow, respectively. The required capacities of air-conditioning components for implementing the IC and ADV strategies are shown in Figure 4.9. In general, the implementation of the ADV strategy

required larger capacities of MAU cooling coil, which can be 3.1 (Chongqing) to 9.4 times (Urumqi) as larger as that for the IC strategy. In contrast, the required capacities of other components (i.e. fans, AHU cooling coil, humidifier and heater) were not larger or equal to that for the IC strategy. This result also offered a good reference for the existing system (i.e. initially adopting the IC strategy) retrofit and new system design. For the full implementation of the ADV strategy in an existing system, only the size of the MAU cooling coil was required to be enlarged while the other components can be unchanged. For the full implementation of the ADV strategy in a new system, compared with the design for the IC strategy, the required capacity of the MAU cooling coil was larger while the required capacities of AHU cooling coil and heater were smaller. It is worth noticing that, when adopting the IC strategy, the required fan power (9.9 kW) in Urumqi was lower than the others. When the enthalpy economizer was activated under dry outdoor conditions adopting the IC strategy, the amount of outdoor air was induced to control indoor relative humidity at its higher limit (i.e. 65%). Due to the dry climatic conditions in Urumqi (Figure 4.8), it is found that the maximum 94% (proportion to total supply airflow) outdoor airflow was required to be induced in the test year. For other cities, which were not as dry as Urumqi, the maximum 100% outdoor air was required to be induced according to the mechanism of the economizer adopting the IC strategy. For a new design of the case in Urumqi, the required MAU fan power (10.5 kW) adopting the ADV strategy was larger than that of adopting the IC strategy (9.9 kW). However, in the retrofitting case (originally designed for adopting the IC strategy), the modification on the MAU fan was not required due to that the fan capacity can almost meet the outdoor air ventilation requirements when the economizer was activated.

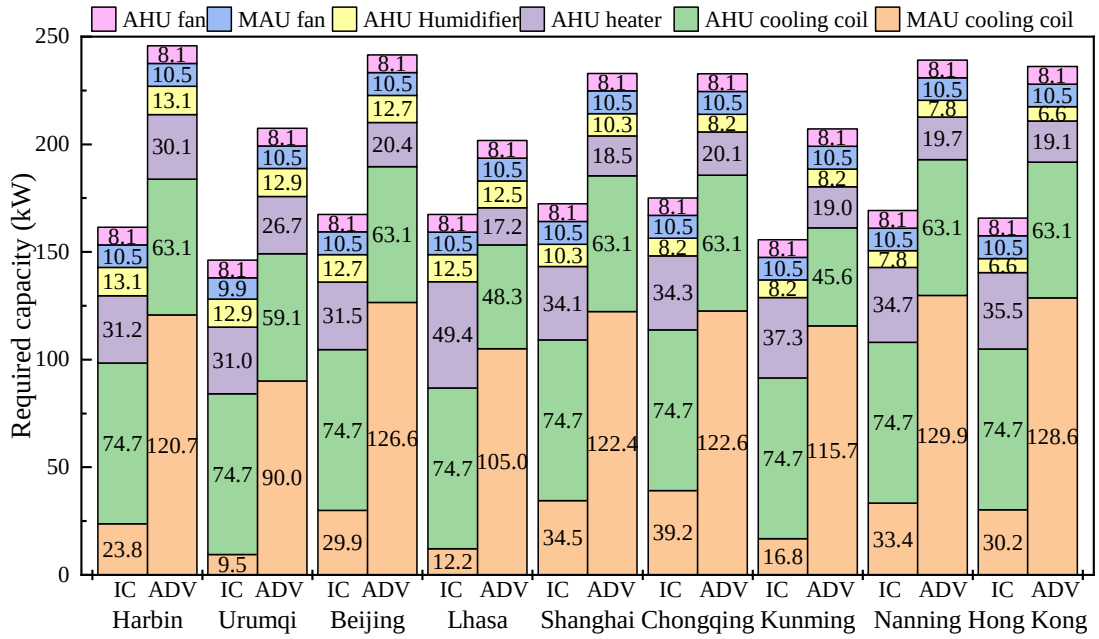

Figure 4.9 Air-conditioning component design capacities for implementing IC and ADV strategies

The payback period (PBP) indicates the number of years needed for the payback of the surplus capital cost for using the ADV strategy to replace the IC strategy. This value is the ratio of capital cost difference and operation cost difference as shown in Eq. 4.1, where ΔC_C and ΔC_O are the increase of system capital cost and the annual operation (electricity) cost saving, respectively. For new system designs, the total capital cost is the sum of component investment costs. For existing system retrofits, the total capital cost includes the component investment costs and refurbishment costs. The component initial cost includes the cost of AHU/MAU cooling coils (Inc_{CC}), AHU/MAU axial fans (Inc_{fan}), AHU electric heater (Inc_{he}) and AHU electric humidifier (Inc_{hu}). The cost estimates, which are the functions of the corresponding component capacities, were based on RSMeans Mechanical Cost Data (Mossman, 2008) as shown in Appendix A, where £$_e$ is the local electricity price (USD/kWh), as shown in Table 4.2. The electricity prices of all cities except for Hong Kong were obtained from National Development and Reform Commission (NDRC, 2018) and the

electricity price of Hong Kong was obtained from China Light & Power Company (CLP Hong Kong, 2018). It is worth noticing that, the component investment cost considering the inflation was used to fit the cost equations. In this study, the component investment cost (in 2019) was used for cost analysis, which was obtained by adding the inflation on the cost data in 2008. It is also recommended to use actual manufacturers' quotations, if reliable, or newly updated cost data for cost analysis. For the retrofitting case, the refurbishment cost of a component (including additional installation cost) was assumed as 30% of its incremental investment cost considering the possible modification and maintenance of accessories and packages (Hang et al., 2014).

$$PBP = \begin{cases} \frac{\Delta C_C}{\Delta C_O} = \frac{(Inc_{cc}+Inc_{he}+Inc_{hu}+Inc_{fan})_{ADV}-(Inc_{cc}+Inc_{he}+Inc_{hu}+Inc_{fan})_{IC}}{£_e\times(E_{tot,IC}-E_{tot,ADV})}, & \text{New system design} \\ \frac{\Delta C_C}{\Delta C_O} = \frac{1.3[(Inc_{cc}+Inc_{he}+Inc_{hu}+Inc_{fan})_{ADV}-(Inc_{cc}+Inc_{he}+Inc_{hu}+Inc_{fan})_{IC}]}{£_e\times(E_{tot,IC}-E_{tot,ADV})}, & \text{Existing system retrofit} \end{cases} \quad (4.1)$$

Table 4.2 Electricity prices (USD/kWh) for non-residential buildings in each simulated city

City	Electricity price (USD/kWh)
Harbin	0.110
Urumqi	0.071
Beijing	0.121
Lhasa	0.106
Shanghai	0.116
Chongqing	0.105
Kunming	0.089
Nanning	0.108
Hong Kong	0.141

Figure 4.10 shows the payback periods for existing system retrofits and new system designs adopting the ADV strategy. Due to the high energy saving potentials adopting ADV strategy, when retrofitting an existing system, the system payback periods in all cities except for Urumqi were all less than 4 years. Due to the required smaller sizes

of the AHU, for new system designs, the system payback periods in all cities except for Urumqi were all less than 2 years. In addition, the cities in hot climate zones (Shanghai, Chongqing, Kunming, Nanning and Hong Kong) had shorter payback periods than that of the cities in cold/severe cold climate zones (Harbin, Beijing and Lhasa). Urumqi required the longest payback periods compared with other cities, which were 13.6 years for the existing system retrofit and 8.3 years for the new system design. The reason is that Urumqi is dry throughout a year, and only slight energy saving (6.8%) can be achieved by adopting the ADV strategy.

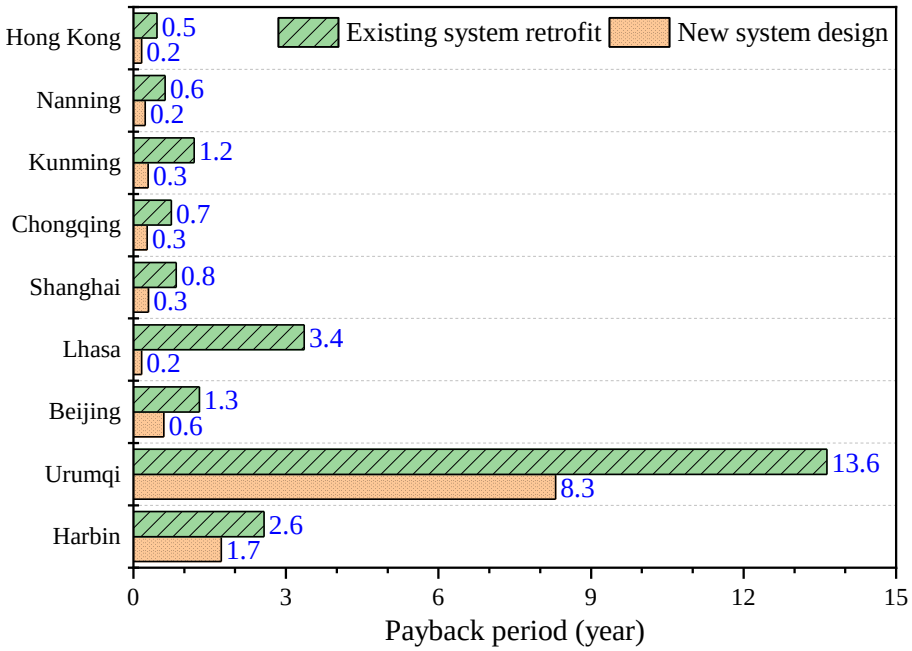

Figure 4.10 Payback periods for existing system retrofit and new system design

The energy and economic performance of the proposed strategy were compared with desiccant cooling strategies, which are the most-updated strategies for indoor temperature and humidity controls. Table 4.3 lists the energy performance and payback periods of desiccant cooling systems compared with conventional vapor compression air-conditioning systems in the existing studies. Compared with the conventional vapour compression air-conditioning systems, although the energy performances of the desiccant cooling systems were superior, both the capital cost and

system complexity of them were increased significantly. Generally, the payback periods of desiccant cooling systems were 2-15 years, with the energy savings of 6-78%, depending on the selection of hybrid systems and climatic conditions.

It is worth noticing that the acceptance of the existing strategies listed in Table 4.3 for cleanroom applications might still be an issue to be confirmed. In these cases, the payback periods presented were those for new system designs. In cases of retrofitting the conventional vapour compression air-conditioning systems, the payback periods of desiccant cooling strategies will be much higher, due to the requirements of replacing the existing equipment. The proposed ADV strategy offers a much better solution for conventional system retrofits. A significant energy saving can be achieved by adopting the proposed ADV strategy while only minor hardware (i.e. sizing) modification is required.

Table 4.3 Overview of desiccant cooling systems for temperature and humidity controls

Author (Year)	City/ Country	System	Energy performance	Payback period (years)
Zhang and Niu (2003)	Hong Kong	Chilled ceiling combined with desiccant cooling	40% primary energy saving	15
Mazzei et al (2005)	Rome	Desiccant wheel hybrid system	23-38% operating cost savings	2-3
Gasparella et al. (2005)	Bolzano	Ground source heat pumps with chemical dehumidification	30% primary energy saving	7.8
Hirunlabh et al. (2007)	Thailand	Solid air-conditioning system	24% electricity saving	4
Khalid et al. (2009)	Karachi	Solar assisted pre-cooled hybrid desiccant cooling system	6% thermal energy saving	14
Ge et al. (2010)	Berlin and Shanghai	Solar driven two-stage rotary desiccant cooling system	78% (Berlin) and 69% (Shanghai) electricity saving	4.7 (Berlin) / 7.2 (Shanghai)
Li et al. (2010)	Hong Kong	Solar-assisted liquid desiccant cooling system	Maximum 59.6% electricity saving	7
Qi et al. (2015)	Singapore	Solar-assisted liquid desiccant cooling system	40% electricity saving	6

4.4 Summary

This chapter presented the energy and economic performance, the required air-conditioning system design and the most suitable operation modes of the proposed ADV strategy for cleanrooms or spaces requiring strict temperature and humidity controls under different climatic conditions. Based on the results of the tests and investigation, some detailed conclusions can be drawn as follows:

i. The ADV strategy offers significant and promising energy savings in different climate zones. The annual energy consumption of the air-conditioning systems could be reduced by 6.8-40.8% when implementing the proposed ADV strategy,

compared with the most commonly used existing interactive control (IC) strategy. It has higher energy saving potentials in humid climates compared with that in dry climates.

ii. When the economizer is not activated, dedicated outdoor air ventilation (DV) mode is highly recommended as the main operation mode of the ADV strategy in severe cold/cold and moderate regions. When the economizer is activated, the "following sensible load" (FS) mode and "lower-limit humidity control" (LL) mode are the recommended operation modes in cold/severe cold climate zones while the "following sensible load" (FS) mode is the recommended operation mode in hot/temperate climate zones.

iii. For the full implementation of the ADV strategy in retrofitting an existing system (i.e. initially adopting the IC strategy), only the size of the MAU cooling coil needs to be enlarged while the other components can keep unchanged. For a new system design, the required capacities of the AHU cooling coil and heater are even smaller compared with those designed for the IC strategy.

iv. The payback periods of existing system retrofits and new system designs could be less than 4 years and 2 years respectively in most climates when the ADV strategy is fully implemented.

CHAPTER 5 UNCERTAINTY-BASED ROBUST OPTIMAL DESIGN OF CLEANROOM AIR-CONDITIONING SYSTEMS

The practical implementation of the ventilation strategy requires proper system design and selection of air-conditioning components. The objective of design optimization is to minimize the life-cycle cost and provide systems with the robustness to operate at high energy efficiency under ever-changing dynamic working conditions. An uncertainty-based robust optimal design method for cleanroom air-conditioning systems is therefore proposed in this chapter. This chapter is organized as follows. Section 5.1 illustrates the problems concerned in the design of multi-zone cleanroom air-conditioning systems. To address these unexpected problems, an uncertainty-based robust optimal design method is proposed and an outline of this method is shown in Section 5.2. The quantification of inherent uncertainties involved, including design input uncertainties and load diversities among zones/spaces, are elaborated in Section 5.3. The detailed procedure of the optimization process is presented in Section 5.4. The proposed design method is tested and validated using an existing pharmaceutical building as a reference building in Section 5.5. Conclusive remarks are presented in Section 5.6.

5.1 Challenges addressed in cleanroom air-conditioning system design

Chapter 4 has presented the required component capacities and design of air-conditioning systems for implementing the proposed ADV strategy, by considering the year-around operation conditions which are certain and presumed at the design stage. The sizing of the components was determined basically using the annual maximum cooling/heating demand. However, the proper and optimal design for cleanroom air-conditioning systems is particularly associated with ever-changing working conditions and the uncertainties of information used. These challenges are summarized as follows, which are the main issues to be addressed.

i. System design should coordinate effectively with certainly preferred ventilation strategy. The air-conditioning systems need to be designed with sufficient consideration on their coordination with a certain properly selected optimal and energy-efficient ventilation strategy to facilitate the systems to work at high energy efficiency under different off-design conditions.

ii. System design should properly consider the accuracy of input data/information which can be rather different from that in real operation. Such inherent deviations are regarded as “uncertainties”. Due to the existence of uncertainties, the actual conditions of air-conditioning systems in operation often deviate significantly from those projected at the design stage.

iii. System design should properly consider the realistic distribution of cooling loads, which could greatly affect the cooling demands on the air-conditioning subsystems associated with a zone, and the corresponding component capacities needed. The uneven distribution issue of the cooling load is regarded as the

diversity of the cooling load distribution. The cooling loads of different spaces in a zone could have large discrepancies at any moment and change with time (Zhou, Yan, Jiang, & Shi, 2016). The load diversities of multiple spaces (including sensible and latent loads), two of the major uncertainties in operation which are usually neglected in system design, affect the operation performance of air-conditioning systems significantly (An, Yan, Hong, & Sun, 2017; Virote & Neves-Silva, 2012; Yu, Fung, Haghighat, Yoshino, & Morofsky, 2011).

5.2 Outline of proposed uncertainty-based robust optimal design method

Figure 5.1 shows the typical configuration of the multi-zone cleanroom air-conditioning systems for multiple spaces requiring strict temperature and humidity controls. It consists of an MAU and a few AHUs. Each AHU might serve a few spaces. It is worth noticing that, different from the system configuration presented in previous chapters (i.e. 2-4) (one MAU and one AHU serve one zone/space), the cleanroom air-conditioning system concerned here is typical in practical applications, which serves multiple zones (i.e. each served by an AHU) and each zone contains multiple spaces. This practically typical system configuration is considered in design optimization.

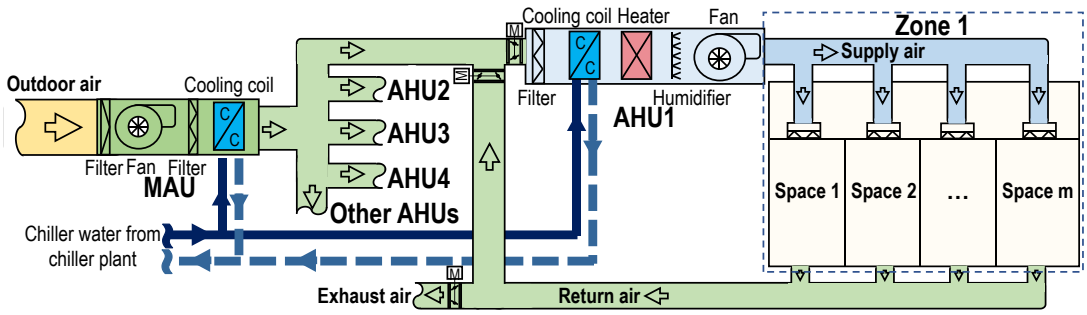

Figure 5.1 System configuration of a typical multi-zone air-conditioning system

Figure 5.2 presents the procedure and major steps of the proposed design method for multi-zone cleanroom air-conditioning systems. The objective of the design optimization is to minimize the life-cycle cost and provide systems with the robustness to operate at high energy efficiency under ever-changing dynamic working conditions. The main challenges to be addressed are associated with the impacts of: *i)* variation of working conditions due to changes of ambient and internal loads; *ii)* the diversities of space latent and sensible loads, particularly sensible heat ratios (SHRs), among different spaces; and *iii)* the uncertainties of the ambient conditions and internal loads as well as their diversities.

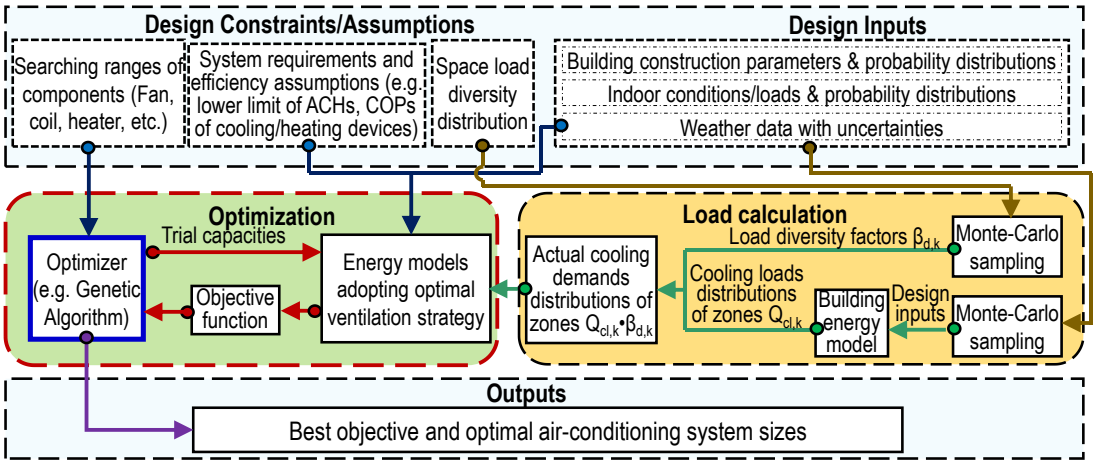

Figure 5.2 Procedure and steps of proposed uncertainty-based robust optimal design method using a probabilistic approach

The objective function for optimization is the overall annualized total cost ($C_{OT,a}$) (i.e. Eq. 5.1), which includes the annualized values of capital cost ($C_{C,a}$), maintenance cost ($C_{M,a}$), operation (or energy) cost ($C_{O,a}$) and penalty cost ($C_{P,a}$). The operation cost includes the total cost of electricity consumed by air-conditioning components (E_{tot}). The penalty cost is introduced to consider the impacts of insufficient cooling and dehumidification capacities to ensure the designed systems with a high level of service satisfaction. The system optimal design consists of three major steps involving the

quantification of these variations/diversities and their inherent uncertainties. *In the first step,* the design inputs (involving uncertainties) and design constraints are selected, including building envelope parameters, design indoor and ambient conditions, assumed efficiency and air-conditioning system constraints as well as the search ranges for the system design parameters (i.e. component capacities) to be optimized. The purpose of this step is to obtain the required information for design optimization. *In the second step,* the annual overall probabilistic sensible/latent cooling demands of individual AHUs in each zone are obtained, which involve quantified uncertainties and diversities of spaces. The design input uncertainties (i.e. weather, building construction and indoor conditions) are considered in the overall zone cooling load calculation with different trials. The diversities of spaces in a zone are considered by adopting a simplified method (namely 'probabilistic diversity factor method'). Two probabilistic load diversity factors are introduced in this method. The probabilistic sensible and latent cooling demands (D_{sen}, D_{lat}) are then obtained using the space sensible and latent load distributions within a zone (Z_{sen}, Z_{lat}) multiplied by the space sensible and latent load diversity factors (with quantified distributions), as shown in Eqs. 5.2-5.3. The probabilistic diversity factors ($\beta_{d,sen}$, $\beta_{d,lat}$) represent the design input uncertainties during sensible and latent load calculations and their asynchrony in multiple spaces. The purpose of this step is to effectively quantify the design input uncertainties and the uncertainties due to the asynchronous behaviours of multiple spaces. *In the third step*, an "optimizer" determines the optimal component capacities by evaluating the overall system performance with various trials of component capacities within their search ranges. The purpose of this step is to find the optimal sizes for air-conditioning components based on the probabilistic cooling load profiles. A system energy model (Eq. 5.4), which is a function of dynamic cooling

demands of zones (D_{sen}, D_{lat}), is used to estimate the energy consumption (E_{tot}) of the systems adopting a selected optimal ventilation control strategy (e.g. adaptive full-range decoupled ventilation strategy). Here COP_c and COP_{he} are the overall coefficients of performance for the central cooling and heating systems, respectively. For the central cooling system, the overall coefficient of performance of the central cooling system (COP_c) including the pumps and the chiller is assumed to be constant as 2.5 when calculating the overall electricity use (Stetiu, 1999; Sun, Wang, & Zhu, 2011). COP of the heating system (COP_{he}) is assumed to be constant as 1.0 due to the heating energy is provided by the electric heaters. $W_{f,MAU}$ and $W_{f,AHU}$ are the fan powers of the MAU and AHUs, respectively. $Q_{cc,MAU}$ and $Q_{cc,AHU}$ are the MAU and AHU cooling loads, respectively. $Q_{he,AHU}$ is the AHU heating load. The detailed optimization process is shown in Figure 5.2 and elaborated as follows.

$$C_{OT,a} = (C_{C,a} + C_{M,a} + C_{O,a}) + C_{P,a} \quad (5.1)$$

$$D_{sen} = Z_{sen} * \beta_{d,sen} \quad (5.2)$$

$$D_{lat} = Z_{lat} * \beta_{d,lat} \quad (5.3)$$

$$E_{tot} = \frac{Q_{cc,MAU}}{COP_c} + W_{f,MAU} + \sum_{i=1}^{k}(\frac{Q_{cc,AHU,i}}{COP_c} + \frac{Q_{he,AHU,i}}{COP_{he}} + W_{f,AHU,i}) = f(D_{sen,i}, D_{lat,i}) \quad (5.4)$$

For retrofitting the air-conditioning systems of existing buildings, the improper sizing problems can be easily addressed through the analysis of the operation data. However, for new buildings in the design phase, various inherent uncertainties exist which need to be considered for accurate cooling load estimations. With the probabilistic estimates of cooling load distributions, the air-conditioning components are of higher probability to be properly designed, to avoid both under-sizing and over-sizing problems. Compared to current engineering practice involving detailed design calculation (Domínguez-Muñoz et al., 2010; Gang, Wang, Shan, & Gao, 2015; Sun et

al., 2014), no additional information is required at the design stage except the information or assumption on the load diversities among multiple zones/spaces. In the design stage, the model inputs required for design include the space control requirements, building layout, envelop parameters, historical weather, internal load conditions and possible distributions of concerned parameters, which are all the same as needed in current design practice when detailed design calculation is conducted. The users can obtain the information from the planning guide, local standards and regulations. However, for the multi-zone air-conditioning systems, each zone may contain several spaces. If the uncertainties in spaces were all considered individually, the calculation process would be very complicated. Therefore, to consider the effects of asynchronous loads in different zones/spaces with reduced computation demand, a probabilistic diversity factor method is proposed, which offers a simplified method to quantify the effects of uncertainties of space load diversities in multiple zones/spaces using diversity factors. More detailed descriptions are shown in Section 5.3.

5.3 Uncertainty quantification in cooling demand calculation

5.3.1 Quantification of design input uncertainties

The uncertainties in design inputs are quantified by adopting the commonly-used Monte Carlo method (Doucet, De Freitas, & Gordon, 2001; Janssen, 2013). Based on inputs (x_1, x_2, …, x_n), the outputs Q (i.e. sensible/latent cooling loads of a space) are obtained using Eq. 5.5. The design inputs involving uncertainties (X) are generated by Monte Carlo simulation using Eq. 5.7, according to their probability distributions (G). The probabilistic cooling loads of a zone (Z), which are usually regarded as the sum of the cooling loads of the corresponding spaces, are then obtained using building energy simulation software.

$$Q = [q_1, q_2, \dots, q_{8760}] = f(x_1, x_2, \dots, x_n) \quad (5.5)$$

$$X = [X_1, X_2, \dots, X_n] \quad (5.6)$$

$$X_i = [x_{j1}, x_{j2}, \dots, x_{jm}]^T, X_i \sim G_i \mid j = 1,2, \dots, n \quad (5.7)$$

$$Z = [Q_1, Q_2, \dots, Q_m]^T = f(X_1, X_2, \dots X_n) \quad (5.8)$$

Three groups of variables *X*, including weather, building construction and indoor conditions, are selected and quantified as the design inputs. For the weather parameter, historical measurements of weather data are used, which is proved to be a better way to account for the weather uncertainties (Sun et al., 2014). For other variables, triangular distributions, normal distributions and uniform distributions are used respectively according to the characteristics of their variations. Latin Hypercube Sampling (LHS) method is used to improve the calculation efficiency (Saltelli, Tarantola, & Campolongo, 2000). By importing the samples into the cooling load calculation software, both the sensible and latent cooling load of the multiple spaces can be obtained.

5.3.2 Quantification of multi-space load diversity effects concerning uncertainties

As a major task and challenge, the diversities of sensible and latent cooling loads of the multiple spaces in a zone are quantified to take their effects and uncertainties into account. To reduce the computation complexity, a probabilistic diversity factor method is proposed, which is a simplified method to quantify uncertain space load diversities by introducing two probabilistic diversity factors ($\beta_{d,sen}$, $\beta_{d,lat}$) for sensible and latent loads respectively. These diversity factors are defined as the ratio of actual sensible (or latent) cooling demand (due to the need for over-cooling) to the sum of the cooling loads of all spaces concerned (Eqs. 5.9-5.10). Probabilistic diversity factors are introduced to quantify the load diversity effects of multiple spaces under

possible load profiles in a zone. Here, AHU supply air temperature (t_s) and humidity (w_s) of a zone are determined according to the air state of the critical space (associated to the zone) in each time step (Eqs. 5.11-5.12). m_s is the supply airflow rate (kg/m^3). t_{space} is the actual space temperature (°C). t_{set} is the space temperature set-point (°C). w_{space} is the actual space humidity (kg/kg). w_{set} is the space humidity set-point (kg/kg). k is the number of a space in a zone. $Q_{sen,k}$ and $Q_{lat,k}$ are the sensible and latent cooling load of space k (kW), respectively. c_p is the air specific heat ratio (kJ/(m^3•°C). h_{fg} is the latent heat of vaporization (kJ/kg).

$$\beta_{d,sen} = \frac{\sum m_{s,k}(t_{space,k}-t_s)}{\sum m_{s,k}(t_{set,k}-t_s)} = f_1\left(Q_{sen,k}\right) \quad | \, k = 1,2,\dots,m \tag{5.9}$$

$$\beta_{d,lat} = \frac{\sum m_{s,k}(w_s-w_k)}{\sum m_{s,k}(w_s-w_{set,k})} = f_2\left(Q_{sen,k}, Q_{lat,k}\right) \quad | \, k = 1,2,\dots,m \tag{5.10}$$

$$t_s = min\ (t_{space,k} - \frac{Q_{sen,k}}{c_p m_{s,k}}) \mid k = 1,2,\dots,m \tag{5.11}$$

$$w_s = min\ (w_{space,k} - \frac{Q_{lat,k}}{h_{fg} G_{s,k}}) \mid k = 1,2,\dots,m \tag{5.12}$$

Both diversities and their probability distributions considering uncertainties among different spaces in a zone will be identified according to the main steps using the probabilistic diversity factor method as shown in Figure 5.3. Based on the sensible and latent cooling load profiles of multiple spaces (i.e. the uncertain load data generated by Monte Carlo simulation in this study) and design constraints, the parameters of two diversity factor models are identified by the "model identification" scheme involving four steps as follows. *In the first step*, the diversity factors of both sensible and latent loads (SLDF/LLDF) are calculated based on the individual space loads as shown in Eqs. 5.9-5.10. *In the second step*, the diversity factors are classified into different clusters using the k-means clustering algorithm (Meesrikamolkul, Niennattrakul, & Ratanamahatana, 2012). *In the third step*, the correlations between the diversity factors and working conditions are identified using the decision-tree method (Quinlan, 1986),

which is one of the most commonly-used data mining approaches. *In the fourth step*, the probability distributions of two diversity factors in each cluster are quantified by fitting the data using typical distribution functions. In this study, the datasets (e.g. ambient conditions, sensible load ratio and space loads) of Zone 1 were used to quantify the diversity factors and train the diversity factor models, while the datasets of Zone 2 and Zone 3 were used to validate the models.

The detailed approaches for the quantification of load diversities of multiple spaces in a zone considering uncertainties are elaborated as follows.

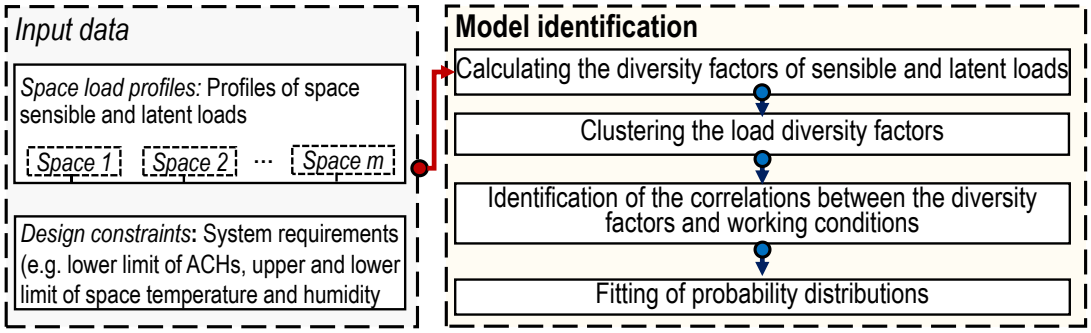

Figure 5.3 Main steps of proposed probabilistic diversity factor method

Clustering the load diversity factors: The task of this step is to categorize the data of the load diversity factors into proper clusters/subgroups, according to their magnitude and pattern. The k-means algorithm (Meesrikamolkul et al., 2012) is employed to ensure: *i).* instances in the same cluster have high similarity, and *ii).* instances in different clusters have low similarities. In the clustering process, the dissimilarity of the diversity factors is evaluated using the Euclidean distance (Han, Pei, & Kamber, 2011) and the optimal number of clusters is evaluated by the Calinski-Harabasz (C-H) criterion (Maulik & Bandyopadhyay, 2002).

Identification of the correlations between the diversity factors and working conditions: The task of this step is to create a decision tree model that predicts the value of *target*

variables based on *predicted variable*s of the dataset. The target variables of the decision tree are the number of a cluster (i.e. Cluster 1, 2, …, n). The predicted variables are the ambient and internal load conditions, including the mean outdoor air temperature (T_{avg}), humidity (W_{avg}) and sensible heat ratio (SHR_{sum}) during the operating period (i.e. 9:00-18:00) of a day, where SHR_{sum} is the ratio of the total sensible cooling load to the total cooling loads of all spaces associated to an AHU, as shown in Eq. 5.13.

$$SHR_{sum} = \frac{\sum_{k=1}^{m} Q_{sen,k}}{\sum_{k=1}^{m} Q_{tot,k}} \tag{5.13}$$

The dataset (including predicted variables and target variables) is automatically and randomly split into two subsets, marked as "training set" (i.e. 3/5 of total data) and "testing set" (i.e. 2/5 of total data). The standard classification and regression trees (CART) algorithm (Breiman, Friedman, Stone, & Olshen, 1984) is employed to generate the decision tree using the training set. The decision tree is validated by cross-validation (using the test set) to estimate the statistical performance of the classification.

Fitting of the probability distribution for clusters: The task of this step is to fit the probability distributions for each cluster. For each cluster, the probability distributions of diversity factors (in each hour) are firstly fitted using four commonly-used probability density functions (PDFs): i.e. Normal distribution, Gamma distribution, Weibull distribution and Lognormal distribution (Forbes, Evans, Hastings, & Peacock, 2011). The detailed functions can be found in Table 5.1. The parameters defining these four PDFs are estimated based on the commonly-used the maximum likelihood method (Holland, Fitz-Simons, & Hopke, 1982) while the Kolmogorov-Smirnov (K-S) test is introduced as the error metric to evaluate the fitness of each PDF (Weber,

Leemis, & Kincaid, 2006). The minimum K-S error of the four distributions is then selected as the target distribution function, where 'K-S error' is the maximum absolute difference between the CDFs of the distributions of the two data vectors, as shown in Eq. 5.14.

$$K - S\ error = max\ (|\hat{F}_1(x) - \hat{F}_2(x)|) \tag{5.14}$$

Table 5.1 Detailed descriptions of four commonly-used probability distribution functions

Distribution	Probability density function	Coefficient description
Normal	$f(x\|\mu,\delta) = \frac{1}{\delta\sqrt{2\pi}} e^{\frac{-(x-\mu)^2}{2\delta^2}}$	μ is the mean parameter, and σ is the standard deviation parameter.
Lognormal	$f(x\|\gamma,\emptyset) = \frac{1}{x\emptyset\sqrt{2\pi}} e^{\frac{-(lnx-\gamma)^2}{2\emptyset^2}}$	γ is the mean parameter of ln(x) and $\emptyset$ is the standard deviation parameter of ln(x)
Gamma	$f(x\|\alpha,\beta) = \frac{x^{\alpha-1}e^{(-\frac{x}{\beta})}}{\beta^{\alpha}\Gamma(\alpha)}$	α is a shape parameter, β is an inverse scale parameter, and $\Gamma(\alpha)$ is a complete Gamma function
Weibull	$f(x\|\lambda,k) = \frac{k}{\lambda}(\frac{x}{\lambda})^{k-1}e^{(-\frac{x}{\lambda})^k}$	λ is the scale parameter, and k is the shape parameter

5.4 Detailed description of optimization method

Energy models are developed in Chapter 3.3 to estimate the energy performance of the air-conditioning systems under different load and ambient conditions, which are controlled ideally by the ventilation strategies concerned respectively. The optimal design of the system for implementing the "adaptive full-range decoupled ventilation (ADV) strategy" is the focus of this study compared with that of the other three ventilation strategies. The ADV strategy is a recommended ventilation strategy for cleanrooms, which takes into account the interaction among different air-conditioning components/zones and provides systems with the robustness to operate at high energy efficiency under ever-changing dynamic working conditions. A Genetic Algorithm

(GA) (Vose, 1999) is used to minimize the overall annualized total cost ($C_{OT,a}$) (i.e. the objective function: Eq. 5.1). The capital cost (C_C) includes the investment (*Inc*) and installation cost (assumed as 30% of the investment cost as shown in Eq. 5.15 (Hang et al., 2014)). The investment cost (*Inc*) includes the costs of major components, such as fans, ducts, cooling coils, heaters, economizer, etc. The unit price of air-conditioning components in this study is presented in Appendix A, where the length of the MAU duct (len_{duct}) is set as 15 m. The annualized maintenance cost ($C_{M,a}$, Eq. 5.16) is assumed as 20% of the annualized capital cost (Henning, 2004). The operation or energy cost (annualized as shown in Eq. 5.17) includes the cost of electricity consumed by the cooling/heating equipment and fans, calculated according to the air-handling processes of the selected ventilation strategy. The electricity cost is calculated using the local electricity price in Hong Kong, which takes the average price of 0.141 USD/kWh (CLP Hong Kong, 2018). The penalty cost (C_P) is introduced as a "virtual expense" to quantify the service quality dissatisfaction due to insufficient cooling or heating capacity. It is quantified by the accumulation of unmet demand multiplied by a penalty price ($£_{pen}$) (Eq. 5.19), where *CRF* is the capital recovery factor, the weighting factor for calculating the present value of an annuity (a series of equal annual cash flows, Eq. 5.20). *i'* is the real discount rate (Eq. 5.21) accounting for the general inflation rate (i_g) and the discount rate (i_d). *i''* is the effective discount rate adjusted for energy inflation (Eq. 5.22) accounting for the general inflation rate (i_g) and the energy inflation rate (i_e). i_d, i_g and i_e are set as typical values of 8%, 4% and 5% respectively (Daud & Ismail, 2012). *N* is the lifetime of air-conditioning systems, which is set as 20 years.

$$C_{C,a} = C_C \cdot CRF(i', N) = C_I(1 + 30\%) \cdot CRF(i', N) \tag{5.15}$$

$$C_{M,a} = C_{C,a} \cdot 20\% \tag{5.16}$$

$$C_{O,a} = C_O \cdot [\frac{CRF(i',N)}{CRF(i'',N)}] \quad (5.17)$$

$$C_{P,a} = C_P \cdot [\frac{CRF(i',N)}{CRF(i'',N)}] \quad (5.18)$$

$$C_P = £_{pen} \cdot \sum_{j=1}^{8760} max(0, D_{emand}(j) - C_{apacity}) \quad (5.19)$$

$$CRF(rate, year) = \frac{rate \cdot (1+rate)^{year}}{(1+rate)^{year}-1} \quad (5.20)$$

$$i' = \frac{i_d - i_g}{1+i_g} \quad (5.21)$$

$$i'' = \frac{i_d - i_e}{1+i_e} \quad (5.22)$$

Different from the ventilation strategies applied in general buildings, such as office buildings and commercial buildings, the ADV strategy is applicable for cleanrooms or spaces requiring strict humidity/temperature controls, such as pharmaceutical cleanrooms, semiconductor/microchip factories and hospitals. The key issue of the ADV strategy is to identify the optimal operation mode under different ambient and internal load conditions. At the design stage, the optimal operation mode when adopting the ADV strategy can be identified based on the information of possible building cooling load profiles and ambient conditions. For the design optimization of the air-conditioning systems facilitating the ADV strategy, an overall trade-off between the satisfaction of service and system costs is made as shown in Figure 5.4. With the decrease of service satisfaction (or component capacities), the operation (energy) cost increases first due to the limited choice of operation modes (from optimum to suboptimum) and then decreases due to the insufficient capacities (i.e. under-provision). The overall total cost decreases first and then increases after it reaches the minimum at point “O”, which is the target point indicating the optimal capacity. Since the performance robustness of air-conditioning systems is the main concern in the design of cleanrooms, a higher penalty price (i.e. greatly larger than

local electricity price in Eq. 5.19) is usually set to avoid insufficient air-conditioning component capacities. When the component capacities are relatively small (i.e. insufficient cooling/heating capacities), the penalty cost can be higher than the operation cost. The decrease in the total cost is mainly due to the decrease in the penalty cost. In contrast, when the component capacities become larger, the required cooling loads of MAU/AHU can be met at most of the operation period, and the penalty cost can be close to zero. The ADV strategy provides various operation modes and, in operation, the most economic mode will be selected in a particular working condition. The ADV strategy has the lowest operation cost and superior energy performance compared with that of adopting the other three existing ventilation strategies (i.e. IC, PD and DV). The optimal design method minimizes the overall annualized total life-cycle cost and therefore makes a proper compromise between the satisfaction of service and system life-cycle costs.

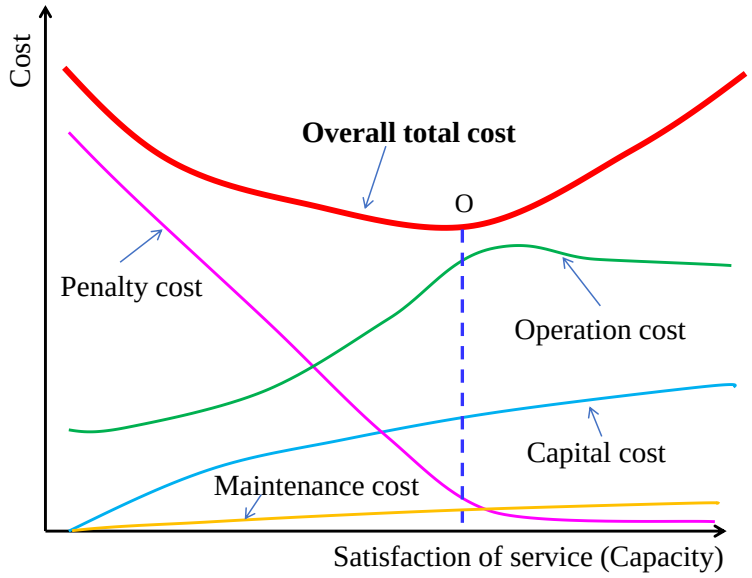

Figure 5.4 Cost vs. capacity of air-conditioning systems facilitating ADV strategy

The method and procedure to estimate the penalty cost due to insufficient capacity are shown in Figure 5.5. The actually available choices of operation modes in a particular

load/ambient condition are subject to the provision of sufficient capacities of all components needed for the operation modes concerned. At each time step of performance evaluation, for the trial component capacities given by the optimizer, the feasibilities of utilizing optimal/suboptimal operation modes are assessed by verifying whether the required component capacities are satisfied. The best available mode is then chosen as the actual operation mode. If required component capacities of all operation modes cannot be satisfied, i.e., the system fails to provide satisfactory performance, a penalty cost (C_p) would be given (that hour is also called as 'unmet hour' (Uh)). Due to the different control modes provided by the ADV strategy, the ADV strategy can choose the optimal mode that can satisfy the control requirements under the given capacities of air-conditioning components and working conditions. This indicates the ADV strategy can offer superior service satisfaction (less unmet hour) due to the operation mode switching compared with other ventilation strategies.

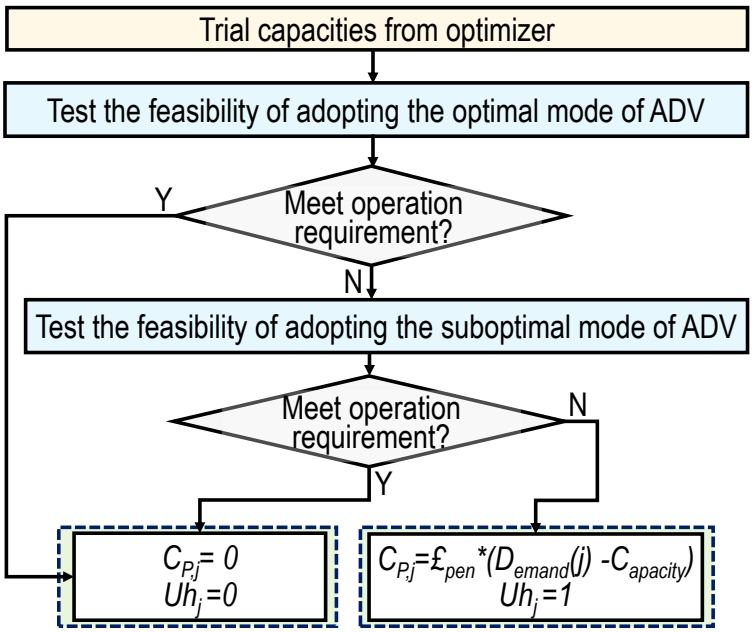

Figure 5.5 Procedure to estimate penalty cost/unmet hour facilitating ADV strategy

5.5 Case study

5.5.1 Building/system description and load characteristics

For the cleanrooms concerned, the configuration of a typical cleanroom air-conditioning sub-system was selected as shown in Table 5.2. In this sub-system, an MAU serves three AHUs, and each AHU serves several cleanrooms on the 2nd floor with constant air flowrate (i.e. 20 ACH). The system configuration of the selected system is similar to Figure 5.1, while the difference is that the humidifier is not adopted due to the humid outdoor conditions in Hong Kong.

Table 5.2 Cleanroom subsystem configuration and control requirements

Floor area of the served zones	Zone 1: Total 100.5 m^2 (9 spaces served by AHU-1)	
	Zone 2: Total 121 m^2 (8 spaces served by AHU-2)	
	Zone 3: Total 151 m^2 (8 spaces served by AHU-3)	
Height of the served zones	2.8 m	
Operating period	9:00-18:00	
Installed fans specification	MAU fan (centrifugal) pressure (Pa)	1,600
	AHU fan (axial) pressure (Pa)	1,350
	Fan efficiency (%)	60
The overall coefficient of performance (COP) of systems	Cooling system (central cooling)	2.5 (constant)
	Heating system (electric heater)	1.0 (constant)
Space control requirements	Temperature (°C)	20±3
	Relative Humidity (%)	55±10
	Supply airflow rate (ACH)	≥20
	Outdoor airflow rate (ACH)	≥2

TRNSYS 18 (2017) was used to calculate the probabilistic sensible and latent cooling loads of the selected multi-zone cleanroom systems considering weather, building and internal load uncertainties. Totally 950 (38×25) sets of samples were used to obtain the uncertain sensible and latent cooling loads for spaces in each zone. The weather

uncertainty was introduced by using historical weather data of 38 years (1979 to 2016) instead of one typical year. Building parameter and internal load uncertainties were introduced by randomly sampling according to their distributions. Eventually, 25 sets of their samples were selected. The weather, building and load parameters and their uncertainties are shown in Table 5.3. It is worth noticing that, the weather and building parameters were sampled and set as the same for all the spaces associated to a zone, while the internal loads were sampled independently for different spaces concerning their asynchronous behaviors.

Table 5.3 Weather, building and load parameters and their uncertainties for cooling load calculation

Group	Parameter	Uncertainty analysis	
		Distribution	Values
Weather	Outdoor dry-bulb air temperature (°C)	Actual data: 1979–2016	
	Outdoor air relative Humidity (%)		
	Global radiation (W/m^2)		
	Diffuse radiation (W/m^2)		
Building parameter	Internal shading coefficient	Normal	$(0.5, 0.1^2)$
	External shading coefficient	Normal	$(0.2, 0.05^2)$
	Conductivity of window ($W/(m^2 \cdot K)$)	Uniform	(1.5, 3)
Indoor condition	Occupant density (m^2/person)	Triangular	10 × triangular (0.3, 1.2, 0.9)
	Lighting density (W/m^2)	Triangular	14 × triangular (0.3, 1.2, 0.9)
	Process sensible load (W/m^2)	Relative normal	45 × normal $(1, 0.06^2)$
	Process latent load (W/m^2)	Relative normal	15 × normal $(1, 0.06^2)$

Figure 5.6 shows the cumulative distribution functions (CDFs) of space/zone loads served by three AHUs. Although the spaces in a zone had similar functions, the cooling load profiles were different. The cooling load (W/m^2) of a zone is the weighted

average of the cooling loads of spaces in this zone. It can also be seen that the peak cooling load of a zone had a high probability to be lower than that of the simple sum of peak loads of individual spaces. In the air-conditioning design, the actual cooling/heating demands of the components (serve for a zone) are significantly influenced by the cooling load of the critical space particularly when both temperature and humidity are controlled. It is especially great for the cleanroom air-conditioning systems which have very high air flow rates and employ CAV systems (Zhou et al., 2016). This indicates that if the total sensible and latent cooling loads of a zone are directly used for sizing the components, the systems will be of high possibility to be undersized significantly. It confirms that the load diversity effects of multiple spaces should be taken into account in the system design.

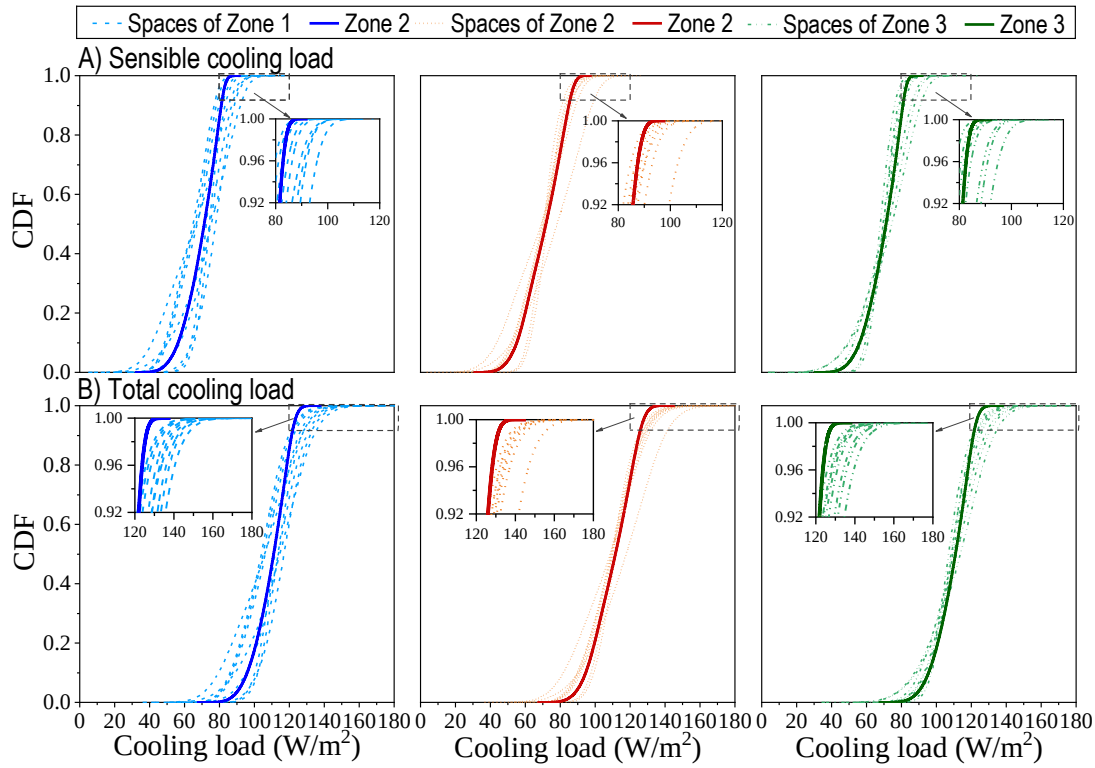

Figure 5.6 Distribution of cooling loads in multiple spaces/zones

5.5.2 Training of diversity factor models

Clustering the load diversity factors: Figure 5.7 shows the distributions of space load diversity factors of Zone 1 calculated by Eqs. 5.9-5.12, by fully considering constraints/interaction among multiple spaces and the cooling loads of the critical space. It can be seen that estimated kernel density estimation functions well matched the histograms of both the diversity factors. 95% confidence interval of sensible/latent cooling load diversity factors were in the range of [1.06, 1.38] and [1.48, 2.89], respectively. This indicates that the actual cooling demands were significantly larger than the cooling loads of the corresponding zone. Figure 5.8 shows the clustering performance evaluated by the Calinski-Harabasz criterion (Caliński & Harabasz, 1974) using the Statistics and Machine Learning Toolbox™ in MATLAB. By comparing the performance of clustering solutions containing two to six clusters, both the diversity factors of sensible cooling load and latent cooling load were grouped into two clusters/subgroups. Figure 5.9 shows the results of categorizing the diversity factors into an optimal number of clusters, where the blue line is the centroid curve of diversity factors in a cluster. The diversity factors of sensible cooling load were categorized into two clusters (i.e. Cluster A-1 and Cluster A-2). Cluster A-1 represents that sensible cooling loads of multiple spaces had high similarity while Cluster A-2 represents that sensible cooling loads of multiple spaces had low similarity. The diversity factors of latent cooling load were categorized into two clusters (i.e. Cluster B-1 and Cluster B-2). Cluster B-1 represents that the latent cooling loads of multiple spaces had low similarity while Cluster B-2 represents that the latent cooling loads of multiple spaces had high similarity.

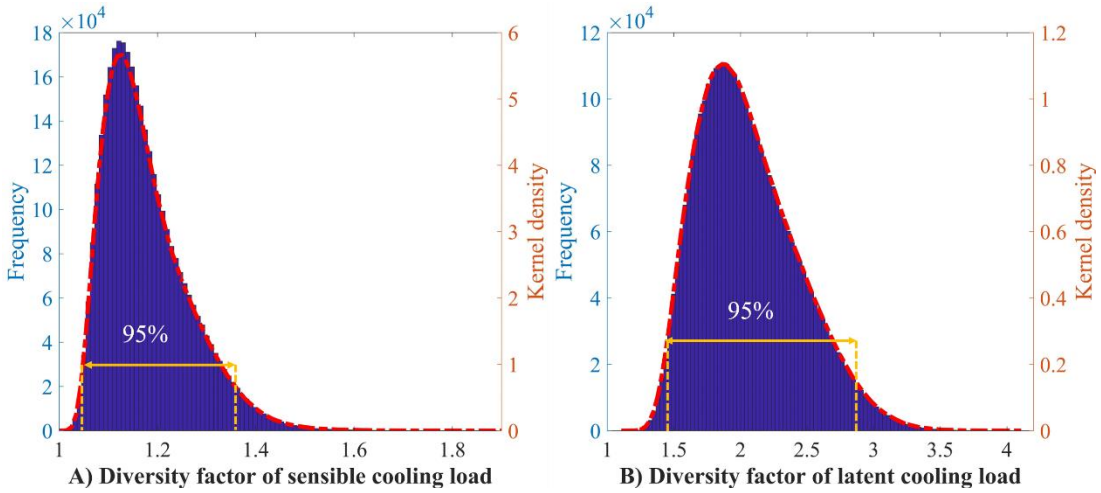

Figure 5.7 Histograms and Kernel density estimation functions of diversity factors

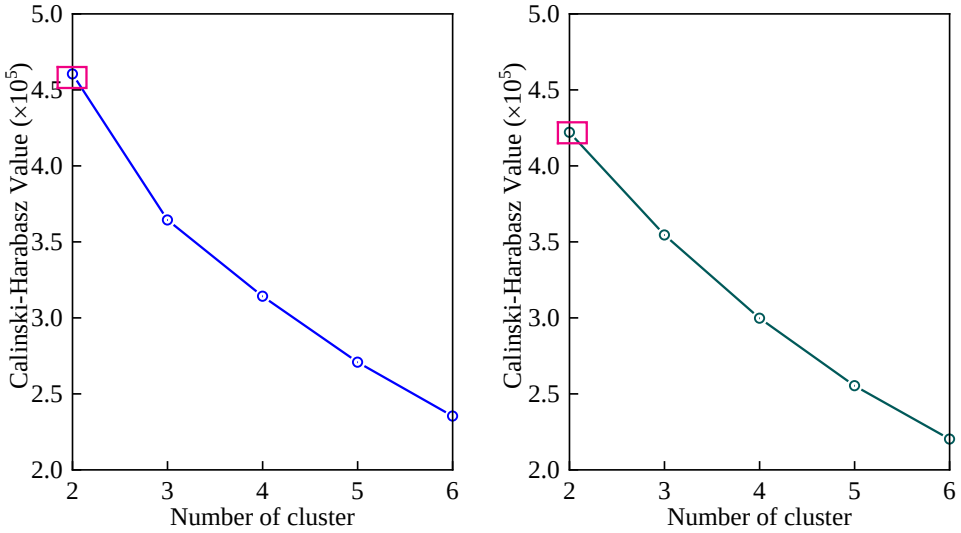

Figure 5.8 Clustering performance for different numbers of clusters

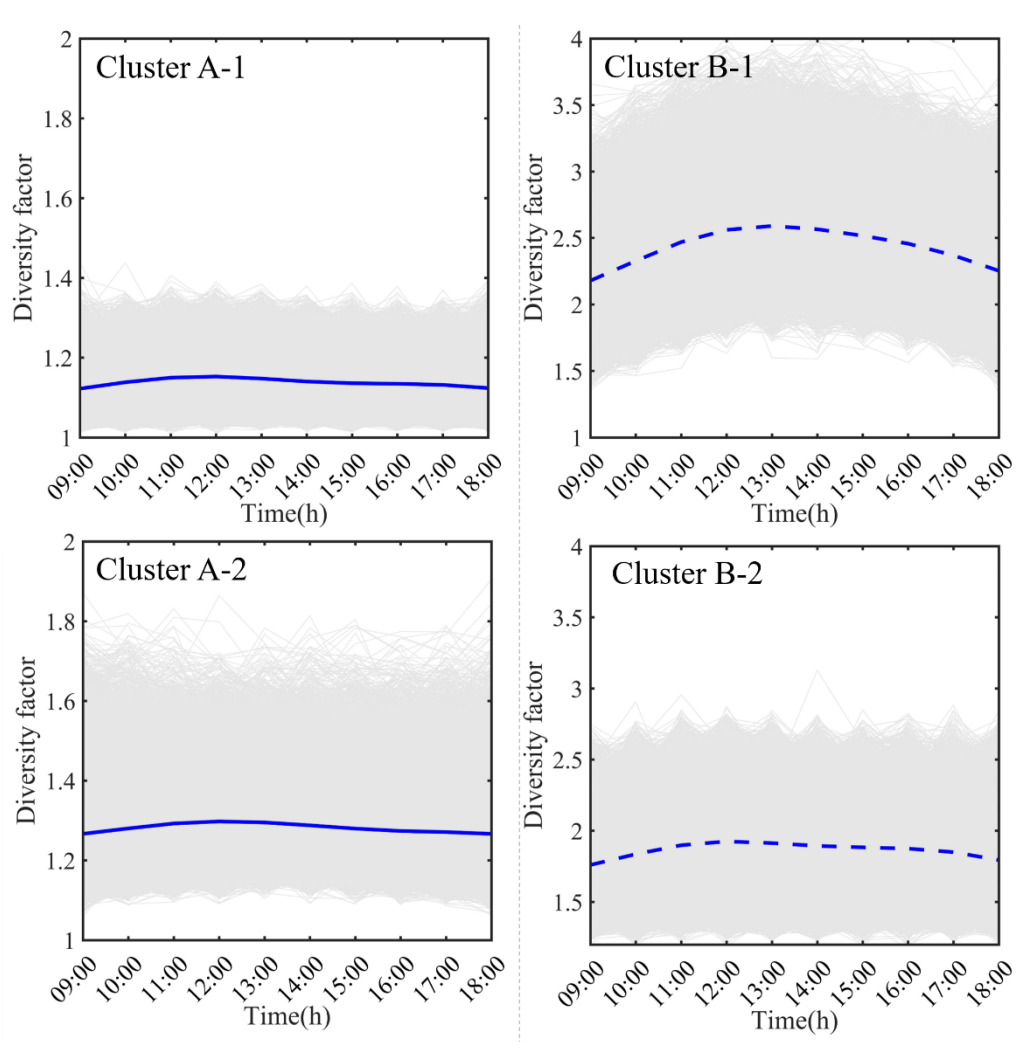

A) Diversity factor of sensible cooling load **B) Diversity factor of latent cooling load**

Figure 5.9 Clustering results for each subgroup

Correlations between the diversity factors and working conditions: Based on predicted variables (i.e. SHR_{sum}, T_{avg} and W_{avg}), decision trees and decision rules can be utilized to predict target variables (i.e. the number of a cluster) as shown in Figure 5.10. The accuracy of the decision trees should be evaluated before being applied to the datasets of other zones (i.e. Zone 2 and 3). Table 5.4 shows that 91.6% and 87.0% of all the training records were correctly classified for the target clusters of sensible cooling load diversity factor (SLDF) and latent cooling load diversity factor (LLDF), respectively. Accordingly, the obtained decision trees were applied to the testing sets and the results are also given in Table 5.4. The result shows that 91.0% and 86.0% of the testing

records were correctly classified for the target clusters of SLDF and LLDF, respectively. This indicates a good accuracy of the decision tree models which can be further applied to a new dataset for classification and prediction.

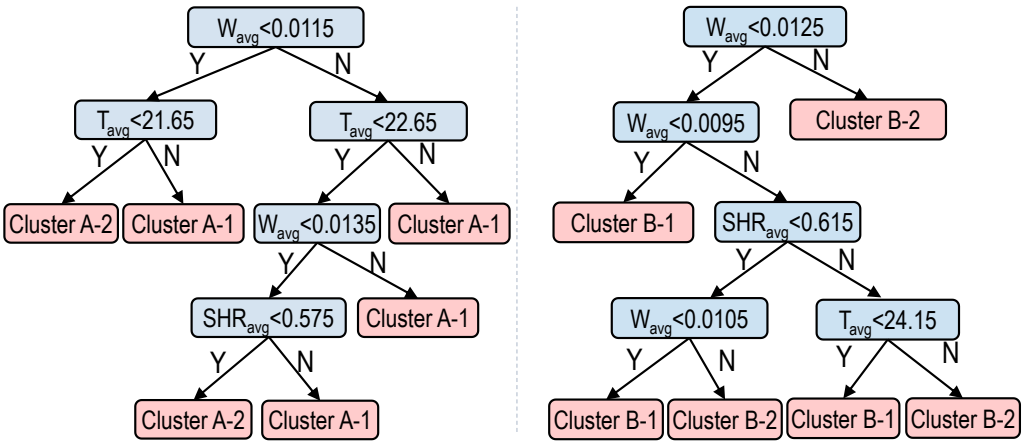

A) Diversity factor of sensible cooling load B) Diversity factor of latent cooling load

Figure 5.10 Decision trees for prediction of target clusters

Table 5.4 Classification performance of the decision tree models

Dataset	Decision tree	Predicted cluster	Correct/total number	Accuracy
Training set	Decision tree for prediction of target clusters (SLDF)	Cluster A-1	141,919/151,046	91.6%
		Cluster A-2	48,757/57,004	
	Decision tree for prediction of target clusters (LLDF)	Cluster B-1	52,630/62,913	87.0%
		Cluster B-2	138,046/145,137	
Testing set	Decision tree for prediction of target clusters (SLDF)	Cluster A-1	111,783/119,762	91.0%
		Cluster A-2	35,737/42,325	
	Decision tree for prediction of target clusters (LLDF)	Cluster B-1	38,885/47,822	86.0%
		Cluster B-2	108,635/114,265	

The probability distribution for clusters/subgroups: The diversity factor in each cluster was then used to fit the probability distributions using the four alternative PDFs listed in Table 5.1. By selecting the distributions with the minimum K-S error, the fitted

PDFs and the identified parameter values of the diversity factors are listed in Table 5.5.

Table 5.5 Identified probability distribution functions and parameter values for the fitted probability density functions of diversity factors

Time	Cluster A-1	Cluster A-2	Cluster B-1	Cluster B-2
	Distribution (Parameter)	Distribution (Parameter)	Distribution (Parameter)	Distribution (Parameter)
9:00	Logn (0.11,0.040)	Logn (0.23, 0.062)	Logn (0.77, 0.126)	Logn (0.56 0.114)
10:00	Logn (0.13,0.043)	Logn (0.25, 0.058)	Logn (0.84, 0.116)	Gam (69.55, 0.026)
11:00	Gam (497.7, 0.002)	Logn (0.25, 0.056)	Logn (0.90, 0.114)	Norm (1.92, 0.246)
12:00	Logn (0.14, 0.045)	Logn (0.26, 0.054)	Logn (0.93, 0.113)	Gam (60.67, 0.032)
13:00	Logn (0.14, 0.044)	Gam (359.1, 0.004)	Logn (0.95, 0.111)	Gam (62.79, 0.032)
14:00	Gam (561.9, 0.002)	Logn (0.25, 0.052)	Logn (0.94, 0.108)	Gam (62.79, 0.030)
15:00	Logn (0.13,0.040)	Logn (0.25, 0.052)	Logn (0.92, 0.105)	Gam (65.82, 0.029)
16:00	Logn (0.13,0.039)	Gam (358.5, 0.004)	Logn (0.89, 0.103)	Gam (68.79, 0.027)
17:00	Logn (0.12,0.039)	Logn (0.24, 0.055)	Logn (0.86, 0.110)	Gam (71.67, 0.026)
18:00	Logn (0.12,0.039)	Logn (0.23, 0.059)	Logn (0.80, 0.126)	Logn (0.58 0.119)

* Note: Logn, Gam, Norm represent Lognormal, Gamma and Normal distribution, respectively.

5.5.3 Validation of diversity factor models

The diversity factor models were validated using the datasets of Zones 2 and 3 (i.e. served by AHU-2 and AHU-3 respectively). Figure 5.11 shows the CDFs of the cooling loads and demands of the two zones. The predicted cooling demands represent the cooling demands calculated using the proposed probabilistic diversity factor method. The actual cooling demands represent the cooling demands calculated by Eqs. 5.9-5.12 when fully considering constraints/interaction among multiple spaces and the cooling loads of the critical space. It can be seen that the distributions of cooling demands of these two zones were very close, while the values of the cooling demands were significantly larger than that of the cooling loads. The index of agreement (*d*) (Heo, Choudhary, & Augenbroe, 2012) was used to evaluate the similarity of the predicted and actual cooling demands, as shown in Eq. 5.23, where *A* and *P* are the

actual and predicted values respectively, sorted in ascending order. The actual average value of the cooling demand is denoted by $\bar{A}$. The range of d lied between 0 and 1, with higher values signifying a good fit between the model and data.

$$d = 1 - \frac{\sum_{i=1}^{n}(A_i - P_i)^2}{\sum_{i=1}^{n}(|P_i - \bar{A}| + |A_i - \bar{A}|)^2} \tag{5.23}$$

By calculating the index of agreement of predicted and actual sensible/latent cooling demands, it is found that the four indexes of cooling demands of two zones (also shown in Figure 5.11) were all higher than 0.95. This confirms that the proposed probabilistic diversity factor method is deemed satisfactory, which can be used to effectively quantify the diversity effects of multiple spaces.

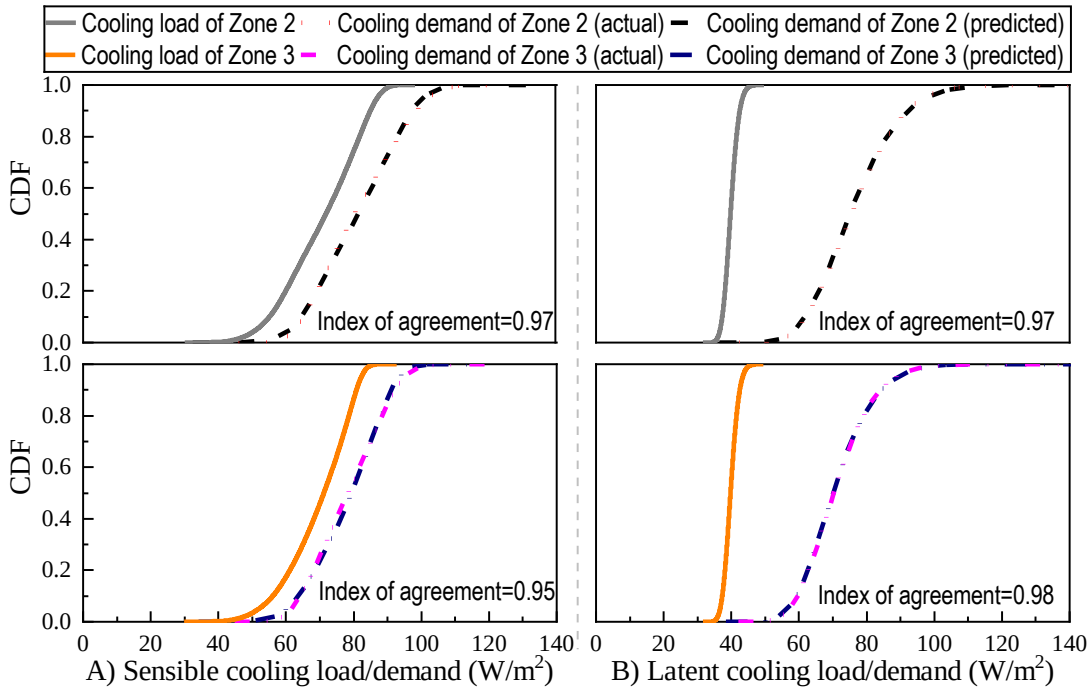

Figure 5.11 Cumulative distribution functions (CDFs) of cooling loads and cooling demands

5.5.4 Performance of air-conditioning systems designed for different ventilation strategies

Referring the actual sizes of the air-conditioning systems and the actual energy consumption of the building, the search ranges for the cooling coil of MAU, the cooling coils of AHUs, the electric heaters of AHUs, and design outdoor air flowrate for different ventilation strategies were set between [0, 300] kW, [0,100] kW, [0, 50] kW and [0.58, 5.80] m^3/s, respectively.

As introduced in Section 5.4, the penalty price affects the design objective. Before a sensitivity study of the penalty price was conducted, the optimization based on a penalty price of 1.41 USD/kWh (i.e. penalty price ratio equals 10) was conducted first and the results are shown in Figure 5.12. In this figure, the "penalty price ratio" (γ_{pen}) is defined as a ratio of penalty price ($£_{pen}$) to the local electricity price ($£_e$) as shown in Eq. 5.24.

$$\gamma_{pen} = \frac{£_{pen}}{£_e} \quad (5.24)$$

Figure 5.12(A) presents the required cooling/heating capacities of the air-conditioning system adopting four different ventilation strategies (ADV, DV, PD and IC). In general, the capacities of components adopting the ADV strategy were in-between that of the other three ventilation strategies. The DV strategy required the highest cooling capacity of MAU, which can be 2.4, 5.8 and 8.9 times that of the ADV, PD and IC strategy, respectively. The PD strategy required the highest heating capacities while the IC strategy required the highest cooling capacities of all three AHUs. Figure 5.12 (B) shows the design outdoor air flowrate for different ventilation strategies. The IC strategy required the largest design volume of outdoor airflow (i.e. 5.26 m^3/s or 18 ACH) due to the involvement of the enthalpy-based economizer. The PD strategy

required the minimum (i.e. 0.58 m^3/s or 2 ACH), while the design outdoor air flowrates for the ADV and DV strategy were 72.6% and 68.2% compared with that of the IC strategy. The overall annualized mean total costs of adopting different ventilation strategies are shown in Figure 5.12(C). It can be seen that the overall annualized mean total cost adopting the ADV strategy was reduced by 18.2%, 13.6% and 6.5% compared with that of using the DV, PD and IC strategy respectively.

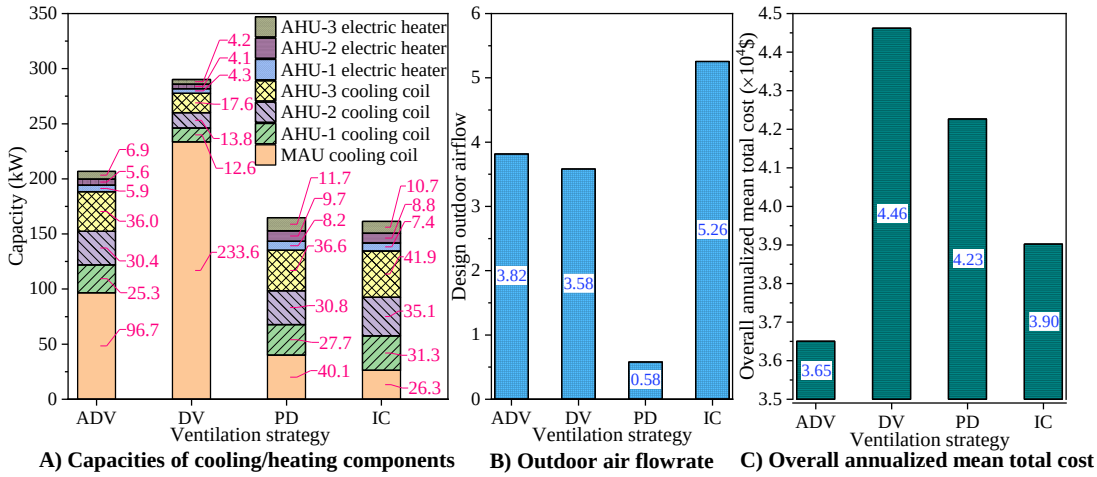

A) Capacities of cooling/heating components **B) Outdoor air flowrate** **C) Overall annualized mean total cost**

Figure 5.12 Optimal air-conditioning sizes and objective value adopting different ventilation strategies

The optimal capacities of the air-conditioning system partially depend on the difference between the electricity price and the penalty price. Therefore, a sensitivity study was conducted to show the effect of the penalty price on the optimal capacities of the air-conditioning system adopting different strategies as shown in Figure 5.13. It can be seen that with the increase of the penalty price ratio, the larger capacities of the components were required. However, when the penalty price ratio was larger than a certain value (i.e. 10), the capacities of air-side components adopting all ventilation strategies varied only with little difference. Under a certain penalty price ratio, the capacities of the components adopting the ADV strategy were in-between that of the other three ventilation strategies.

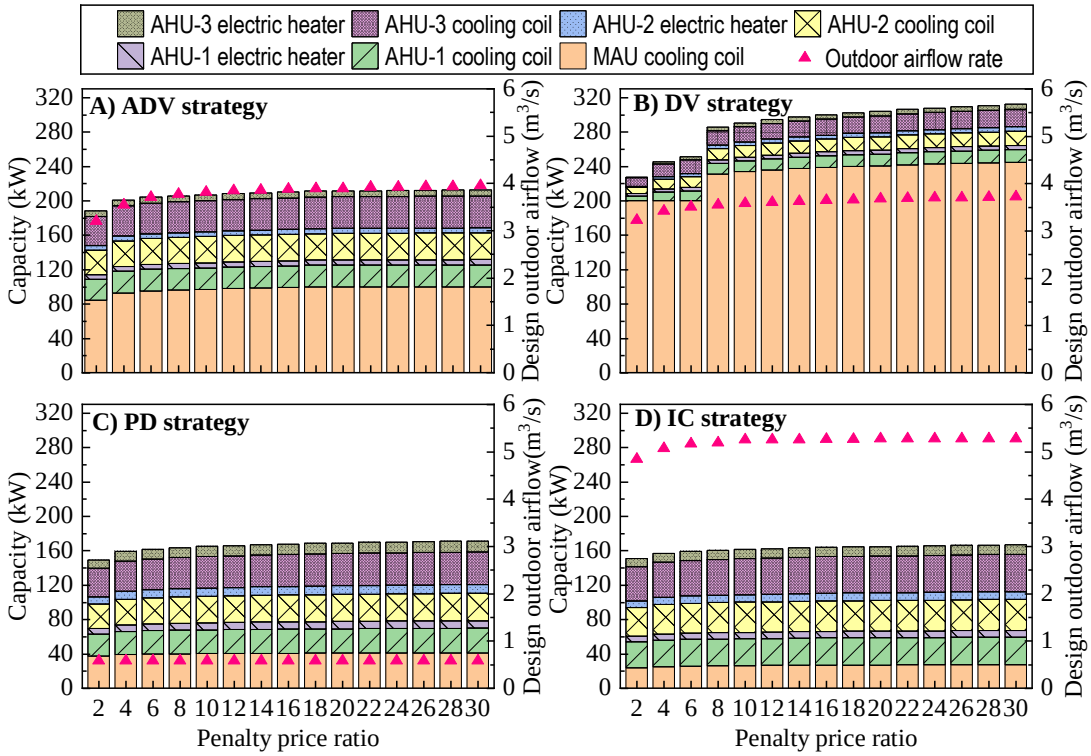

Figure 5.13 Optimal sizes at different penalty price ratios adopting different ventilation strategies

In some practical cases, the number of hours when the cooling or heating capacity cannot meet the required demands (namely unmet hour) are also concerned by the designers to quantify the deficiency in the cooling or heating capacity (i.e. the dissatisfaction of service). It is worth noticing that, in this study, the unmet hour was also affected by the ventilation strategy selected due to the coordination and interaction among these components/processes in different operation conditions. The overall annualized mean total cost (objective) and the corresponding annual mean unmet hour adopting the four ventilation strategies at different penalty price ratios are shown in Figure 5.14. In general, the annual mean unmet hour decreased with the increase of the overall annualized mean total cost. However, both the overall annualized mean total cost and annual mean unmet hour of systems adopting the ADV strategy were significantly lower than that of the other three strategies, especially for the cases with high penalty price ratios (i.e. larger than 2). This indicates the air-

conditioning system, which was designed for the ADV strategy using the proposed design method, can offer superior energy and economic performance as well as the satisfaction of service (represented by the unmet hour) than the other three ventilation strategies. It is also worth noticing that a higher penalty price would ensure the air-conditioning system with a higher level of service satisfaction (more cooling/heating demands can be met and lower annual mean unmet hours). Under a low penalty price ratio (i.e. penalty price ratio=2), the annual mean unmet hour of the air-conditioning system adopting the ADV strategy was about 468 h, slightly higher than that of adopting the IC strategy (450 h), significantly lower than that adopting the DV (1,223 h) and PD strategies (856 h). When the penalty price ratio was larger than 10, the annual mean unmet hour was smaller than 35 h by adopting the ADV strategy, significantly lower than that associated to the other three ventilation strategies. This indicates that the penalty price ratio should be properly set especially for the cleanroom system requiring a high level of service satisfaction.

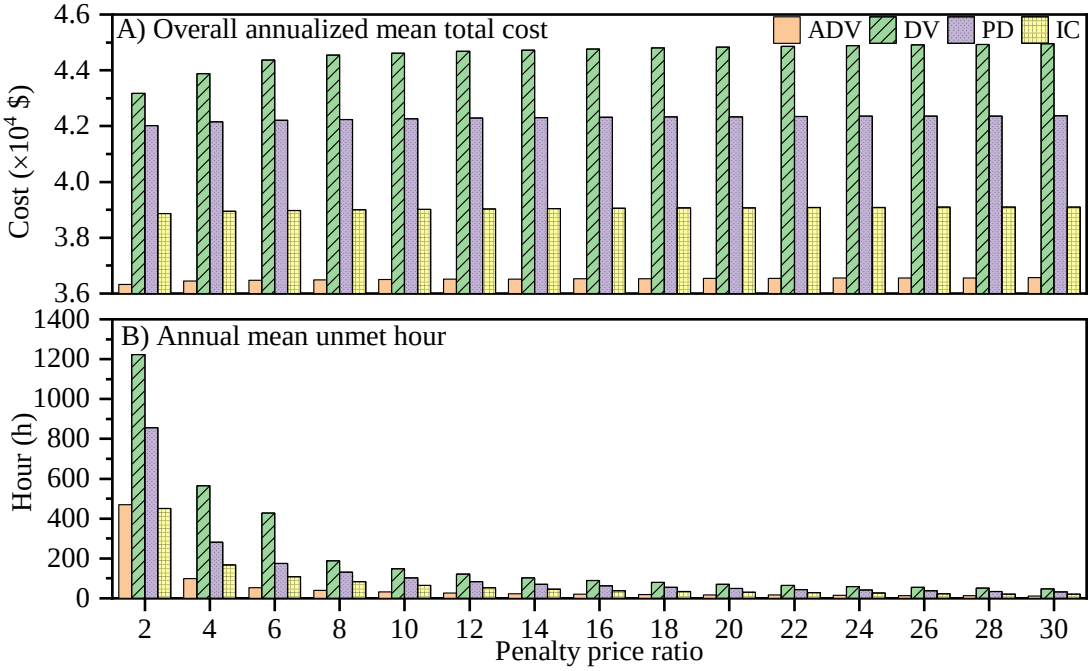

Figure 5.14 Overall annualized mean total cost and annual mean unmet hour at different penalty price ratios

5.6 Summary

An uncertainty-based robust optimal design method of air-conditioning systems was developed for cleanrooms/spaces requiring strict temperature and humidity controls, which facilitates optimal ventilation control strategies to be implemented successfully under uncertainties. To consider the effects of asynchronous loads in different zones/spaces with reduced computation demand, a probabilistic diversity factor method was proposed, which is a simplified method to quantify the uncertainty of space load diversity in multiple zones/spaces using a diversity factor. The proposed design method was implemented and validated in the design optimization of air-conditioning systems for implementing four different ventilation control strategies with full consideration of possible and uncertain off-design conditions. Based on the results and analysis of a case study, detailed conclusions can be made as follows.

i. The proposed uncertainty-based robust optimal design method offers optimal and energy-efficient alternatives for cleanroom air-conditioning system design, facilitating different ventilation control strategies.
ii. The air-conditioning system, which is designed for the "adaptive full-range decoupled ventilation (ADV) strategy" using the proposed design method, offers the superior economic performance and satisfaction of service compared with systems designed for other ventilation strategies. The overall annualized mean total cost of the systems designed for the ADV strategy could be reduced by 18.2%, 13.6% and 6.5% compared with that of the systems designed for the DV, PD and IC strategy respectively in the selected case.
iii. The diverse behaviour of multiple zones/spaces has significant effects on the cooling demand of components, and thus the sizing of optimal design. The design

approach without considering the diverse behaviour of multiple spaces will result in undersized problems for some components. It is recommended to conduct uncertainty quantification of load diversity when estimating the cooling loads of system and components at the design stage.

iv. The introduction of two probabilistic diversity factors using the proposed probabilistic diversity factor method is very effective to quantify the effects of load diversities in multiple zones/spaces.

v. The optimal capacities of the components are affected significantly by penalty prices. The optimal component capacities become larger at higher prices. In the selected case, when the penalty price ratio was larger than 10, the optimal design capacities of air-side components vary only within a small range. The penalty price ratio needs to be properly set, in order to obtain a system with desirable life-cycle costs and satisfaction of service.

It is worth noticing that the diversity factor models were trained using the building simulation tools and validated in specific cases in this study. To improve/ensure the accuracy of the diversity factor models in a particular application, operation or simulation data of typical representative working conditions relevant to the application case are needed in the model training. To obtain more generic models to extend their application scope, different types of building data, such as the number of spaces, zone orientation, space function, working schedules, etc., are also needed for training the models.

It is also worth noticing that, in this study, the design optimization of the cleanroom air-conditioning systems was conducted under the condition that ideal controls were adopted to achieve the intended operation of specific ventilation strategies. For the ADV strategy, the required system configuration was the same as that of the existing

ventilation strategies. However, the successful implementation of the ADV strategy requires the supervisory controller to identify the best operation mode. In actual applications, an online control strategy is needed to ensure the actual achievement of the ventilation strategy systems concerning measurement uncertainties and component degradation, which needs further investigations.

CHAPTER 6 RISK-BASED ONLINE ROBUST OPTIMAL CONTROL OF CLEANROOM AIR-CONDITIONING SYSTEMS CONSIDERING MEASUREMENT UNCERTAINTIES

Besides appropriate design, online supervisory control is also essential for the successful implementation of the ADV strategy, in order to achieve energy-efficient operation of cleanroom air-conditioning systems in practical applications. In this chapter, a risk-based online robust optimal control strategy for multi-zone cleanroom air-conditioning systems is proposed, which minimizes the energy consumption by properly selecting the control mode considering measurement uncertainties and component performance degradation. The proposed control strategy is tested and implemented in a dynamic simulation platform based on an existing pharmaceutical industrial building in Hong Kong located in a subtropical region.

This chapter is organized as follows. The challenges concerned in the online control of cleanroom air-conditioning systems are presented in Section 6.1. Section 6.2 presents the overall structure of the risk-based online robust optimal control strategy. Section 6.3 presents the detailed procedure and steps of the risk-based online robust optimal control strategy. Section 6.4 presents a real-time dynamic simulation platform of a pharmaceutical building and its air-conditioning systems, which is developed to implement the proposed control strategy. In addition, the coefficients of the adaptive models are identified. Section 6.5 presents the test and implementation results of the

proposed online control strategy on the simulation platform. Conclusive remarks are given in Section 6.6.

6.1 Challenges addressed for cleanroom air-conditioning system control

The proposed "adaptive full-range decoupled ventilation (ADV) strategy" includes various modes for different ambient and internal load conditions. However, due to the complexity of air-conditioning systems with counteractant processes and the dynamic nature of the working conditions, errors and uncertainties in measurements might lead to improper selection of system operation modes, which often results in huge energy waste. These challenges are the main issues to be addressed in developing the risk-based online robust optimal control strategy, which are summarized as follows:

i. Different sources of measurement uncertainties are needed to be quantified effectively. The measurements in the cleanroom air-conditioning systems, such as temperature, humidity and air flowrate, suffer easily from measurement noises, outliers and biases. The measurement errors can significantly influence system online control decisions.
ii. Models for online use are needed to be adaptive to component performance degradation. Even if the models can be well trained at the initial stage, the model prediction errors of component capacities can be significant due to changes of component performance.
iii. The correlations between different control modes are needed to be identified. To evaluate the performance of different control modes online, the energy

performance of other operation modes is needed to be evaluated/predicted using the available data of current operation mode.

iv. An online optimal decision-making scheme is needed to select the optimal mode by compromising between the risks and benefits of adopting different control modes.

6.2 Assessment of decision-making risks due to measurement uncertainties

A risk-based approach is adopted to support robust decision-making, "aiming for an optimal balance between acceptable levels of risk and the costs of further risk reduction" in the face of uncertain information (Kuklicke & Demeritt, 2016). This approach can be found in marketing (Hult, Craighead, & Ketchen David J, 2010), financial (Kuklicke & Demeritt, 2016), ecological (Peterman & Anderson, 1999) and civil infrastructure (Ellingwood & Wen, 2005) fields, which provides flexibility for decision-makers in responding to possible changes that are uncertain or as yet unknown. The main advantage of this approach is that the risks and benefits of decisions are evaluated by quantifying the propagation of "aggregated uncertainties" instead of considering the uncertainty of each source.

6.2.1 Overall structure of risk-based online robust optimal control strategy

Figure 6.1 shows the overall structure of the risk-based online robust optimal control strategy, which involves decision-making approaches and adaptive control at two levels. At the local level, local feedback process controllers control the process outputs at their optimum or predetermined set-points according to the control mode determined at the upper level. At the upper level, the optimal control modes for

individual AHUs are determined by the "online optimal decision-making scheme". The scheme compares the risks/benefits of different control modes and selects the optimal mode for each AHU, to achieve energy-efficient and reliable temperature and humidity controls. The control modes available to the system are PD and DV. The differences of control logics between the two modes are highlighted by the different line styles in Figure 6.1.

Control mechanism of PD mode: The fan speed and cooling coil valve opening of the MAU are modulated by pressure and temperature controllers respectively to maintain the air static pressure (i.e. at the sensor location) and outlet temperature at a lower limit (i.e. much lower than indoor air dew-point temperature). The heater output of each AHU is modulated (by a humidity controller) to control the space relative humidity within its allowable range. The cooling of each AHU is modulated (by a temperature controller) to control the supply air temperature at its set-point ($T_{AHU,sp}$). The supply air temperature set-point ($T_{AHU,sp}$) is adjusted (by a temperature reset controller) according to the indoor air temperature. The make-up air damper for each AHU is modulated (by an airflow controller) to control the outdoor airflow at its lower limit ($V_{fh,PD}$), which is the minimum outdoor airflow rate required for maintaining the acceptable indoor air quality or space positive pressure.

Control mechanism of DV mode: The DV mode differs from the PD mode in two ways. First, the setpoint of outdoor airflow ($V_{fh,DV}$) is adjusted (by a humidity controller) according to the indoor air relative humidity (i.e. indoor latent load). Second, the heating of each AHU is seldom used due to the fully decoupled temperature and humidity control loops.

To select the optimal control mode online, two objectives of the online optimal decision-making scheme need to be addressed, including *i*) risk and benefit evaluation of operation modes, and *ii*) optimal control mode. The need and benefits of developing the decision-making scheme are outlined in Section 6.2.2. The mechanism of optimal control mode selection is illustrated in Section 6.2.3. The development of adaptive models to identify the correlations between different modes considering uncertainties for risk and benefit evaluation is presented in Section 6.2.4.

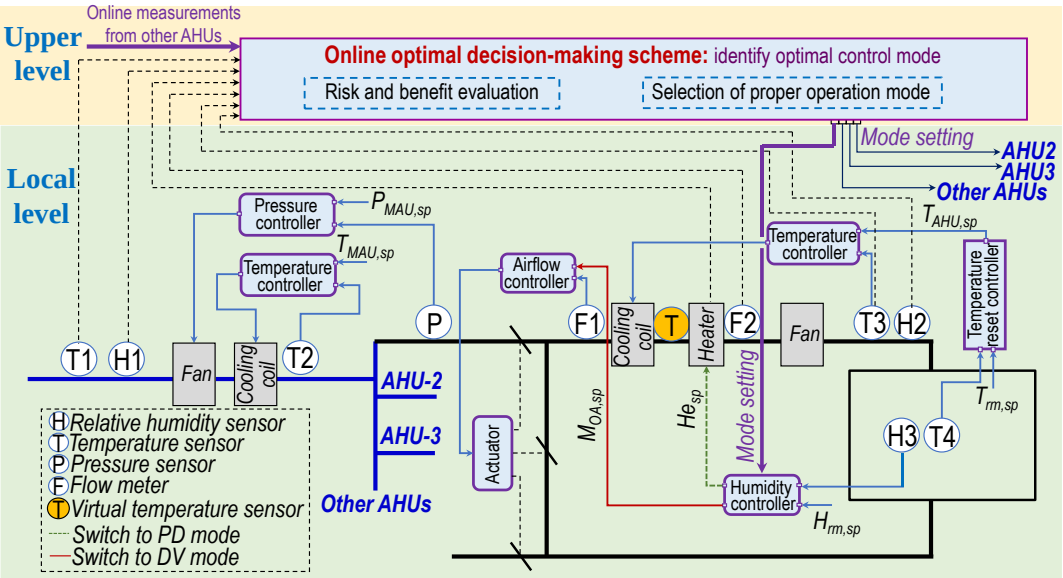

Figure 6.1 Overall structure of developed risk-based online robust optimal control strategy

6.2.2 The requirements and benefits of risk-based decision-making

Multiple control modes are available in many control systems. However, because the optimal control mode varies according to the working conditions, its identification is an important challenge, especially when the systems suffer from component performance degradation and measurement uncertainties. Figure 6.2 presents a typical case for cleanroom air-conditioning control systems, which shows the optimal control

modes under different indoor load regions. The figure was plotted under a given outdoor condition, assuming that the component capacities can satisfy the cooling demands. The SHR is defined as the sensible heat or cooling load divided by the total heat or cooling load. Under the same total cooling load, a lower SHR indicates that a higher moisture load needs to be handled. The SHR is used to represent the load characteristics in cleanrooms. When a space has a comparatively high SHR (Region 1), both the PD and DV modes have the same energy performance, because all of the indoor latent load can be removed by the MAU to avoid the need for overcooling and reheating counteraction processes. When a space has a medium SHR (Region 2), the DV mode outperforms the PD mode, because the energy saving (i.e. by avoiding counteraction processes) exceeds the energy waste (i.e. by introducing intensively high-enthalpy outdoor air). When a space has low SHR (Region 3), PD outperforms DV, because the energy saving of the latter is less than the energy waste. With the decrease of outdoor air enthalpy, the boundary line between Region 2 and 3 moves down and the area of Region 2 increases, eventually subsuming Region 3. More details can be found in Section 3.4.2.

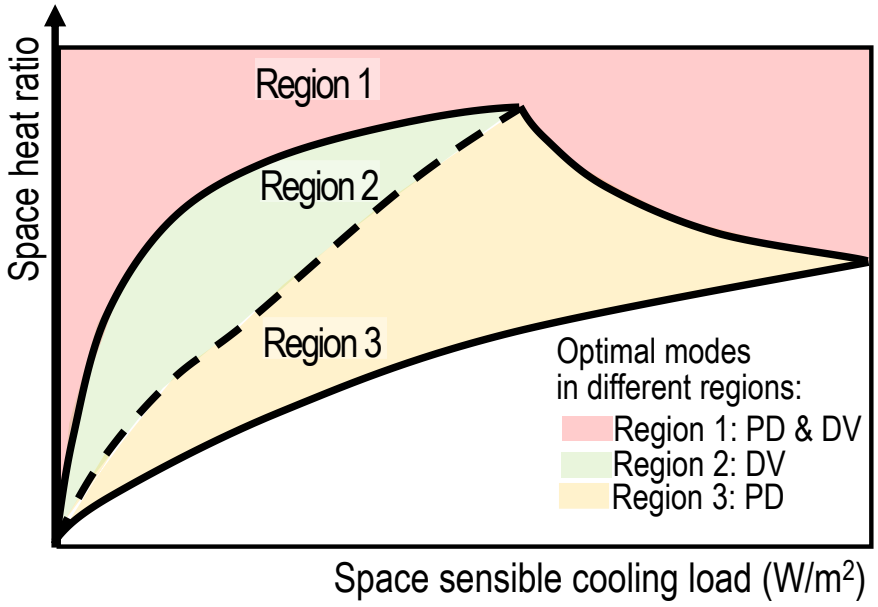

Figure 6.2 Optimal modes under different indoor load regions and a given outdoor condition

The major task of the proposed online control strategy is to identify the optimal control mode (i.e. DV or PD), which is defined as the mode that enables the system to operate at the highest energy efficiency and reliability. However, the actual performance of a system is significantly influenced by the actual MAU cooling capacity and load. Figure 6.3A shows the required MAU cooling demand under different latent cooling load (Q_{lat}) conditions for multiple zones (using three zones as an example). The conservative mode is a safe mode that can always maintain acceptable control and moderate energy consumption because the MAU cooling demand is kept at a low level (lower than the MAU cooling capacity) in all three regions. The aggressive mode is a highly economical but risky mode, which offers satisfactory energy performance over all three regions but carries a high failure risk due to high ventilation cooling demands. The MAU cooling demand is maintained at a low level in Regions 1 and 3 while the cooling demand increases with the increase of space latent load in Region 2. In real applications, an MAU usually treats and supplies the outdoor air to multiple AHUs.

Therefore, the control mode should be properly set to avoid control failure (i.e. MAU demand exceeding its capacity), especially when the latent loads of all zones are in Region 2. The optimal mode is determined based on the online decision-making scheme by selecting between conservative and aggressive control modes, to avoid control failure while minimizing energy consumption. For instance, if the component cooling capacity can meet the required cooling demand under the aggressive mode, this mode is optimal as its energy performance is better than that of the conservative mode. In contrast, if the component cooling capacity cannot meet the required cooling demand under the aggressive mode, the conservative mode is optimal due to its high reliability (i.e. the aggressive mode will consume more energy when control failure occurs). Figure 6.3B shows the four possible operation options when the latent loads of all zones are high (i.e. in Region 2). For Option 1, all zones adopt the aggressive mode (DV mode). Therefore, high MAU cooling demand is required for dehumidification purposes, which exceeds the MAU cooling capacity and results in control failure. For the other three options, one zone adopts the conservative mode and the other zones adopt the aggressive mode. Options 2-4 all ensure successful system operation, although the optimal option (endowing systems with the highest energy-efficiency and reliability) must be determined according to their actual energy performance, which is further elaborated in Section 6.3.3. In real applications, the actual cooling demand and capacity are difficult to accurately estimate due to component performance degradation and measurement uncertainties, which significantly influences the proper selection of control modes. To avoid the failure of the selected control modes, a decision-making scheme considering the possible uncertainties is needed.

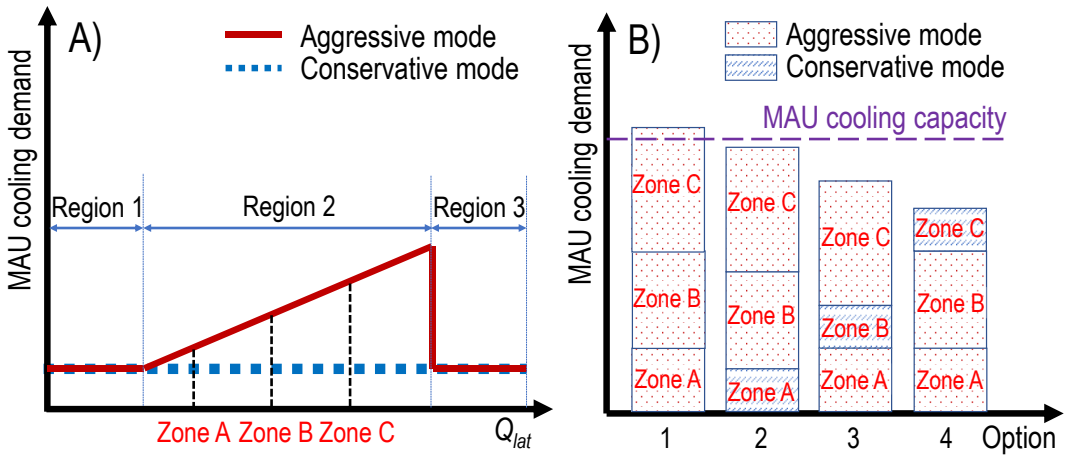

Figure 6.3 Problems affecting the selection of control modes for multiple zones *(A. MAU cooling demand under different latent load conditions; B. MAU cooling demand versus MAU cooling capacity in different options)*

6.2.3 Mechanism of risk-based control mode selection

A compromise between the failure risks and energy benefits is made using a probabilistic approach for selecting between the aggressive and the conservative control modes. Such a selection is commonly faced in applications at medium/high indoor load conditions (e.g. pharmaceutical cleanrooms and labs), especially in humid climates. The mechanism of compromising in making a robust online decision in this situation is illustrated in Figure 6.4. The optimal control mode of individual AHUs is determined as a compromise between the energy benefit in case of success and the energy waste in case of failure. When the cooling demand is low (i.e. lower than cooling capacity), adopting the aggressive mode (DV) offers a significant energy benefit (E_b) compared with the conservative mode (PD) if the decision is correct. However, when the cooling demand becomes higher (i.e. higher than cooling capacity), the failure risk (P_f) of adopting the aggressive mode increases. The aggressive mode becomes unachievable in practice when the component cooling capacity is lower than its cooling demand. There will be much energy waste (E_w) if the decision is wrong,

resulting in control failure (denoted as "aggressive mode failure"). The optimal switching point for the control mode should be the point at which Q_D=Q_C in principle, but the actual estimation of this point is itself uncertain due to the uncertainties in estimating the cooling demand and cooling capacity. When the selected switching point moves to the right, the failure risk (P_f) increases, as shown in the figure.

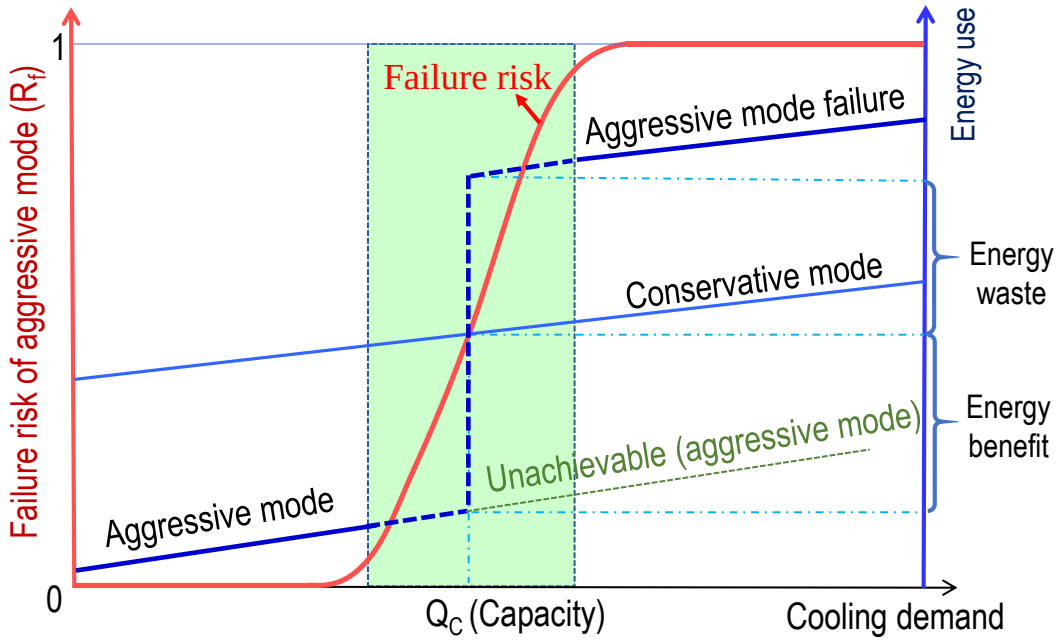

Figure 6.4 Probabilistic optimal decisions for selecting the optimal control mode

The compromise-based decision will keep the system in the aggressive control mode until the expected net energy benefit (E_{nb}) is less than a predetermined threshold (E_{thr}) as shown by Eq. 6.1. Here, E_{nb} is a weighted value considering the energy benefit (E_b)/waste (E_w) and the corresponding modes' probabilities of success (R_s)/failure (R_f). A dead band (ΔE) is introduced to avoid situations where switching between the two modes is too frequent. The evaluation of energy benefit/waste and their probabilities is further elaborated in Section 6.3.3.

$$\begin{cases} E_{nb} = \int E_b R_s - E_w R_f \geq E_{thr} + \frac{\Delta E}{2} & \rightarrow aggressive\ mode \\ E_{nb} = \int E_b R_s - E_w R_f < E_{thr} - \frac{\Delta E}{2} & \rightarrow conservative\ mode \end{cases} \quad (6.1)$$

6.2.4 Adaptive models for risk evaluation considering component performance degradation and measurement uncertainties

Due to the component performance degradation and measurement uncertainties, the actual cooling capacity (Q_c) and cooling demand (Q_d) are challenging to accurately estimate through direct measurements. In this study, the maximum ($V_{fh,max}$) and the demanded outdoor air flowrate (V_{fh}), which represent the correlations between Q_c and Q_d as described by Eq. 6.2, are used to evaluate the failure risks of a prospective decision. Here, $V_{fh,max}$ is the maximum outdoor airflow rate that the MAU can handle under constant outlet temperature (i.e. at dew-point). V_{fh} is the outdoor airflow that the system currently requires. For the conservative mode, there is no risk that the demanded outdoor airflow will be higher than $V_{fh,max}$ because the demanded outdoor airflow ($V_{fh,PD}$) is always maintained at its lower limit. For the aggressive mode, $V_{fh,DV}$ is adjusted according to the indoor latent load, and can exceed its lower limit. Hence there is a risk that the demanded outdoor airflow will be higher than $V_{fh,max}$ especially when the indoor latent load and outdoor air enthalpy are high. When the system operates in the aggressive mode, the demanded outdoor air flowrate ($V_{fh,DV}$) can be directly measured. The critical issue is to evaluate the value of $V_{fh,DV}$ at which the system decides to shift from the conservative mode to the aggressive mode. The correlations between different control modes can be identified by comparing the air states of two modes under the same or similar indoor load conditions (i.e. similar supply air and indoor air states) as elaborated in Section 6.3.2.

$$\frac{V_{fh,max}}{V_{fh}} = \frac{Q_c}{Q_d} \quad (6.2)$$

Adaptive models (Eqs. 6.3 and 6.4) are developed to predict the $V_{fh,max}$ and the $V_{fh,DV}$ using measured data. The outdoor air enthalpy, h_{fh}, which is a function of the measured outdoor air temperature and relative humidity, is used to predict the $V_{fh,max}$. The adaptive models are built by assuming the component capacities are unchanged in a short period. A "fictitious" AHU cooling coil outlet temperature ($T_{fic,PD}$, in the conservative mode) is introduced to predict the $V_{fh,DV}$ in the aggressive mode. $T_{fic,PD}$ is estimated by assuming a virtual temperature sensor located on the AHU cooling coil outlet, as marked in Figure 6.1. $T_{fic,PD}$ is a function of the measured AHU supply air temperature (T_s) and heating load of heaters (Q_{he}) as shown in Eq. 6.5, where a_1, a_2, b_1 and b_2 are correlation coefficients with certain distributions needed to be quantified, aggregating the component performance degradation, measurement biases and noises. $T_{rise,fan}$ and m_s are the air temperature rise (K) due to the fan motor and supply mass airflow (kg/s), respectively, which are constant for a constant air volume (CAV) system. Q_{he} is evaluated using the heater output and rated power (kW).

The correlations between $T_{fic,PD}$ and $V_{fh,DV}$ (Eq. 6.4) are based on the assumption that the MAU outlet air state is in a steady state (e.g. 13 °C, 95%). When the system operates using the aggressive control mode, the demanded outdoor airflow is proportional to the space latent load as shown in Eq. 6.6. When the system resorts to overcooling and reheating to remove indoor latent heat using the conservative mode, $T_{fic,PD}$ is the apparatus dewpoint. The moisture content ($w_{out,PD}$) is linearly related to apparatus dewpoints (ASHRAE, 2013). Therefore, the AHU cooling coil outlet temperature has negative linear relationship to the indoor latent cooling load (Q_{lat}) and demanded outdoor airflow of the aggressive mode (as shown in Eq. 6.7). Eq. 6.4 can then be derived by combining Eqs. 6.6-6.7.

$$V_{fh,max} = \frac{a_1}{h_{fh}} + a_2 \tag{6.3}$$

$$V_{fh,DV} = b_1 T_{fic,PD} + b_2 \tag{6.4}$$

$$T_{fic,PD} = T_s - T_{rise,fan} - \frac{Q_{he}}{m_s} = f(T_s, Q_{he}) \tag{6.5}$$

$$V_{fh,DV} \propto Q_{lat} \tag{6.6}$$

$$T_{fic,PD} \propto w_{out,PD} \propto Q_{lat} \propto -V_{fh,DV} \tag{6.7}$$

The coefficients of the adaptive models are fitted offline using measured data. Figure 6.5(A) shows the correlation between h_{fh} and $V_{fh,max}$, which is affected by the performance degradation of the MAU. The solid curve represents the performance of a new MAU and the dashed curve represents the degraded MAU affected by the aging/fouling. The correlations are obtained by assuming that the outlet temperature (i.e. at the dew-point) of the MAU cooling coil is constant (i.e. 13 °C). Figure 6.5(B) shows the correlations between $T_{fic,PD}$ and $V_{fh,DV}$ of different zones. For zones with the same volume, the trends of $T_{fic,PD}$ and $V_{fh,DV}$ should be the same, as shown by the solid red line if no uncertainties are involved. The correlations are obtained by assuming that the temperature rise due to heat generation from the AHU fan motor is constant and identical under the same supply air flowrate. However, due to measurement uncertainties in each zone, the slope and intercept of the lines differ between zones. The measurement uncertainties (noises and biases) are thus aggregated into the adaptive models by identifying the model coefficients. The coefficients of the adaptive models are updated regularly, considering the changes in the uncertainties and the component performance degradation.

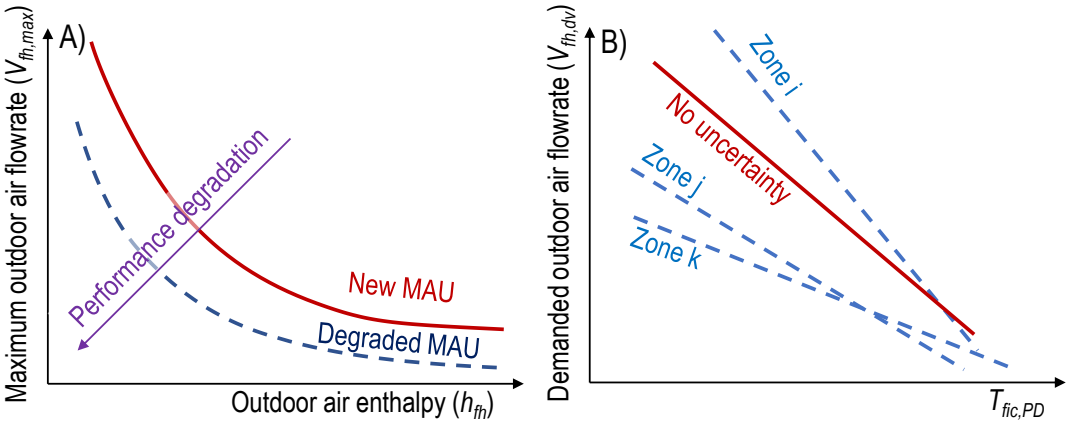

Figure 6.5 Adaptive models considering component performance degradation and measurement uncertainties *(A. outdoor air enthalpy versus maximum outdoor air flowrate; B. fictitious AHU cooling coil outlet temperature of conservative mode versus demanded outdoor air flowrate of aggressive mode)*

6.3 Detailed steps of risk-based online robust optimal control strategy

The detailed steps of the proposed risk-based online robust optimal control strategy considering the measurement uncertainties are shown in Figure 6.6. The first of the three main steps is to remove the outliers and identify the steady-state measurements. The second step is to identify the coefficients of the adaptive models. Both the maximum and demanded outdoor air flowrate models are fitted in advance using the measured data. The MAU fan energy model can be fitted using measurements or manufacturers' performance data. These models are updated regularly considering the measurement uncertainties and component performance degradation. The third step is to evaluate the risks and benefits of each control mode based on the possibilities of both the maximum and demanded air flowrate, as well as the predicted fan energy power, for online decision-making. These steps are elaborated in detail in the subsections below.

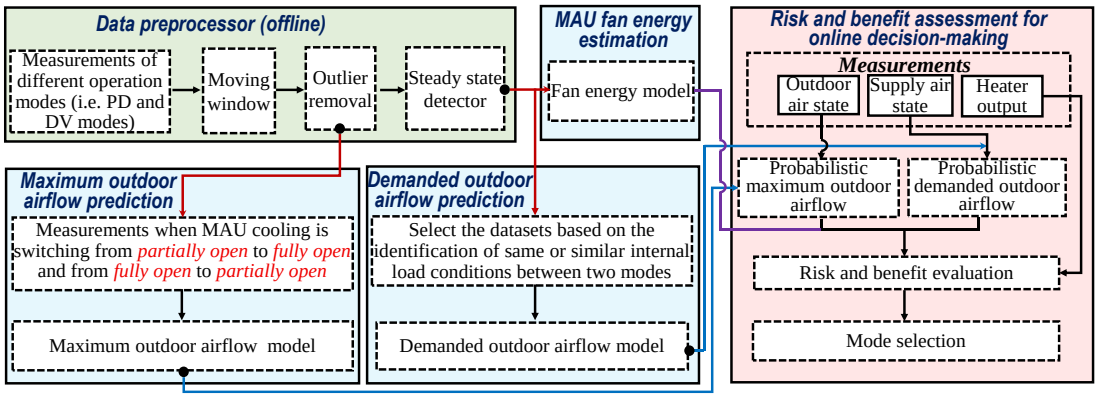

Figure 6.6 Detailed steps of risk-based online robust optimal control under measurement uncertainties

6.3.1 Outlier removal and steady-state identification

The measurements of temperature, humidity and air flowrate are highly susceptible to measurement noises, outliers and biases (Huang, Wang, Xiao, & Sun, 2009; Wang & Xiao, 2004). Taking measurement noises and biases into account, the reading given by a sensor is described by

$$\hat{m} = m^r + e + \beta \tag{6.8}$$

where m^r is the true value of $\hat{m}$, e is white noise and β denotes the sensor biases. A moving window is used to reduce the effects of measurement noise and outliers, which is defined as a matrix with dimension $L_w \times n_p$ as shown in Eq. 6.9. L_w and n_p are the length of the moving window and the number of variables, respectively. k is the time instant. To simplify the data preprocessing, two conventional assumptions are made (Kuklicke & Demeritt, 2016): *(i)* Measurement noises are normally distributed. *(ii)* Measurement biases are unknown constants within the moving window.

$$\begin{bmatrix} m_{1,1} & m_{2,1} & \cdots & m_{n_p,1} \\ m_{1,2} & m_{2,2} & & m_{n_p,2} \\ \vdots & & \ddots & \vdots \\ m_{1,L_w} & m_{2,L_w} & \cdots & m_{n_p,L_w} \end{bmatrix}_k \tag{6.9}$$

Figure 6.7 shows the flowchart of the outlier removal and steady-state identification. The three-sigma rule (Smirnov & Dunin-Barkowski, 1963) is used to detect the outlier and steady-state within a moving window. If the measurements in the defined window are more than three scaled median absolute deviations (MAD) away from the median, the system may experience significant dynamics or the measurements are outliers. The dynamic measurements and outliers are then removed from the datasets. A further step of the dynamic filter is applied. If the standard deviation (δ) of a measurement from the mean value in the window is larger than a threshold α_t, this measurement is regarded as dynamic and removed from the database. Because the measurement noise e has zero expectation, $\bar{m}$ will be close to ($m^r + \beta$) when L_w is large enough as shown in Eq. 6.10. Taking the mean value ($\bar{m}$) of the moving windows reduces the influence of sensor noises.

$$\bar{m}_k = m_k^r + \mathbb{E}(e) + \beta \approx m_k^r + \beta,\ e \sim N(0, \sigma^2) \tag{6.10}$$

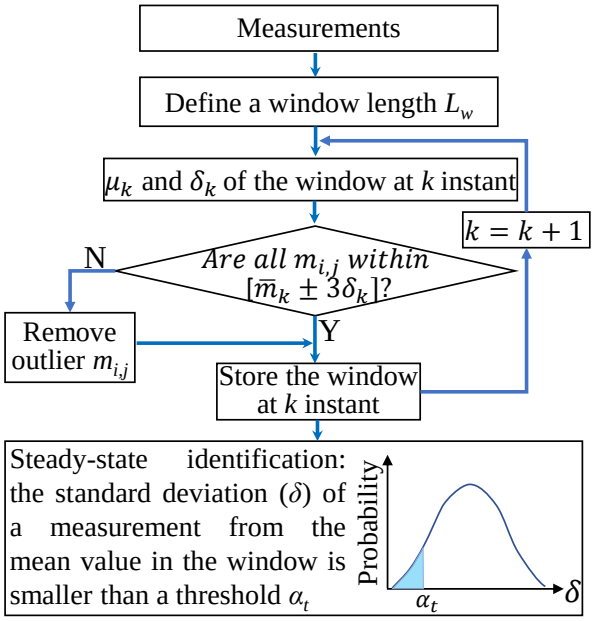

Figure 6.7 Outlier removal and steady-state identification

6.3.2 Identification of model coefficients

In this study, both the maximum and demanded outdoor air flowrate models are modelled "probabilistically" and their coefficients are identified in specific ranges (confidence intervals) with proper distributions rather than deterministic values. The MAU fan model is a regular deterministic model and its coefficients are deterministic constants. A probabilistic model is necessary because both the maximum and demanded outdoor air flowrate have significant implications for the selection of the control mode, as shown in Section 6.2.4, and the risk of each prospective mode due to these erratic flowrate data needs to be carefully addressed.

Maximum outdoor airflow model: The data for fitting this model (i.e. Eq. 6.3) are selected based on the assumption that when the MAU cooling valve is switched from *partially open to fully open* and vice versa, the MAU capacity is equal to its measured cooling load. Figure 6.8 shows an actual profile of the cooling valve position of an MAU in a pharmaceutical cleanroom subsystem during a summer day. Due to the insufficient capacity of the MAU, its cooling valve was fully open between 12:20 and 13:40 and between 17:00 and 18:30. Vf_1, Vf_2, Vf_3 and Vf_4 are thus the switching points as mentioned above. The corresponding data of the outdoor airflow and outdoor air states are selected to form the model training database.

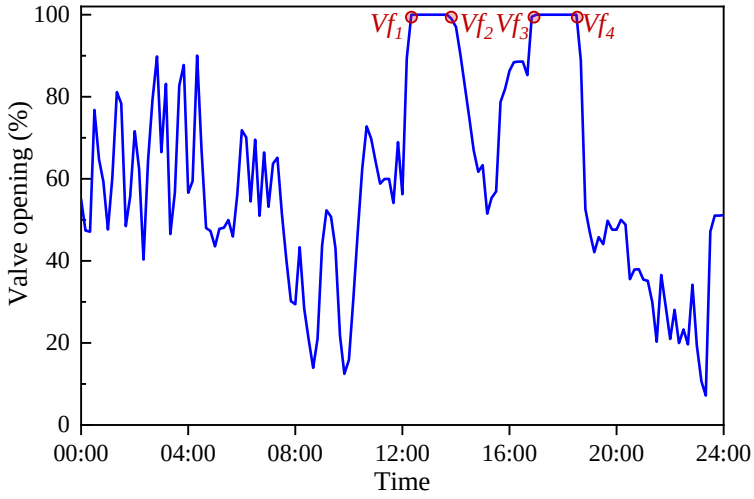

Figure 6.8 Opening status of the MAU cooling valve on a summer working day

Demanded outdoor airflow model: The data for fitting this model (Eq. 6.4) are selected by identifying the similarity of the indoor load conditions between the two modes, which involves two steps. In the first step, the "distances" (Eq. 6.11) between two sets of measurements, taken under the aggressive mode and the conservative mode respectively, are calculated. The distances are used to quantify the similarities of the indoor load conditions under the two control modes. Here, T_r and T_s are room and supply air temperature (°C). RH_r and RH_s are the room and supply air relative humidity (%). In the second step, the sets of measurements with the distances lower than a threshold γ_t are selected and used as visible operational states in the two different control modes under the same indoor load conditions. The corresponding data of heater output, supply air temperature and outdoor air flowrate are selected to form the model training database.

$$d_k = \sqrt{\left(\hat{T}_{r,PD} - \hat{T}_{r,DV}\right)_k^2 + \left(\widehat{RH}_{r,PD} - \widehat{RH}_{r,DV}\right)_k^2 + \left(\hat{T}_{s,PD} - \hat{T}_{s,DV}\right)_k^2 + \left(\widehat{RH}_{s,PD} - \widehat{RH}_{s,DV}\right)_k^2} \quad (6.11)$$

MAU fan energy model: The MAU fan power is approximated as a three-order polynomial function of the volumetric flowrate as shown in Eq. 6.12, where c_1, c_2, c_3 and c_4 are deterministic constants fitted using the measured outdoor flowrate (V_{fh}) and

fan power (P_{fan}). In real applications, if the fan power data are not available, the fan power can also be estimated using the manufacturer's performance data (Salimifard, Delgoshaei, Xu, & Freihaut, 2014). This will not seriously affect the decision-making process because the energy consumed by the fan motor is much smaller than cooling/heating energy. The accuracy of fan energy estimation thus has little impact on the final decision.

$$P_{fan} = c_1 V_{fh}^3 + c_2 V_{fh}^2 + c_3 V_{fh} + c_4 \quad (6.12)$$

6.3.3 Quantification of risks/benefits and selection of optimal control modes

As mentioned in Section 6.2.3, the critical issue when selecting the optimal operation/control mode is to evaluate the expected net energy benefit ($E_{nb,}$ Eq. 6.1). This is a weighted value considering the energy benefit (E_b)/waste (E_w) and the corresponding success (R_s)/failure probabilities (R_f) of the modes, elaborated as follows.

Energy benefit (E_b) and waste (E_w) evaluation: The energy benefit (E_b) of using the aggressive mode can be calculated using Eq. 6.13. The first two terms represent the additional energy uses (MAU cooling and fan energy) compared with the conservative mode, due to the introduction of excessive outdoor airflow. The third term represents the energy saving due to the prevention of overcooling and reheating. The energy waste (E_w) when using the aggressive mode can be calculated using Eq. 6.14. When failure occurs, a "penalty" is introduced by assuming that 100% outdoor airflow would be induced (i.e. the outdoor air damper is fully open). In addition, the AHUs resort to overcooling and reheating processes to ensure the indoor environment can be controlled within the allowable range. Here, h_r (kJ/kg) is the room air enthalpy under the design conditions (i.e. 23 °C, 63%). ρ_{fh} and ρ_s are the air density (kg/m^3) of the

outdoor air and supply air, respectively. COP_c and COP_{he} are the overall coefficient of performance of the cooling system and heating system, assumed to be constant as 2.5 and 1.0, respectively. $V_{fh,full}$ is the 100% outdoor air flowrate (L/s), which is equal to the supply air flowrate (V_s). P_{fan} is a function of the volumetric flowrate, as shown in Eq. 6.12.

$$E_b = \frac{\rho_{fh}(V_{fh,DV}-V_{fh,PD})(H_{oa}-H_r)}{COP_C} + [P_{fan}(V_{fh,DV}) - P_{fan}(V_{fh,PD})] + \rho_s V_s Q_{he}(\frac{1}{COP_C} + \frac{1}{COP_{he}}) \quad (6.13)$$

$$E_w = \frac{\rho_{fh}(V_{fh,full}-V_{fh,PD})(H_{oa}-H_r)}{COP_C} + [P_{fan}(V_{fh,full}) - P_{fan}(V_{fh,PD})] \quad (6.14)$$

<u>*Evaluation of success and failure probabilities:*</u> The failure probability (R_f) and success probability (R_s) of the different control modes are estimated using Eqs. 6.15 - 6.16. The failure probability refers to the probability that the maximum outdoor air flowrate ($V_{fh,max}$) will be less than the demanded outdoor air flowrate ($V_{fh,DV}$), while the success probability is the probability that $V_{fh,max}$ will be higher than the $V_{fh,DV}$. Here, f_1 and f_2 are probability density functions (PDFs) of $V_{fh,max}$ and $V_{fh,DV}$ respectively under a certain working condition, obtained from the adaptive models (Eqs. 6.3-6.4). When the system adopts the aggressive mode (Figure 6.9A), R_f is the integral of f_1 over the range between -∞ and the measured outdoor airflow ($\hat{V}_{fh}$). R_s is the integral of f_1 over the range between $\hat{V}_{fh}$ and +∞. When the system operates in the conservative mode (Figure 6.9B), R_f is the overlap area of f_1 and f_2. R_s is the integral of *[f_2-min (f_1, f_2)]*.

$$R_s = \begin{cases} \int f_1(V_{fh,DV})\, dV_{fh,DV} \quad |V_{fh,DV} < \hat{V}_{fh} & \text{, under superior mode} \\ \int f_2(V_{fh,DV}) - min[f_1(V_{fh,DV}), f_2(V_{fh,DV})]\, dV_{fh,DV} & \text{, under conservative mode} \end{cases} \quad (6.15)$$

$$R_f = \begin{cases} f_1(V_{fh,DV}) dV_{fh,DV} \quad |V_{fh,DV} \geq \hat{V}_{fh}, & \text{under superior mode} \\ min[f_1(V_{fh,DV}), f_2(V_{fh,DV})]\, dV_{fh,DV}, & \text{under conservative mode} \end{cases} \quad (6.16)$$

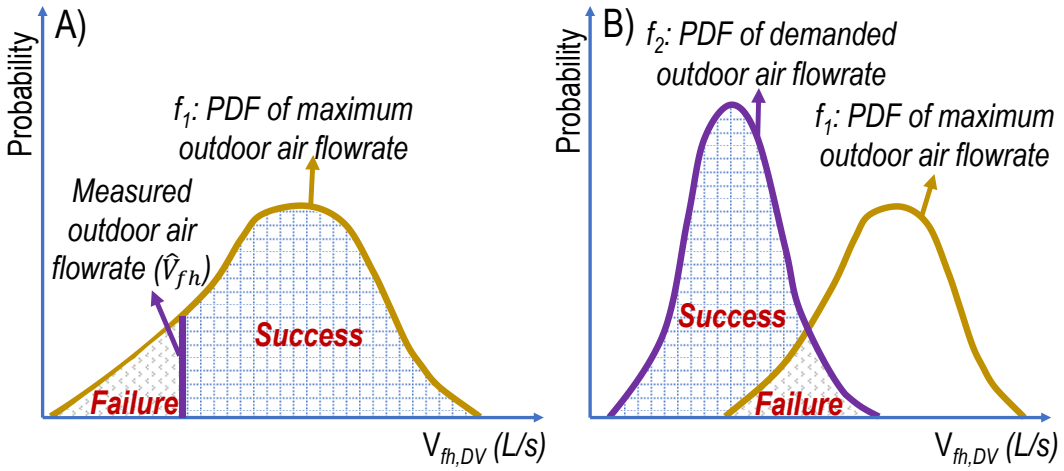

Figure 6.9 Failure and success probability evaluation *(A. under aggressive mode B. under conservative mode)*

Because E_b, E_w, R_f and R_s are all functions of the outdoor airflow rate ($V_{fh,DV}$), Eq. 6.1 can be rewritten as Eq. 6.17.

$$E_{nb} = \int \{R_s(V_{fh,DV})E_b(V_{fh,DV}) - R_f(V_{fh,DV})E_w(V_{fh,DV})\}\, dV_{fh,DV} \qquad (6.17)$$

Figure 6.10 illustrates the detailed steps of selecting the optimal control modes for individual AHUs. In the first step, the measurements, including supply air state, outdoor air state and heater status, are preprocessed using a low-pass filter (Eq. 6.18), to reduce the influence of random noises. Here, θ_{otp} is the filtered output. λ is the filtering weight factor. θ_{inp} is the actual measurement, and *j* and *j-1* are the current and previous sampling instants. In the second step, the failure risks and energy benefits of the different control modes are evaluated. If the cooling capacity of the MAU is estimated to be insufficient, the zone(s) with least heater energy use (estimated by Eq. 6.5) will adopt the conservative mode (i.e. the heaters of the corresponding AHU will be activated). In the third step, the decision is made, aiming to avoid unnecessary overcooling and reheating while ensuring that the system can operate at a low failure risk.

$$\theta_{otp,j} = \lambda\theta_{otp,j-1} + (1-\lambda)\theta_{inp,j} \qquad (6.18)$$

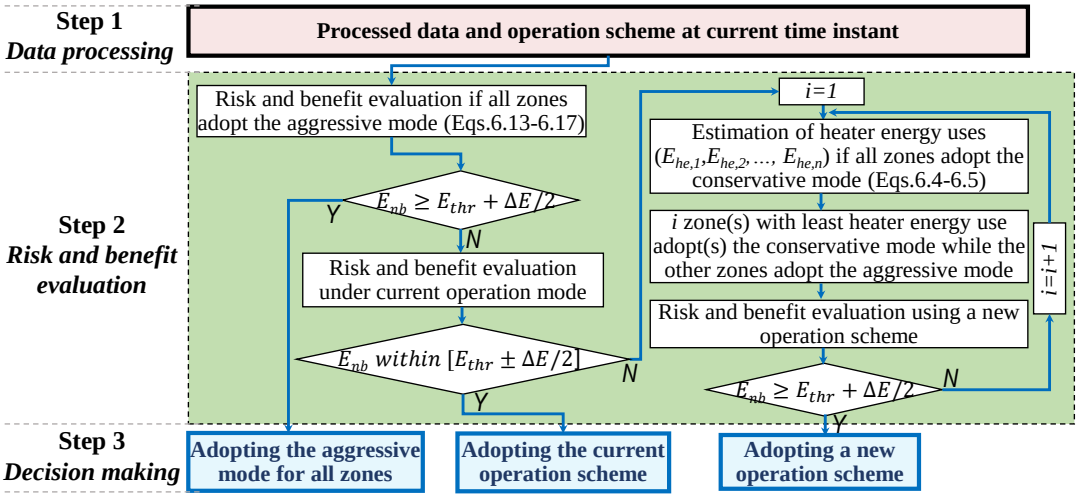

Figure 6.10 Procedure of risk-based online decision making for individual AHUs

6.4 Test platform and identification of model coefficients

6.4.1 TRNSYS-MATLAB co-simulation testbed and test conditions

A virtual simulation platform was constructed using dynamic models developed in TRNSYS [34] to test the effectiveness of the proposed control strategy for cleanroom air-conditioning systems. To take advantage of its powerful computational capabilities, MATLAB was used to program the supervisory controller (which determines the optimal control mode on the basis of risks and benefits). The combined use of TRNSYS and MATLAB is presented in Figure 6.11. The detailed physical models, building envelop and major components (e.g. fans, hydraulic network, air ducts, cooling coils and heaters) of an air-conditioning subsystem were included in this dynamic simulation platform. The dynamic processes of hydraulics, heat transfer, airflow/pressure balancing, energy conservation and control were simulated for the entire system. The models used in the test platform were calibrated using real site operational data (Wang, 1998, 1999). The building's thermal performance under the influences of weather, occupancy, and air-conditioning systems were characterized

using the model type 56 in TRNSYS. The cleanroom air-conditioning subsystem mainly consists of an MAU and three AHUs, having the configuration shown in Figure 6.1. This type of system is the most popular in real building projects of this kind and hence was selected for the testing and implementation of the proposed strategy. The simulated air-conditioning system was modified based on such a system from an actual pharmaceutical building in Hong Kong and the main design parameters (i.e. the inputs of the simulation platform) are presented in Table 6.1.

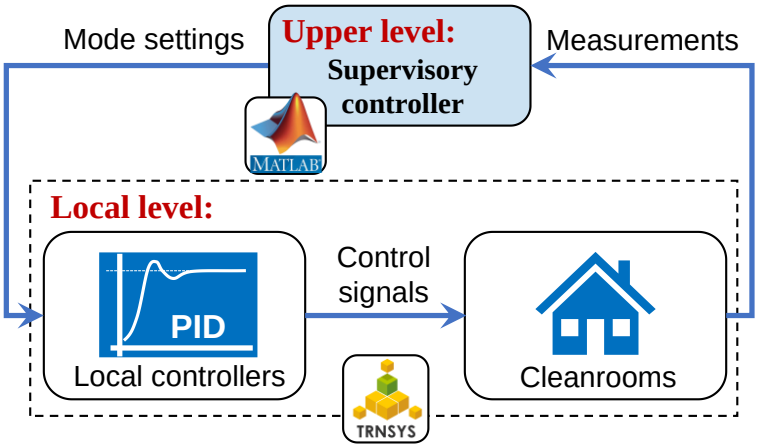

Figure 6.11 TRNSYS-MATLAB co-simulation testbed for performance evaluation of control strategies

The studied cleanrooms are designed as ISO class 8 (ISO, 2015). The minimum total supply and outdoor airflow rates are designed as 20 air change rates per hour (ACH) and 2 ACH respectively to meet the requirements of indoor cleanliness and pressurization (ASHRAE 62.1, 2016; ISO, 2015). Three typical air-conditioned zones in this building were selected, served by one MAU and three AHUs. The upper limits of indoor temperature and relative humidity were set at 23 °C and 63% respectively, which are slightly lower than the upper limits of their allowable ranges. The actual MAU cooling capacity in operation was assumed to be degraded by 20% (i.e. 112 kW) compared with its rated cooling capacity. The reference control strategies and the

proposed control strategy were all tested on the same platform to avoid the effects of model errors and obtain reliable performance data of the proposed control strategy.

Table 6.1 Design room conditions, equipment configuration and control requirements

Description	Parameter	Value
Envelope details	Wall ($W/m^2 \cdot K$)	1.5
	Roof ($W/m^2 \cdot K$)	0.8
	Window ($W/m^2 \cdot K$)	2.7
	Window to wall ratio (WWR)	0.2
Indoor design conditions	Temperature (°C)	21 ± 3
	Relative humidity (RH) (%)	55 ± 10
	Floor area (m^2)	Zone A: 105 (served by AHU-1) Zone B: 78.6 (served by AHU-2) Zone C: 99.8 (served by AHU-3)
	Height (m)	2.8
Internal loads (sensible and latent heat)	Lighting (W/m^2)	13.9 + 0 (all zones)
	Occupants (W/m^2)	22 + 37 (all zones)
	Equipment (W/m^2)	151 + 55 (Zone A), 142 + 55 (Zone B), 144 + 52 (Zone C)
Outdoor and supply airflow rate	Outdoor air changes per hour (h^{-1})	≥2
	Supply air changes per hour (h^{-1})	≥20
Installed fans	Rated power (kW)	34 (MAU), 16 (AHU-1), 14 (AHU-2), 15 (AHU-3)
Cooling coils	Rated cooling capacity (kW)	140 (MAU), 38 (AHU-1), 32 (AHU-2), 35 (AHU-3)
Multi-stage heaters	Rated power of each heater (kW)	2.4 (AHU-1), 2.1 (AHU-2), 2.0 (AHU-3)
	Number of stages	5 (AHU-1), 4 (AHU-2), 5 (AHU-3)

To test the robustness of the proposed control strategy, measurement uncertainties (including biases and noises) were set for each type of sensor as summarized in Table 6.2.

Table 6.2 Sensor noises and biases introduced for case study

Measurement	Unit	Bias	Noise
MAU outlet temperature	°C	1.0	N (0,0.12)
MAU air flowrate	L/s	-54	N (0,5.43)
AHU-1 supply air temperature	°C	0.9	N (0,0.12)
AHU-1 supply air RH	%	2.0	N (0,0.78)
AHU-1 outdoor air flowrate	L/s	20	N (0,5.43)
AHU-1 supply air flowrate	L/s	-62	N (0,5.43)
AHU-2 supply air temperature	°C	-2.2	N (0,0.12)
AHU-2 supply air RH	%	1.5	N (0,0.76)
AHU-2 outdoor air flowrate	L/s	-17	N (0,5.43)
AHU-2 supply air flowrate	L/s	32	N (0,5.43)
AHU-3 supply air temperature	°C	-0.7	N (0,0.12)
AHU-3 supply air RH	%	-2.0	N (0,5.43)
AHU-3 outdoor air flowrate	L/s	-16	N (0,5.43)
AHU-3 supply air flowrate	L/s	-45	N (0,5.43)

6.4.2 Identification of model coefficients for risk and benefit evaluation

The normal operational data for calculating the model coefficients (Eqs. 6.3, 6.4, 6.12) were generated by simulating the cleanroom air-conditioning systems over a wide range of ambient and indoor load conditions. Two sets of operational data were generated: one was free of measurement errors, while the other was obtained after introducing the measurement errors. Figure 6.12 shows the theoretical and adaptive models of the maximum outdoor airflow and demanded outdoor air flowrate. It can be seen that due to the MAU performance degradation and measurement uncertainties, the predicted values deviate far from the theoretical values under the given working conditions. The coefficients of the theoretical and adaptive maximum and demanded outdoor air flowrate models (Eqs. 6.4-6.5) are listed in Table 6.3. The coefficients of the adaptive models are uncertain while those of the theoretical models are deterministic.

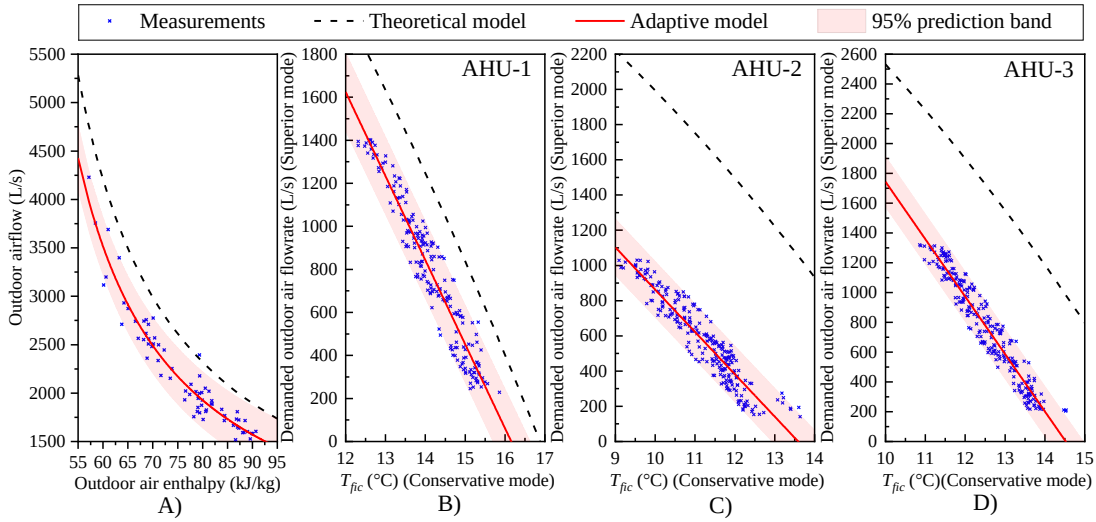

Figure 6.12 Comparison of theoretical and adaptive models *(A. maximum outdoor air flowrate models; B-D. demanded outdoor air flowrate models for AHU-1, AHU-2 and AHU-3)*

Table 6.3 The coefficients of theoretical and adaptive models

Coefficient	Identified value for theoretical models (*deterministic value*)	Identified value for adaptive models (*with 95% confidence bounds*)
a_1	4.35×10^5	3.40×10^5 (3.15×10^5, 3.65×10^5)
a_2	-3057	-2294 (-2626, -1963)
$b_{1,1}$	-387.8	-390.7 (-406.8, -374.6)
$b_{2,1}$	6630	6312 (6084, 6541)
$b_{1,2}$	-257.2	-240.3 (-251.5, -229.1)
$b_{2,2}$	4566	3266 (3140, 3391)
$b_{1,3}$	-368.6	-385.4 (-398.4, -372.5)
$b_{2,3}$	6302	5598 (5435, 5760)

The fan power model was fitted using the "measured" outdoor airflow as shown in Figure 6.13. Eq. 6.19 was used to estimate the fan power under a given outdoor airflow.

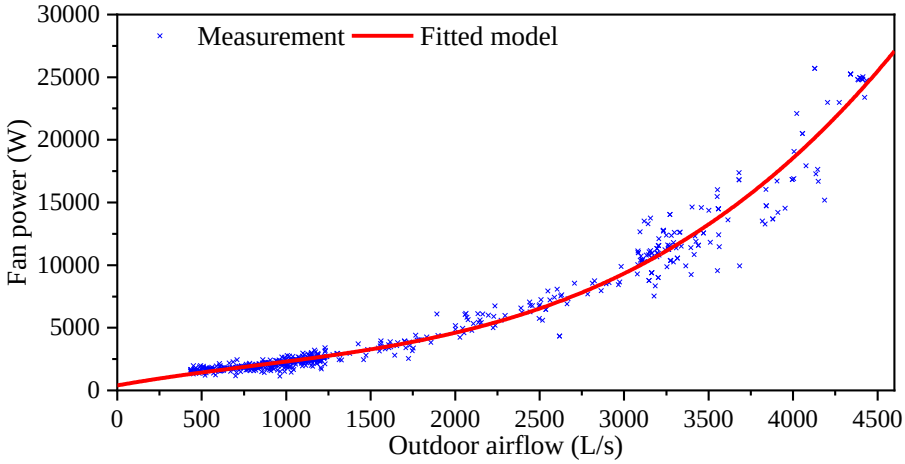

Figure 6.13 Estimated fan power using the measured outdoor airflow

$$P_{fan} = 3.4 \times 10^{-7}\, V_{fh}^3 - 0.0008 V_{fh}^2 + 2.39 V_{fh} + 398.47 \qquad (6.19)$$

6.5 Performance tests and evaluation of proposed risk-based optimal control strategy

6.5.1 Reference control strategies and load conditions

To demonstrate the control performance and energy efficiency of the cleanroom air-conditioning system using the proposed risk-based online optimal control strategy (Strategy #5), four control strategies were selected for comparison as shown in Table 6.4. Strategies #1, #2 and #3 each adopt a single control mode while Strategies #4 and #5 enable dynamic selection of the control mode from multiple options during operation. Strategy #1 adopts IC, the most commonly used control strategy in cleanroom air-conditioning systems. The MAU outlet temperature is controlled at 18 °C by modulating the MAU cooling coil valve. Zone temperature and relative humidity are controlled by adjusting the AHU cooling coil valve and heater output. Strategy #2 adopts PD, and has the same mechanism and settings as the PD mode of Strategy #5. In Strategy #3, the control mode is DV, under the same mechanism and

settings as the DV mode of Strategy #5. Meanwhile, Strategy #4 allows both DV and PD modes, and selects between them by comparing their predicted energy performance based on the theoretical models. The difference between Strategy #4 and #5 is that the component performance degradation and measurement uncertainties are not considered in Strategy #4.

Note that only local process controls are involved for Strategies #1, #2 and #3 while both local-level process controls and upper-level supervisory controls are required for Strategies #4 and #5. For Strategies #3, #4 and #5, when the MAU cooling demand exceeds its capacity, control failure may occur (i.e. the indoor temperature and relative humidity will go outside of the allowable ranges). In this study, to ensure the control reliability of the systems, subcooling and reheating processes of the AHU are adopted for Strategy #3 when control failure occurs (for a minimum of 10 mins). For Strategies #4 and #5, inside the critical zone (i.e. the zone with least estimated heater energy use), the control mode is switched from aggressive to conservative when control failure occurs. The threshold (E_{thr}) and dead band (ΔE) in Eq. 6.1 are selected as 0 kW and 5 kW respectively.

Table 6.4 Description of the control strategies

	Strategy	Description	Supervisory control
Reference strategies	Strategy #1	MAU outlet temperature is controlled at 18 °C. Outdoor air flowrate is set at minimum. System resorts to sub-cooling and reheating processes for indoor air temperature and humidity control.	×
	Strategy #2	MAU outlet temperature is controlled at 13 °C. Outdoor air flowrate is set at minimum. System resorts to sub-cooling and reheating processes when the indoor latent load is high.	×
	Strategy #3	MAU outlet temperature is controlled at 13 °C. Outdoor air flowrate is adjusted according to the indoor latent load.	×
	Strategy #4	MAU outlet temperature is controlled at 13 °C. The system selects the best operation mode by comparing energy performances of modes based on the theoretical models. Performance degradation and measurement uncertainties are not considered using this strategy.	√
Proposed	Strategy #5	MAU outlet temperature is controlled at 13 °C. The system selects the best operation mode based on the risk-based online optimal decision-making scheme. Performance degradation and measurement uncertainties are considered using this strategy.	√

A typical day in Hong Kong was selected to test the performance of the proposed control strategy. The ambient conditions and load settings are shown in Figure 6.14. The patterns of lighting and occupants of all three zones were set as constants (i.e. 1.0 and 0.5 respectively) on the test day.

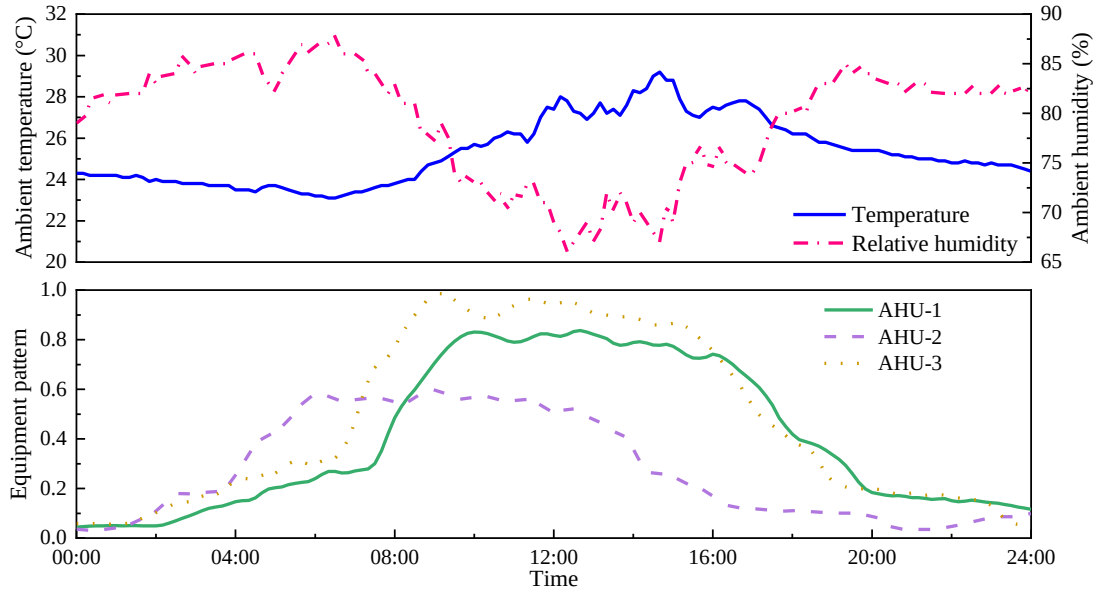

Figure 6.14 Ambient conditions and load patterns for performance evaluation

Note: The load patterns are given as fractions of their respective design values

6.5.2 Energy performance comparison of proposed and reference strategies

To demonstrate the mechanism of energy-efficient control under the proposed control strategy, the outdoor air flowrate, cooling and heating output in the dynamic simulation are compared with the reference strategies. Figure 6.15 shows the outdoor air flowrates and cooling value of the MAU using the different strategies. Strategies #1 and #2 always induced the minimum required outdoor air flowrate, and the MAU cooling valve opening was less than in the other three control strategies throughout the day. Under Strategies #3, #4 and #5, the minimum required outdoor air flowrates were induced for a short period (00:00-02:00) during which the indoor latent load in the three zones was low, but these outdoor air flowrates were above their lower limits for most of the day (02:00-24:00) due to the need of dehumidification in the MAU. However, for Strategy #3, during 09:40-16:30 the cooling valve of the MAU was frequently fully open, indicating that the dehumidification capacity of the MAU was insufficient to handle the complete indoor latent load of all three zones. The

insufficient MAU capacity resulted in a large amount of outdoor air being introduced, leading to system control failure. For Strategy #4, the cooling valve of the MAU was likewise fully open during 09:40-10:00, resulting in a brief episode of control failure. This failure can be attributed to the neglect of measurement uncertainties and component performance degradation in Strategy #4, which jeopardized the accuracy of the estimated MAU cooling demand and cooling capacity. For Strategy #5, the cooling valve of the MAU was never fully open, indicating that its cooling capacity met its cooling demand throughout the day thanks to the judicious choice of control modes for individual zones.

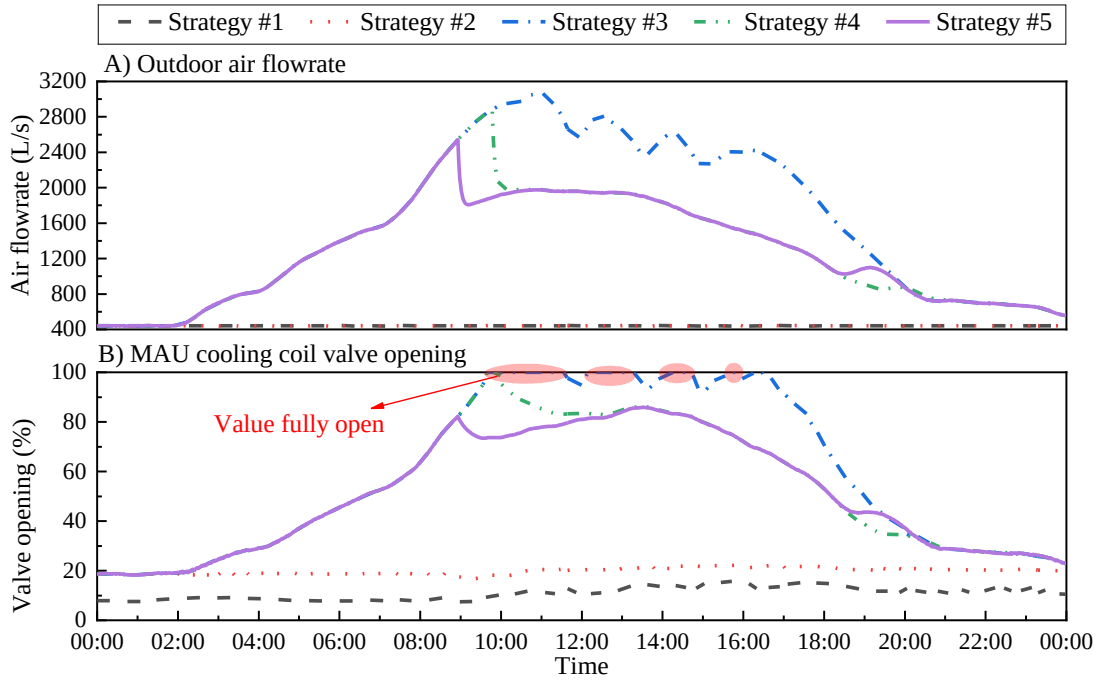

Figure 6.15 Outdoor air flowrate and cooling valve opening of MAU using five control strategies

For the sake of energy efficiency of air-conditioning systems, unnecessary sub-cooling and reheating processes should be avoided. Figure 6.16 shows the heater stages of the AHUs using the five control strategies. For Strategy #1, the three AHUs experienced overcooling and reheating counteraction processes throughout the day. For Strategy

#2, overcooling and reheating were avoided during certain times (e.g. from 00:00 to 02:00) compared with Strategy #1 under conditions of low indoor latent load. For Strategy #3, the three AHUs likewise underwent counteraction processes due to the insufficient MAU cooling capacity around 10:00-16:30. For Strategies #4 and #5, the counteraction processes only occurred in Zone C (served by AHU-3), while the heaters in the other two AHUs (associated with Zone A and Zone B) were not activated at any time during the day. However, the activation of heaters was delayed under Strategy #4 compared with Strategy #5. The schemes for control mode selection (represented by the heater output) differed between Strategies #4 and #5 due to the existence of measurement uncertainties and different decision-making schemes.

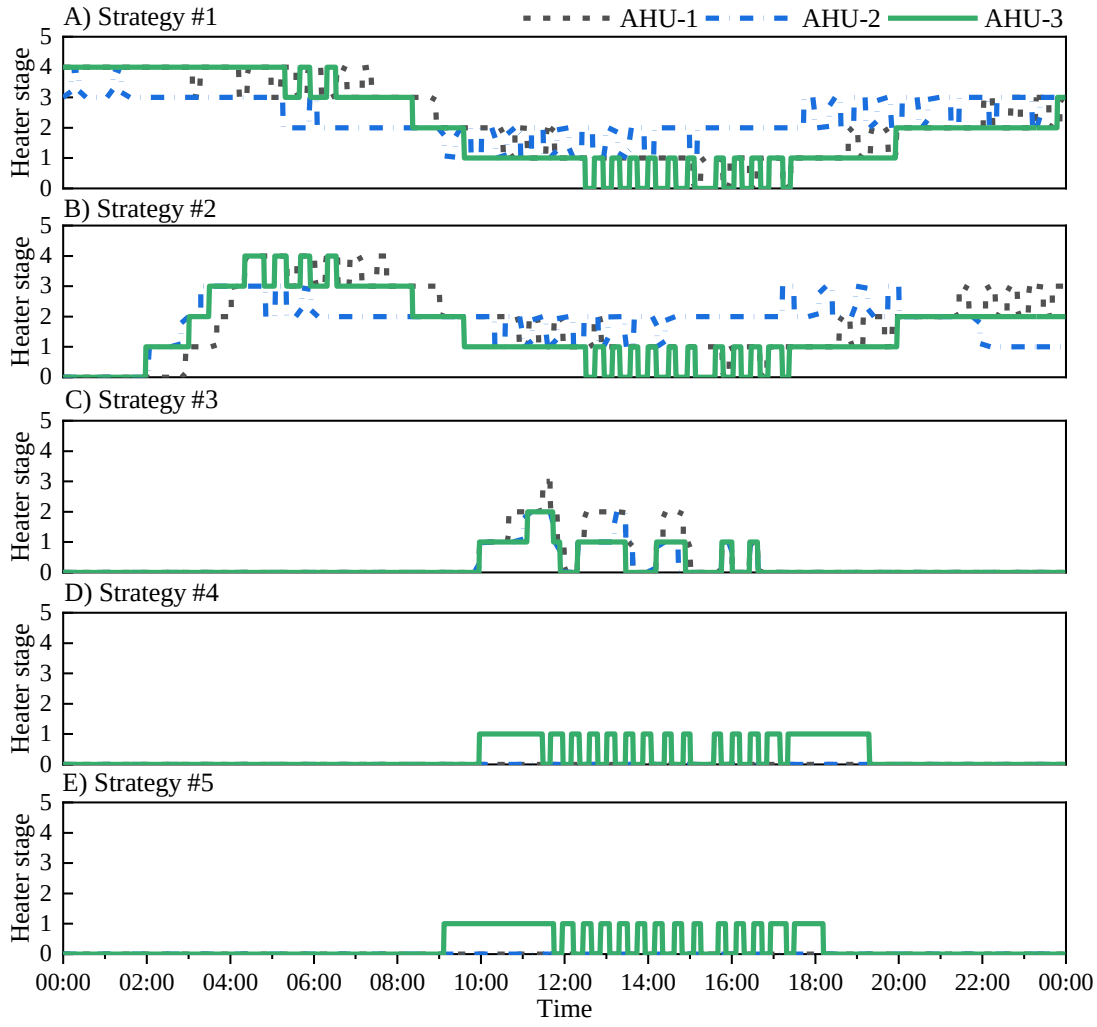

Figure 6.16 Heater stage of AHUs using five control strategies

The energy consumption terms, including the cooling coils, heaters and fans as well as the entire air-conditioning systems, using the five control strategies are shown in Table 6.5. Compared with the conventional Strategy #1, Strategy #2 saved both the cooling and heating energy by 5.8% and 24.0% due to the avoidance of overcooling and reheating under low space latent load. For Strategies #3, #4 and # 5, the heating energy use was significantly decreased by 89.5%, 96.5% and 96.6% respectively due to the decoupling temperature and humidity control loops. However, the cooling energy use increased by 18.4%, 5.9% and 5.4% respectively due to the introduction of excessive high-enthalpy outdoor air flowrates. Compared with Strategy #1, the overall energy savings of Strategies #2, #3, #4 and #5 were 9.3%, 9.2%, 19.4% and 19.9%, respectively.

Table 6.5 Energy consumptions using five control strategies on the test day

	Strategy #1	Strategy #2	Strategy #3	Strategy #4	Strategy #5
MAU fan consumption (kWh)	31.7	31.7	99.7	73.9	71.0
MAU cooling consumption (kWh)	110.5	180.1	661.5	532.8	523.5
AHU cooling consumption (kWh)	552.1	444.1	122.7	168.9	174.8
AHU heating consumption (kWh)	345.6	262.6	36.4	12.0	11.8
AHU fan consumption (kWh)	259.2	259.2	259.2	259.2	259.2
Overall energy consumption (kWh)	1299.1	1177.8	1179.6	1046.8	1040.2
Cooling energy saving (%)	-	5.8	-18.4	-5.9	-5.4
Heating energy saving (%)	-	24.0	89.5	96.5	96.6
Overall energy saving (%)	-	9.3	9.2	19.4	**19.9**

6.5.3 Control reliability of proposed strategy compared with reference strategies

For cleanroom air-conditioning systems, the reliability of indoor temperature and relative humidity control is a major issue. Reliability implies that the indoor

temperature and relative humidity can be controlled within the allowable ranges during operation, meaning that satisfactory services can be offered. Figure 6.17 shows the indoor air temperature and relative humidity profiles of the three zones using the five control strategies. Generally, the indoor air temperature and relative humidity were controlled within the allowable range using Strategies #1, #2 and #5. However, for Strategies #3 and #4, control failure occurred around 09:50-10:10 due to the insufficient MAU cooling capacity for dehumidification. For Strategy #5, the indoor air temperature and relative humidity of the zones were controlled within the allowable ranges throughout the test day. This indicates that the proposed risk-based online optimal control strategy can fulfil the requirements of indoor environment control and thus offer satisfactory service.

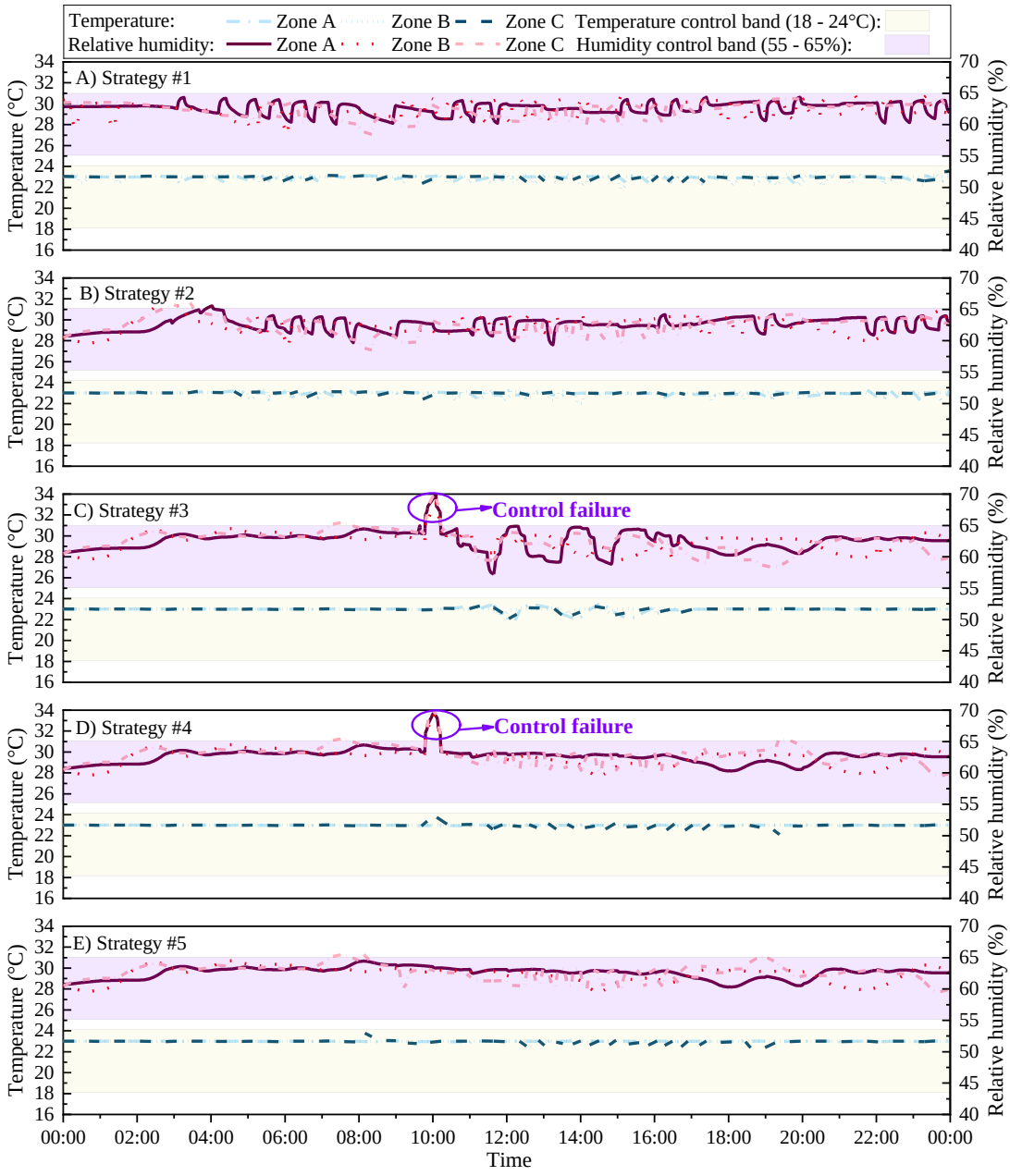

Figure 6.17 Indoor air temperature and relative humidity profiles using five control strategies

Figure 6.18 shows the control mode selection (i.e. the number of zones adopting the aggressive mode) of Strategies #4 and #5, demonstrating the importance of considering the component performance degradation and measurement uncertainties in upper-level supervisory control. It can be seen that the systems adopting Strategy #5 shifted from the aggressive to the conservative control mode in the critical zone in advance (i.e. at 08:55) to avoid control failure, based on the risk assessment. In

contrast, aggressive mode failure occurred under Strategy #4, due to the inaccurate estimation of MAU cooling demand and capacity. In addition, compared with Strategy #5, the mode shifting was delayed under Strategy #4, causing more energy waste.

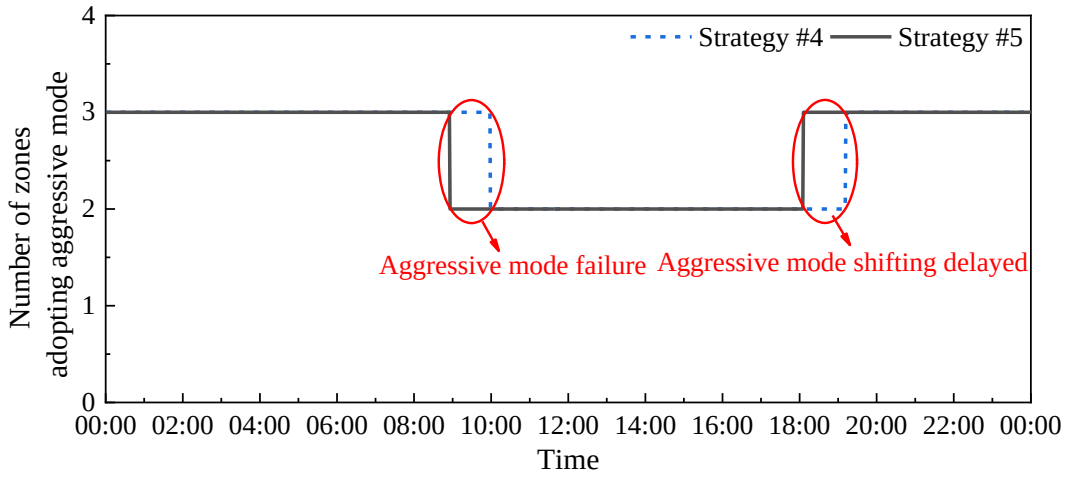

Figure 6.18 Number of zones adopting aggressive mode using Strategies #4 and #5

Figure 6.19 presents the risks and expected net energy benefits in the decision-making process when adopting Strategy #5, evaluated under the assumption that all zones adopt the aggressive mode. The selected control modes for individual zones in the decision-making process are shown in Table 6.6. When the space latent load stayed at a low level (i.e. in periods 1 and 3), the failure probability was also estimated to be low, if all zones in the aggressive mode. Therefore, all of the zones selected this mode because of the high expected net energy benefits estimated by the decision-making scheme. When the indoor latent load increased (i.e. in period 2), the control strategy determined the control mode for each zone based on the expected net energy benefits. Zone C (served by AHU-3), which was estimated to use the least heater energy (Eqs. 6.4-6.5), switched from the aggressive to the conservative mode, to ensure that the other two zones could operate under the aggressive mode successfully.

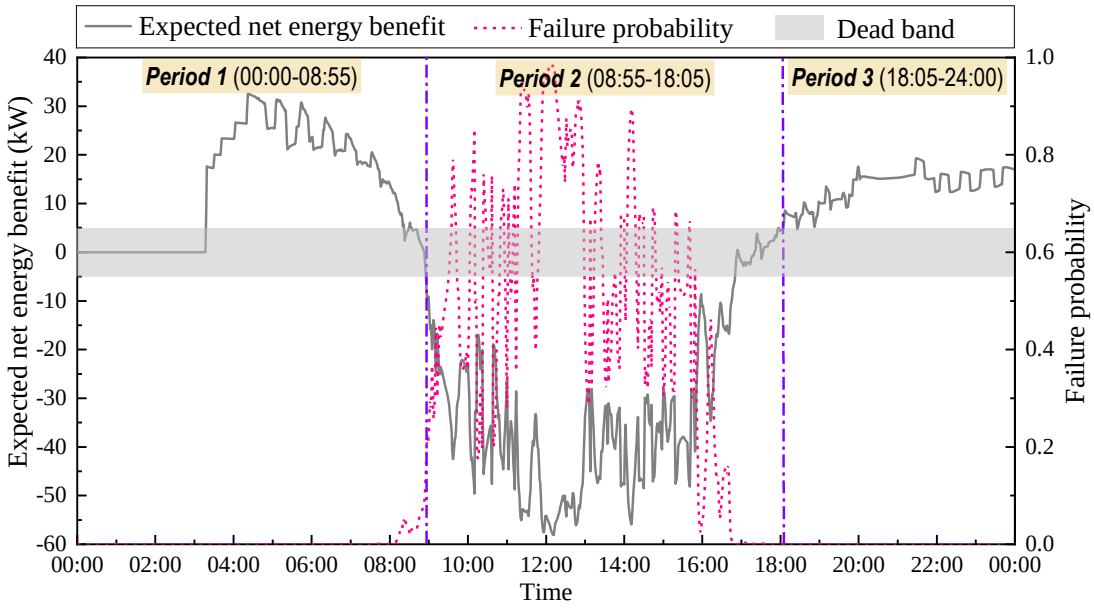

Figure 6.19 Risks and expected net energy benefits in decision-making process

Table 6.6 Control mode at different periods using risk-based decision-making approach

	Period 1 (00:00-08:55)	Period 2 (08:55-18:00)	Period 3 (18:00-24:00)
Zone A	Aggressive mode	Aggressive mode	Aggressive mode
Zone B	Aggressive mode	Aggressive mode	Aggressive mode
Zone C	Aggressive mode	***Conservative mode***	Aggressive mode

6.6 Discussion

Energy-efficient control strategies in the operation of cleanroom air-conditioning systems reduce energy consumption and operational costs, and maintain more reliable control of the cleanroom environment. The results of performance tests indicated that the proposed risk-based control strategy appropriately selected or shifted the control modes to achieve energy-efficient and reliable operation of environmental control systems. This is especially important for industrial applications, where the integrity of cleanroom production environments must be preserved and highly sophisticated and knowledge-intensive manufacturing processes are involved.

Based on the performance tests of the developed strategy and a review of the existing literature, several issues still need to be addressed in further studies for the successful implementation of the risk-based control strategy in practice:

i. Concerning measurement, there is a need to collect data regularly under different operation states (i.e. failure or success) of the control modes. The data can be used to update the component performance model and improve the accuracy of risk/benefit evaluation. For instance, in the selected test case, if aggressive control fails, the outdoor air flowrate induced in practice can be obtained from actual measurements. The flowrate measurements can then be used for quantifying the energy waste of the aggressive mode.

ii. Concerning the model prediction, there is a need for sensitivity and uncertainty analysis to identify the impacts of errors of different sensors on the performance of the control strategies. This would reduce the need for data collection, and simplify the risk/benefit analysis, hence facilitating online decision-making. For instance, Shan et al. (2013) conducted a sensitivity analysis of measurements and found that the accuracy of the outdoor airflow meter had the most significant impact on the performance of the ventilation control strategy.

iii. The successful implementation of the risk-based control strategy requires the predictive models to be adaptive to the changes of working conditions. In this study, the parameters of the models were identified using operational data under normal conditions. There is a need for a robust approach to self-tune the coefficients/parameters of predictive models in cases of control failure. In practical applications, control failure (i.e. due to improper decision making) may occur due to either changes of working conditions or sensor errors. An online learning and estimation approach is required to re-calculate and update the

coefficients of the predictive models and preserve the model accuracy when the working conditions change or the component performance is degraded.

iv. The cost function (for evaluating risk and benefit) for decision-making must be modified for cleanrooms requiring higher cleanliness levels. In such applications, due to the higher requirements of environmental control, the tolerance for control failure is lower. The cost function must be updated to ensure that the systems operate with high reliability. This can be achieved by properly setting the penalty for unsatisfactory service.

6.7 Summary

A risk-based online optimal control strategy for multi-zone cleanroom air-conditioning systems was proposed. As the core of the control strategy, an online optimal decision-making scheme was developed based on a compromise between the risks and benefits of various control modes, to select the optimal mode, allowing for component performance degradation and measurement uncertainties. The proposed control strategy was tested and implemented on a simulation platform. Based on the results of the tests and implementation, some detailed conclusions can be drawn:

i. The proposed strategy can successfully determine the optimal control mode allowing for component performance degradation and measurement uncertainties, enabling air-conditioning systems to operate with both high reliability and energy efficiency.

ii. The online optimal decision-making scheme is effective in quantifying the correlations between different control modes and evaluating the energy benefits and failure risks of these modes under uncertainties.

iii. In the test period, the proposed strategy based on risk-assessment achieved approximately 20% overall energy saving compared with interactive control, the most commonly used method.

The proposed risk-based online decision-making approach can also be applied for other systems with multiple control modes that may require mode shifting under certain conditions. In real applications, due to various uncertainties, engineers usually prefer to select a conservative/safe mode rather than an aggressive mode (i.e. with more energy-saving potential but higher risks), to ensure highly reliable operation (Teng & Ho, 1996). In this study, a quantification method of risks and benefits was developed for decision-making accounting for measurement uncertainties, offering a promising means for engineers to exploit the potential benefits of control mode shifting.

Notably, the coefficients of the adaptive models were fitted using building simulation tools and implemented in specific cases in this study. In real applications, operational data of typical working conditions under different control modes are needed to identify these coefficients.

It is also worth noting that in this study, in the case of mode failure, a penalty was incurred by assuming that 100% outdoor airflow is induced associated with simultaneous cooling and heating processes, forcing the system to provide satisfactory environmental control. In real applications, the penalty should be properly set according to the environmental control requirements.

More importantly, on-site implementation and comprehensive validation of the proposed online control strategy and the corresponding control schemes, are needed under real conditions matching the system requirements. On-site test results will be

essential for updating the strategy to achieve satisfactory performances in practical applications. Further tests and validation of the proposed online control strategy in real buildings would be of considerable value in future studies.

CHAPTER 7 CONCLUSIONS AND RECOMMENDATIONS

This PhD thesis presented a novel "adaptive full-range decoupled ventilation (ADV) strategy", an uncertainty-based robust optimal design method, and a risk-based robust online optimal control strategy for achieving energy-efficient air-conditioning systems for cleanrooms or spaces requiring strict humidity and temperature control. The developed ventilation strategy, design and control methods were tested and validated based on the actual air-conditioning systems in an existing pharmaceutical building.

This chapter presents the overall conclusions and recommendations, which is organized as follows. Section 7.1 presents a summary of the main contributions of this PhD study. The conclusions based on the work done are summarized in Section 7.2. The recommendations for future work are presented in Section 7.3.

7.1 Summary of main contributions

The main contributions of this PhD study are summarized as follows:

i. An "adaptive full-range decoupled ventilation (ADV) strategy" is developed for cleanroom air-conditioning systems. This strategy can offer superior energy performance over the full range of internal load and ambient conditions. It minimizes system energy consumption by avoiding sub-cooling and reheating as far as beneficial via the best use of MAU and economizer for dehumidification.
ii. The energy and economic performance, as well as the preferable operation modes of the ADV strategy are fully explored when implemented in different climate

regions. The new design and the needs of modifications in retrofitting existing systems are presented for implementing the ADV strategy in cleanroom air-conditioning systems under different climatic conditions.

iii. An uncertainty-based robust optimal design method is developed for cleanroom air-conditioning systems facilitating the adaptive ventilation strategy under uncertainties. A probabilistic diversity factor method is proposed to quantify the effects of asynchronous loads in different zones/spaces. The robust optimal design offers systems high energy efficiency at a wide range of internal loads and ambient conditions, taking into account design input uncertainties and load diversities.

iv. A risk-based online robust optimal control strategy is developed, which determines the optimal control mode and settings in order to minimize energy use taking account of component performance degradation and measurement uncertainties. An "online optimal decision-making scheme" is developed by compromising between the risks and benefits of control modes, to select the best control mode allowing for uncertainties.

7.2 Conclusions

On the "adaptive full-range decoupled ventilation strategy"

Compared with the existing ventilation strategies, the developed "adaptive full-range decoupled ventilation (ADV) strategy" has superior energy performance over the full range of internal load and ambient conditions.

Under hot and humid outdoor conditions, while the economizer is not activated, the proposed strategy can minimize system energy consumption by avoiding sub-cooling and reheating as far as beneficial via the best use of MAU for dehumidification. Under

dry and cool outdoor conditions, while the economizer is activated, the proposed strategy can optimize the outdoor air intake by the full use of the outdoor air "free cooling" and "free dehumidification" capacities.

On the performance and applications of ADV strategy in different climate zones

The developed ADV strategy offers air-conditioning systems significant and promising energy savings in different climate zones. Concerning its short payback period, it is attractive for both existing system retrofits and new system designs in most climates.

The test results show that the annual energy consumption of the air-conditioning systems could be reduced by 6.8-40.8% when adopting the proposed ADV strategy, compared with the most commonly used existing interactive control (IC) strategy. It has higher energy saving potentials in humid climates compared with that in dry climates.

When the economizer is not activated, dedicated outdoor air ventilation mode is highly recommended as the main operation mode of the ADV strategy in severe cold/cold and moderate regions. When the economizer is activated, the "following sensible load" (FS) and "lower-limit humidity" (LL) control modes are the recommended operation modes in cold/severe cold climate zones, while the "following sensible load" (FS) mode is the recommended operation mode in hot/temperate climate zones.

For the full implementation of ADV strategy in retrofitting an existing system (i.e. initially adopting the IC strategy), only the size of the MAU cooling coil needs to be enlarged while the other components can keep unchanged. For a new system design, the required capacities of the AHU cooling coil and heater are even smaller compared with those designed for the IC strategy. The payback periods of existing system

retrofits and new system designs could be less than 4 years and 2 years respectively in most climates when the ADV strategy is fully implemented.

On the uncertainty-based robust optimal design method

The uncertainty-based robust optimal design method can offer cleanroom air-conditioning system superior economic performance and satisfaction of service, facilitating the developed ADV strategy under uncertainties.

The diverse behaviour of multiple zones/spaces has significant effects on the cooling demand of components, and thus the sizing of optimal design. The design approach without considering the diverse behaviour of multiple spaces will result in undersized problems for some components. The introduction of two probabilistic diversity factors using the developed probabilistic diversity factor method is very effective to quantify the effects of load diversities in multiple zones/spaces.

The case study shows that the overall annualized mean total cost of the system designed for the ADV strategy could be reduced by up to 18% compared with that for existing ventilation control strategies. The optimal capacities of the components are affected significantly by penalty prices. When the penalty price is over a threshold, the optimal design capacities of air-side components vary only within a small range.

On the risk-based online robust optimal control

The risk-based online optimal control strategy developed can successfully determine the best operation allowing for component performance degradation and measurement uncertainties. This strategy ensures the cleanroom air-conditioning systems to operate at high reliability and energy efficiency. The “online optimal decision-making scheme” is effective for decision-making by quantifying the correlations between different

operation modes and evaluating the energy benefits and failure risks of different operation modes under uncertainties.

Test results show that this risk/benefit-based control strategy could achieve up to 20% overall energy saving with high control reliability compared with the conventional control strategies.

7.3 Recommendations for future work

The major efforts of this PhD study have been made on the development of the optimal ventilation strategy, as well as the optimal design and control methods for implementing the developed ventilation strategy under uncertainties. It would be very desirable and valuable to make further efforts on the following aspects to improve the quality of the research and to bring these methods into practical applications.

- Effective and accessible tools are necessary to implement the proposed design methods considering uncertainties. More generic models are needed to be developed to quantify the load diversities of multiple spaces, which are the key sources of uncertainty in the performance of air-conditioning systems. It will be much more helpful if such tools can be integrated with popular building energy simulation tools, such as EnergyPlus and TRNSYS.
- The design and control methods for other cleanroom configurations are required to be further developed. For instance, for the cleanroom with higher cleanliness requirements (i.e. higher air changes rate per hour), the optimization of air recirculation systems (i.e. air distribution and flow pattern) is a challenge worth undertaking. The cleanroom air conditioning systems integrated with advanced

heat recovery devices are also needed to be optimized to achieve minimum life-cycle costs.

- On-site implementation and validation of the proposed online control strategy and the corresponding schemes are needed when the real conditions can meet the requirements. The on-site test results are very important to update them and to achieve desirable and satisfactory performances in practical applications. It would be an energy-consuming task and considerable efforts need to be paid to test and validate the proposed online control strategy in the practical buildings in future studies.

APPENDIX A INVESTMENT COST MODELS OF COMPONENTS

The investment costs of air-side components are the functions of the corresponding component capacities in this study. The investment costs (USD) of the centrifugal fan, axial fan, duct, cooling coil, electric heater and electric humidifier can be estimated by Eqs. A.1-A.6 based on RSMeans Mechanical Cost Data (Mossman, 2008). The RSMeans Mechanical Cost Data was built based on continuously monitoring the available costs from the manufacturers in the construction industry. Considering the inflation, the component investment cost (*Inc*) used in this study is calculated as Eq. A.7. Here, the *Nc* is the investment cost provided by RSMeans Data. *i* is the annual inflation rate set as 4% (Daud & Ismail, 2012), and *n* is the number of time periods (years) past, selected as 11 years in this study. The investment cost of the economizer is estimated as 8 USD/m^2 of the floor area considering the installation of additional dampers, sensors and actuators (Fisk, Black, & Brunner, 2012).

$$Inc_{fan,cen} = 1125.9flow + 3375.1 \qquad flow \in [0.5, 6] \qquad \text{(A.1)}$$

$$Inc_{fan,axi} = 297.0flow + 1406.4 \qquad flow \in [0.5, 6] \qquad \text{(A.2)}$$

$$Inc_{duct} = (3.0flow^3 - 29.2flow^2 + 138.9flow + 7.68) \times len_{duct} \quad flow \in 0.5, 6] \qquad \text{(A.3)}$$

$$Inc_{cc} = -1.33CAP_{cc}^2 + 165.1CAP_{cc} + 1746.7 \qquad CAP_{cc} \in [2, 55] \qquad \text{(A.4)}$$

$$Inc_{he} = 221.0CAP_{he} + 211.1 \qquad CAP_{he} \in [0.5{,}20] \qquad \text{(A.5)}$$

$$Inc_{hu} = 74.8CAP_{hu} + 3353.1 \qquad CAP_{hu} \in [5{,}90] \qquad \text{(A.6)}$$

$$Inc = Nc(1 + i)^n \qquad \text{(A.7)}$$

where, CAP_{cc} (kW), CAP_{he} (kW), CAP_{hu} (kW) and *flow* (m^3/s) are the capacities of the cooling coil, electric heater, electric humidifier and design air flowrate, respectively. len_{duct} is the length of the MAU duct. It is worth noticing that when the design capacities of the cooling coil, electric heater and electric humidifier are larger than the upper limit of the ranges (e.g. 55 kW for cooling coil), several same components would be selected. For example, if the design cooling coil capacity is 100 kW, the investment cost of the cooling coil is the sum of the investment costs of two cooling coils, each with a capacity of 50 kW.

REFERENCES

An, J., Yan, D., Hong, T., & Sun, K. (2017). A novel stochastic modeling method to simulate cooling loads in residential districts. *Applied Energy*, *206*, 134-149.

ASHRAE. (2007). *ASHRAE Handbook: HVAC applications.* American Society of Heating, Refrigerating and Air Conditioning Engineers, Atlanta, GA.

ASHRAE. (2013). *ASHRAE Handbook: Fundamentals.* American Society of Heating, Refrigerating and Air Conditioning Engineers, Atlanta, GA.

ASHRAE. (2016). *ASHRAE Handbook: HVAC systems and equipment.* American Society of Heating, Refrigerating, and Air Conditioning Engineers, Atlanta, GA.

ASHRAE 62.1. (2016). *Ventilation for Acceptable Indoor Air Quality.* American Society of Heating, Refrigerating and Air-Conditioning Engineers, Atlanta, GA.

Bichiou, Y., & Krarti, M. (2011). Optimization of envelope and HVAC systems selection for residential buildings. *Energy and Buildings*, *43*(12), 3373-3382.

Breiman, L., Friedman, J., Stone, C. J., & Olshen, R. A. (1984). *Classification and regression trees*. The Wadsworth Statistics/Probability Series. Chapman and Hall, New York.

Brohus, H., Frier, C., Heiselberg, P., & Haghighat, F. (2012). Quantification of uncertainty in predicting building energy consumption: A stochastic approach. *Energy and Buildings*, *55*, 127-140.

Brown, W. K. (1990). Makeup air systems energy-saving opportunities. *ASHRAE Transactions*, *96*, 609-615.

Budaiwi, I. M. (2001). Energy performance of the economizer cycle under three climatic conditions in Saudi Arabia. *International Journal of Ambient Energy, 22*(2), 83-94.

Burnett, J., Yik, W., Lee, W., Powell, G., & Tang, A. (2001). *Hong Kong building environmental assessment method. HK-BEAM version 5/04 existing buildings*. HK-Beam Society, Hong Kong.

Caliński, T., & Harabasz, J. (1974). A dendrite method for cluster analysis. *Communications in Statistics-Theory and Methods, 3*(1), 1-27.

Cheng, Q., Wang, S. W., & Yan, C. C. (2016). Robust optimal design of chilled water systems in buildings with quantified uncertainty and reliability for minimized life-cycle cost. *Energy and Buildings*, *126*, 159-169.

Cho, J., Lim, T., & Kim, B. S. (2012). Viability of datacenter cooling systems for energy efficiency in temperate or subtropical regions: Case study. *Energy and Buildings*, *55*, 189-197.

Cho, K., Chang, H., Jung, Y., & Yoon, Y. (2017). Economic analysis of data center cooling strategies. *Sustainable Cities and Society*, *31*, 234-243.

CLP Hong Kong. (2018). *Tariff review presentation*. Retrieved from https://www.clpgroup.com/en/Media-Resources-site/Current Releases Documents/20171212_Appendix_en.pdf.

Cui, J., Watanabe, T., Ryu, Y., Akashi, Y., & Nishiyama, N. (1999). Numerical simulation on simultaneous control process of indoor air temperature and humidity. *Sixth International IBPSA Conference, Proceedings*, *2*, 1005-1012.

Daud, A.-K., & Ismail, M. S. (2012). Design of isolated hybrid systems minimizing costs and pollutant emissions. *Renewable Energy*, *44*, 215-224.

De Wit, S., & Augenbroe, G. (2002). Analysis of uncertainty in building design evaluations and its implications. *Energy and Buildings*, *34*(9), 951-958.

Domínguez-Muñoz, F., Cejudo-López, J. M., & Carrillo-Andrés, A. (2010). Uncertainty in peak cooling load calculations. *Energy and Buildings*, *42*(7), 1010-1018.

Doodman, A. R., Fesanghary, M., & Hosseini, R. (2009). A robust stochastic approach for design optimization of air cooled heat exchangers. *Applied Energy*, *86*(7-8), 1240-1245.

Doucet, A., De Freitas, N., & Gordon, N. (2001). *An introduction to sequential Monte Carlo methods.* Sequential Monte Carlo Methods in Practice. Statistics for Engineering and Information Science. Springer, New York, 3-14.

Dounis, A. I., & Caraiscos, C. (2009). Advanced control systems engineering for energy and comfort management in a building environment—A review. *Renewable and Sustainable Energy Reviews*, *13*(6-7), 1246-1261.

Duić, N., Guzović, Z., Kafarov, V., Klemeš, J. J., vad Mathiessen, B., & Yan, J. (2013). Sustainable development of energy, water and environment systems. *Applied Energy*, *101*, 3-5.

Ellingwood, B. R., & Wen, Y. (2005). Risk-benefit-based design decisions for low-probability/high consequence earthquake events in Mid-America. *Progress in Structural Engineering and Materials*, *7*(2), 56-70.

EMSD. (2018). *Hong Kong Energy End-use Data 2018*. The Energy Efficiency Office Electrical & Mechanical Services Department, Hong Kong.

ENVB. (2015). *Energy Saving Plan for Hong Kong's Built Environment 2015-2025+*. Environment Bureau, Development Bureau and Transport and Housing Bureau, Hong Kong.

Fasiuddin, M., & Budaiwi, I. (2011). HVAC system strategies for energy conservation in commercial buildings in Saudi Arabia. *Energy and Buildings, 43*(12), 3457-3466.

Ferreira, P. M., Ruano, A. E., Silva, S., & Conceicao, E. Z. E. (2012). Neural networks based predictive control for thermal comfort and energy savings in public buildings. *Energy and Buildings, 55*, 238-251.

Fisk, W. J., Black, D., & Brunner, G. (2012). Changing ventilation rates in US offices: Implications for health, work performance, energy, and associated economics. *Building and Environment, 47*, 368-372.

Forbes, C., Evans, M., Hastings, N., & Peacock, B. (2011). *Statistical distributions*, 4th edition. John Wiley & Sons, New York, US.

Gang, W. J., Wang, S. W., Shan, K., & Gao, D. C. (2015). Impacts of cooling load calculation uncertainties on the design optimization of building cooling systems. *Energy and Buildings, 94*, 1-9.

Gasparella, A., Longo, G. A., & Marra, R. (2005). Combination of ground source heat pumps with chemical dehumidification of air. *Applied Thermal Engineering, 25*(2-3), 295-308.

Ge, T. S., Ziegler, F., Wang, R. Z., & Wang, H. (2010). Performance comparison between a solar driven rotary desiccant cooling system and conventional vapor compression system (performance study of desiccant cooling). *Applied Thermal Engineering, 30*(6-7), 724-731.

Goyal, S., Ingley, H. A., & Barooah, P. (2012). Effect of various uncertainties on the performance of occupancy-based optimal control of HVAC zones. *2012 IEEE 51st IEEE Conference on Decision and Control (CDC)*, 7565-7570.

Ham, S. W., Park, J. S., & Jeong, J. W. (2015). Optimum supply air temperature ranges of various air-side economizers in a modular data center. *Applied Thermal Engineering*, *77*, 163-179.

Han, J., Pei, J., & Kamber, M. (2011). *Data mining: concepts and techniques*, 3rd Edition. Morgan Kaufmann Publishers, San Francisco, CA, US.

Hanby, V. I., & Angelov, P. P. (2000). Application of univariate search methods to the determination of HVAC plant capacity. *Building Services Engineering Research and Technology*, *21*(3), 161-166.

Hang, Y., Qu, M., Winston, R., Jiang, L., Widyolar, B., & Poiry, H. (2014). Experimental based energy performance analysis and life cycle assessment for solar absorption cooling system at University of Californian, Merced. *Energy and Buildings*, *82*, 746-757.

Henning, H. M. (2004). *Solar-assisted air-conditioning in buildings: a handbook for planners.* Springer, New York, US.

Heo, Y., Choudhary, R., & Augenbroe, G. A. (2012). Calibration of building energy models for retrofit analysis under uncertainty. *Energy and Buildings*, *47*, 550-560.

Hirunlabh, J., Charoenwat, R., Khedari, J., & Teekasap, S. (2007). Feasibility study of desiccant air-conditioning system in Thailand. *Building and Environment*, *42*(2), 572-577.

Holland, D. M., Fitz-Simons, T., & Hopke, P. K. (1982). Fitting statistical distributions to air quality data by the maximum likelihood method. *Atmospheric Environment*, *16*(5), 1071-1076.

Hopfe, C. J., Augenbroe, G. L. M., & Hensen, J. L. M. (2013). Multi-criteria decision making under uncertainty in building performance assessment. *Building and Environment*, *69*, 81-90.

Hu, S. C., & Chuah, Y. K. (2003). Power consumption of semiconductor fabs in Taiwan. *Energy*, *28*(8), 895-907.

Hu, S. C., & Tsao, J. M. (2007). A comparative study on energy consumption for HVAC systems of high-tech FABs. *Applied Thermal Engineering*, *27*(17-18), 2758-2766.

Huang, G. S., Wang, S. W., Xiao, F., & Sun, Y. (2009). A data fusion scheme for building automation systems of building central chilling plants. *Automation in Construction*, *18*(3), 302-309.

Huang, P., Huang, G., Augenbroe, G., & Li, S. (2018). Optimal configuration of multiple-chiller plants under cooling load uncertainty for different climate effects and building types. *Energy and Buildings*, *158*, 684-697.

Huang, P., Huang, G., & Sun, Y. (2018). Uncertainty-based life-cycle analysis of near-zero energy buildings for performance improvements. *Applied Energy*, *213*, 486-498.

Hult, G. T. M., Craighead, C. W., & Ketchen David J, J. (2010). Risk uncertainty and supply chain decisions: a real options perspective. *Decision Sciences*, *41*(3), 435-458.

ISO. (2015). 14644-1: 2015, *Cleanrooms and associated controlled environments–Part 1: Classification of air cleanliness by particle concentration*. International Organization for Standardization, Geneva, Switzerland.

Janssen, H. (2013). Monte-Carlo based uncertainty analysis: Sampling efficiency and sampling convergence. *Reliability Engineering & System Safety*, *109*, 123-132.

Jin, X., & Du, Z. (2006). Fault tolerant control of outdoor air and AHU supply air temperature in VAV air conditioning systems using PCA method. *Applied Thermal Engineering*, *26*(11-12), 1226-1237.

Jo, M. S., Shin, J. H., Kim, W. J., & Jeong, J. W. (2017). Energy-saving benefits of adiabatic humidification in the air conditioning systems of semiconductor cleanrooms. *Energies*, *10*(11), 1774.

Jouhara, H. (2009). Economic assessment of the benefits of wraparound heat pipes in ventilation processes for hot and humid climates. *International Journal of Low-Carbon Technologies*, *4*(1), 52-60.

Khalid, A., Mahmood, M., Asif, M., & Muneer, T. (2009). Solar assisted, pre-cooled hybrid desiccant cooling system for Pakistan. *Renewable Energy*, *34*(1), 151-157.

Kircher, K., Shi, X., Patil, S., & Zhang, K. M. (2010). Cleanroom energy efficiency strategies: Modeling and simulation. *Energy and Buildings*, *42*(3), 282-289.

Kuklicke, C., & Demeritt, D. (2016). Adaptive and risk-based approaches to climate change and the management of uncertainty and institutional risk: The case of future flooding in England. *Global Environmental Change*, *37*, 56-68.

Lee, K.P., & Chen, H.L. (2013). Analysis of energy saving potential of air-side free cooling for data centers in worldwide climate zones. *Energy and Buildings*, *64*, 103-112.

Lee, W.S., Chen, Y., & Wu, T. H. (2009). Optimization for ice-storage air-conditioning system using particle swarm algorithm. *Applied Energy*, *86*(9), 1589-1595.

Li, H., Lee, W. L., & Jia, J. (2016). Applying a novel extra-low temperature dedicated outdoor air system in office buildings for energy efficiency and thermal comfort. *Energy Conversion and Management, 121*, 162-173.

Li, H., He, H., Shan, J., & Cai, J. (2018). Innovation efficiency of semiconductor industry in china: A new framework based on generalized three-stage DEA analysis. *Socio-Economic Planning Sciences*, *66*, 136-148.

Li, Y., Lu, L., & Yang, H. (2010). Energy and economic performance analysis of an open cycle solar desiccant dehumidification air-conditioning system for application in Hong Kong. *Solar Energy*, *84*(12), 2085-2095.

Lin, T., Hu, S. C., & Xu, T. (2015). Developing an innovative fan dry coil unit (FDCU) return system to improve energy efficiency of environmental control for mission critical cleanrooms. *Energy and Buildings, 90*, 94-105.

Lu, Y. (2008). *Practical Handbook of heating and air conditioning design.* China Building Industry Press, Beijing, China.

Marion, W., & Urban, K. (1995). *User's Manual for TMY2s: Typical Meteorological Years: Derived from the 1961-1990 National Solar Radiation Data Base*. National Renewable Energy Laboratory, Golden, CO, USA

Mathew, P. (2008). *An estimate of energy use in laboratories, cleanrooms, and data centers in New York*. Lawrence Berkeley National Laboratory Report, Berkeley, CA, US.

Maulik, U., & Bandyopadhyay, S. (2002). Performance evaluation of some clustering algorithms and validity indices. *IEEE Transactions on Pattern Analysis and Machine Intelligence*, *24*(12), 1650-1654.

Mazzei, P., Minichiello, F., & Palma, D. (2005). HVAC dehumidification systems for thermal comfort: a critical review. *Applied Thermal Engineering*, *25*(5-6), 677–707.

Meesrikamolkul, W., Niennattrakul, V., & Ratanamahatana, C. A. (2012). Shape-Based Clustering for Time Series Data. *Pacific-Asia Conference on Knowledge Discovery and Data Mining*, 530-541.

Mills, E. (1996). *Energy efficiency in California laboratory-type facilities*. Lawrence Berkeley National Laboratory Report, Berkeley, CA, US.

Mills, E., Shamshoian, G., Blazek, M., Naughton, P., Seese, R. S., Tschudi, W., & Sartor, D. (2008). The business case for energy management in high-tech industries. *Energy Efficiency*, *1*(1), 5-20.

MOHURD. (1993). *Thermal design code for civil building (GB 50176-93)*. Ministry of Housing and Urban-Rural Development, People's Republic of China.

MOHURD. (2015). *Design Standard for Energy Efficiency of Public Buildings (50189-2015)*. Ministry of Housing and Urban-Rural Development, People's Republic of China.

Mossman, M. J. (2008). *RSMeans mechanical cost data*. A Division of Reed Construction Data Construction Publishers & Consultants, Kingston.

Nassif, N., Kajl, S., & Sabourin, R. (2005). Optimization of HVAC control system strategy using two-objective genetic algorithm. *HVAC&R Research*, *11*(3), 459-486.

NDRC. (2018). *Announcement on Changing the Electricity Price on the Grid*. National Development and Reform Commission, People's Republic of China.

Peterman, R. M., & Anderson, J. L. (1999). Decision analysis: a method for taking uncertainties into account in risk-based decision making. *Human and Ecological Risk Assessment: An International Journal*, *5*(2), 231-244.

PG&E. (2011). *A design guideline sourcebook: High performance cleanrooms*. San Francisco: Pacific Gas and Electric Company.

Qi, R., Lu, L., & Huang, Y. (2015). Parameter analysis and optimization of the energy and economic performance of solar-assisted liquid desiccant cooling system under different climate conditions. *Energy Conversion and Management*, *106*, 1387–1395.

Wang, Q., & Zhang, M. (2015). Introduction of the standard for energy efficient building evaluation. *Sustainable Cities and Society*, *14*, 1–4.

Quinlan, J. R. (1986). Induction of decision trees. *Machine Learning*, *1*(1), 81-106.

Remund, J., Kunz, S., & Lang, R. (1999). *METEONORM: Global meteorological database for solar energy and applied climatology*. Solar Engineering Handbook, Bern, Meteotest.

Salimifard, P., Delgoshaei, P., Xu, K., & Freihaut, J. D. (2014). Comparison of actual supply air fan performance data to ASHRAE 90.1 Standard-2010 and DOE Commercial Reference Buildings part load fan energy use formula. *ASHRAE/IBPSAUSA Building Simulation Conference*, 386-393.

Saltelli, A., Tarantola, S., & Campolongo, F. (2000). Sensitivity anaysis as an ingredient of modeling. *Statistical Science*, *15*(4), 377-395.

Schneider, R. K. (2001). Designing clean room HVAC systems. *ASHRAE Journal*, *43*(8), 39.

Sekhar, S. C., & Tan, L. T. (2009). Optimization of cooling coil performance during operation stages for improved humidity control. *Energy and Buildings*, *41*(2), 229-233.

Shan, K., & Wang, S. W. (2017). Energy efficient design and control of cleanroom environment control systems in subtropical regions–A comparative analysis and on-site validation. *Applied Energy*, *204*, 582-595.

Shan, K., Wang, S. W., Xiao, F., & Sun, Y. J. (2013). Sensitivity and uncertainty analysis of measurements in outdoor airflow control strategies. *HVAC&R Research*, *19*(4), 423-434.

Shehabi, A. (2008). *Energy implications of economizer use in California data centers.* Lawrence Berkeley National Laboratory Report, Berkeley, CA, US.

Shiue, A., Den, W., Kang, Y. H., Hu, S. C., Jou, G., Lin, C. H., Hu, V., & Lin, S. I. (2011). Validation and application of adsorption breakthrough models for the chemical filters used in the make-up air unit (MAU) of a cleanroom. *Building and Environment*, *46*(2), 468-477.

Smirnov, N. V, & Dunin-Barkowski, I. V. (1963). *Mathematische statistik in der technik.* Deutscher Verl. Der Wissenschaften.

Son, J. E., & Lee, K. H. (2016). Cooling energy performance analysis depending on the economizer cycle control methods in an office building. *Energy and Buildings*, *120*, 45-57.

Stetiu, C. (1999). Energy and peak power savings potential of radiant cooling systems in US commercial buildings. *Energy and Buildings*, *30*(2), 127-138.

Sun, Y., Gu, L., Wu, C. F. J., & Augenbroe, G. (2014). Exploring HVAC system sizing under uncertainty. *Energy and Buildings*, *81*, 243–252.

Sun, Z. W., Wang, S. W., & Zhu, N. (2011). Model-based optimal control of outdoor air flow rate of an air-conditioning system with primary air-handling unit. *Indoor and Built Environment*, *20*(6), 626-637.

Suzuki, H., Hanaoka, H., Ohkubo, Y., Yamazaki, Y., Shirai, Y., & Ohmi, T. (2000). Energy saving in semiconductor fabs by out-air handling unit performance improvement. *Proceedings of ISSM2000. Ninth International Symposium on Semiconductor Manufacturing (IEEE Cat. No. 00CH37130)*, 293-296.

Teng, S. G., & Ho, S. M. (1996). Failure mode and effects analysis. *International Journal of Quality & Reliability Management*, *13*(5), 8-26.

TRNSYS. (2017). *Transient System Simulation Tool*. University of Wisconsin, USA: Solar Energy Laboratory.

Tsao, J. M., Hu, S. C., Chan, D. Y. L., Hsu, R. T. C., & Lee, J. C. C. (2008). Saving energy in the make-up air unit (MAU) for semiconductor clean rooms in subtropical areas. *Energy and Buildings*, *40*(8), 1387-1393.

Tschudi, W., Sartor, D., Mills, E., & Xu, T. (2002). *High-performance laboratories and cleanrooms.* Lawrence Berkeley National Laboratory Report, Berkeley, CA, US.

Tschudi, W., & Xu, T. (2001). *Cleanroom energy benchmarking results.* Lawrence Berkeley National Laboratory Report, Berkeley, CA, US.

Virote, J., & Neves-Silva, R. (2012). Stochastic models for building energy prediction based on occupant behavior assessment. *Energy and Buildings*, *53*, 183-193.

Vose, M. D. (1999). *The simple genetic algorithm: foundations and theory*. MIT Press, Cambridge, MA, US.

Wang, G., & Song, L. (2012). Air handling unit supply air temperature optimal control during economizer cycles. *Energy and Buildings*, *49*, 310-316.

Wang, S. W. (1998). Dynamic simulation of a building central chilling system and evaluation of EMCS on-line control strategies. *Building and Environment*, *33*(1), 1-20.

Wang, S. W. (1999). Dynamic simulation of building VAV air-conditioning system and evaluation of EMCS on-line control strategies. *Building and Environment*, *34*(6), 681-705.

Wang, S. W., & Chen, Y. M. (2002). Fault-tolerant control for outdoor ventilation air flow rate in buildings based on neural network. *Building and Environment*, *37*(7), 691-704.

Wang, S. W., & Ma, Z. J. (2008). Supervisory and optimal control of building HVAC systems: A review. *HVAC&R Research*, *14*(1), 3-32.

Wang, S. W., & Xiao, F. (2004). AHU sensor fault diagnosis using principal component analysis method. *Energy and Buildings*, *36*(2), 147-160.

Weber, M. D., Leemis, L. M., & Kincaid, R. K. (2006). Minimum Kolmogorov–Smirnov test statistic parameter estimates. *Journal of Statistical Computation and Simulation*, *76*(3), 195-206.

West, S. R., Ward, J. K., & Wall, J. (2014). Trial results from a model predictive control and optimisation system for commercial building HVAC. *Energy and Buildings*, *72*, 271-279.

Wright, J. A. (1996). HVAC optimisation studies: sizing by genetic algorithm. *Building Services Engineering Research and Technology*, *17*(1), 7-14.

Xu, T. (2003). *Efficient Airflow Design for Cleanrooms Improves Business Bottom Lines*. Lawrence Berkeley National Laboratory Report, Berkeley, CA, US.

Yan, B., Li, X., Malkawi, A. M., & Augenbroe, G. (2017). Quantifying uncertainty in outdoor air flow control and its impacts on building performance simulation and fault detection. *Energy and Buildings*, *134*, 115-128.

Yang, X. Bin, Jin, X. Q., Du, Z. M., Fan, B., & Zhu, Y. H. (2014). Optimum operating performance based online fault-tolerant control strategy for sensor faults in air conditioning systems. *Automation in Construction*, *37*, 145–154.

Yao, Y., & Wang, L. (2010). Energy analysis on VAV system with different air-side economizers in China. *Energy and Buildings*, *42*(8), 1220-1230.

Yau, Y. H. (2007). Application of a heat pipe heat exchanger to dehumidification enhancement in a HVAC system for tropical climates—a baseline performance characteristics study. *International Journal of Thermal Sciences*, *46*(2), 164-171.

Yu, Y., Woradechjumroen, D., & Yu, D. (2014). A review of fault detection and diagnosis methodologies on air-handling units. *Energy and Buildings*, *82*, 550-562.

Yu, Z., Fung, B. C. M., Haghighat, F., Yoshino, H., & Morofsky, E. (2011). A systematic procedure to study the influence of occupant behavior on building energy consumption. *Energy and Buildings*, *43*(6), 1409-1417.

Zhang, L. Z., & Niu, J. L. (2003). A pre-cooling Munters environmental control desiccant cooling cycle in combination with chilled-ceiling panels. *Energy*, *28*(3), 275-292.

Zhou, X., Yan, D., Jiang, Y., & Shi, X. (2016). Influence of asynchronous demand behavior on overcooling in multiple zone AC systems. *Building and Environment*, *110*, 65-75.